Università degli Studi di Ferrara

DOTTORATO DI RICERCA IN
"Farmacologia e Oncologia Molecolare"

CICLO XXVII

COORDINATORE Prof. Antonio Cuneo

# CANNABINOID $CB_2$ AND μ-OPIOID RECEPTORS SIGNALLING IN MICROGLIAL CELLS: POTENTIAL TARGETS TO INCREASE CLINICAL EFFICACY OF OPIOIDS

Settore Scientifico Disciplinare BIO/14

**Dottorando**
Dott.ssa Debora Fazzi

**Tutore**
Dott.ssa Stefania Merighi

Anni 2012/2014

# TABLE OF CONTENTS

# Cannabinoid $CB_2$ receptors modulate ERK-1/2 kinase signalling and NO release in microglia cells stimulated with bacterial lypopolysaccharide

# Introduction

## Cannabinoid receptors signalling

Due to diverse physiological effects of cannabinoids, the endocannabinoid system has attracted major attention as a potential therapeutic target for a broad range of diseases. In the nervous system, neurotransmission and neuroinflammation are mediated by the endocannabinoid signalling system (Fernández-Ruiz, 2009; Marrset al., 2010). To date, two cannabinoid (CB) receptors have been identified by molecular cloning, namely, $CB_1$ and $CB_2$. $CB_1$ receptors are expressed by the neurones and regulate the release of neurotransmitters, while $CB_2$ receptors are expressed by the microglia, regulating their motility and immunomodulator production (Howlett et al., 2002; Pertwee et al., 2010; receptor nomenclature follows Alexander et al., 2011). Endogenous ligands for the cannabinoid receptors were discovered soon after their characterization. The two major known endogenous ligands are anandamide (AEA) and 2-arachidonoylglycerol (2-AG). Both are arachidonic acid derivatives produced from phospholipid precursors through activity-dependent activation of specific phospholipase enzymes (Massi et al., 2013). 2-AG is high efficacy agonist at $CB_2$, while AEA has a low efficacy at $CB_2$, often functioning as a weak partial agonist (Atwood et al., 2010).

Both $CB_1$ and $CB_2$ receptors are $G_{i/o}$-protein-coupled and are able to signal through the three main components of the MAPK pathway, namely, ERK, JNK and p38 (Howlett et al., 2002). However, activation of CB receptors is heavily influenced by cell type specificity, and their signalling is remarkably complex (Figure 1) (Bosier et al., 2010); indeed, they are able to exploit a wide variety of pathways to regulate the activities of MAPKs. In fact, CB receptor coupling to MAPKs is extremely dependent on the cellular context and a wide range of activation and inhibition has been observed dependent on cell type, cell differentiation status and co-modulators of MAPK cascades (Howlett, 2005).

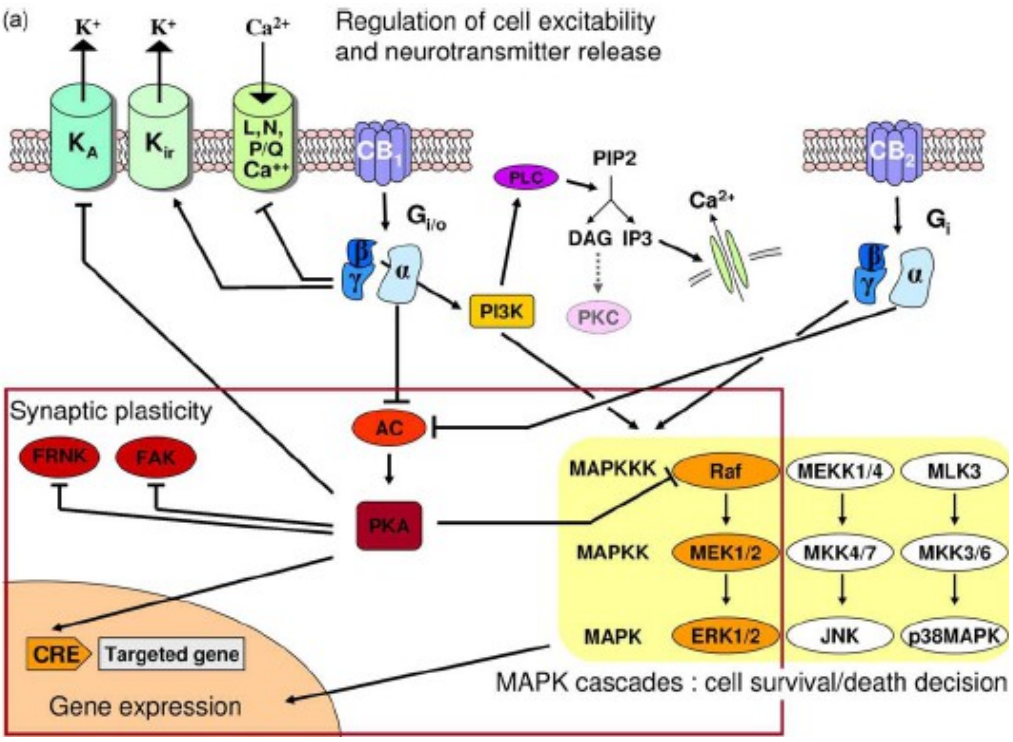


**Figure 1: Cannabinoid receptors signalling. Bosier et al., Biochem Pharmacol 80 (2010) 1-12.**

In the nervous system, activation of $CB_1$ and $CB_2$ receptors is induced by the endocannabinoids, AEA and 2-AG, produced by the neurons and glia (Massi et al, 2013). However, ample evidence suggests that additional receptors may contribute to the behavioral, vascular and immunological actions of $\Delta^9$-tetrahydrocannabinol (THC), the major psychoactive constituent of marijuana, and endocannabinoids (Begg et al., 2005). In particular, it has been established that GPR55 is an additional novel cannabinoid receptor (Lauckner et al., 2008; Bondarenko 2014).

During CNS inflammation, both $CB_1$ and $CB_2$ receptors mediate the induction of MAPK phosphatase-1 (MKP-1) by the endocannabinoid AEA. Rapid AEA-induced MKP-1 expression switches off MAPK signal transduction in microglial cells and thereby protects neurons from inflammatory damage (Eljaschewitsch et al., 2006). Furthermore, it has recently been reported that both the pharmacological stimulation of $CB_2$ receptors and the manipulation of endocannabinoid tone by inhibiting AEA hydrolysis in microglia, could modify the cytokine milieu, thereby contributing to the accumulation of anti-inflammatory microglia at lesion sites in multiple sclerosis (Correa et al., 2010; 2011). Moreover, another recent study has demonstrated that administration of 2-AG ameliorates both acute and chronic experimental autoimmune encephalomyelitis, a widely used model of multiple sclerosis (Lourbopoulos et al., 2011).

# Microglia

Microglia, which may constitute as many as 12% of the cells in the central nervous system (CNS), were described by del Rio-Hortega as a distinct cell type within the CNS with characteristic morphology and specialized staining characteristics that differentiated them from other glial cells and neurons. In recent years the advent of monoclonal antibodies to define cell surface determinants has led to the identification of microglia as a specialized macrophage population in the CNS, quiescent in the normal brain. However, after CNS injury or upon LPS interaction with Toll-like receptor (TLR)-4 during bacterial infection (González-Scarano and Baltuch, 1999), these cells can be activated by cytokines, produced by infiltrating immune effector cells. Thus, LPS stimulation of the microglia is a useful model for the study of mechanisms underlying neuronal injury by various pro-inflammatory and neurotoxic factors released by activated microglia (Jung et al., 2010). Microglial activation results in changes in morphology (e.g., complement receptors, scavenger receptors), and changes in function (Figure 2) (e.g., migration to sites of damage phagocytosis and the release of oxygen radicals, proteases, pro-inflammatory cytokines and NO) (Fricker et al., 2012; Grace et al., 2014). Cumulative evidence shows that, while the NO free radical may play an important role in host defence against certain intracellular pathogens, it may also contribute to neuropathology (Hanisch and Kettenmann, 2007). Hence, agents that suppress microglial cell activation may be beneficial in the treatment of neurodegenerative diseases.

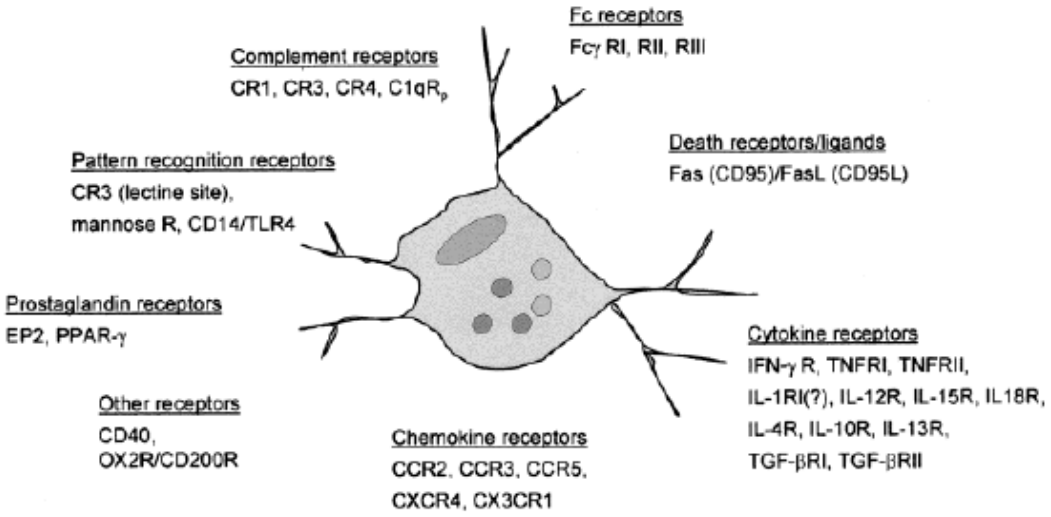


**Figure 2: Signalling to microglia. Under inflammatory condition, a variety of constitutively expressed and inducible receptors may promote migration as well as induce or downregulate immune effector functions of microglia. Aloisi, Glia 36 (2001) 165-179.**

# Cannabinoid $CB_2$ receptors

Cannabinoid $CB_2$ receptor is a G protein-couple receptor expressed mainly in microglia and peripheral immune cells, modulating antigen presentation, cytokine/chemokine production, and cell migration. The expression of $CB_2$ receptor was increased in brain injury and many types of neurodegenerative diseases including Alzheimer's disease, amyotrophic lateral sclerosis, Huntington's chorea (Lei Ma et al., 2015). $CB_2$ is an attractive therapeutic target; activation of $CB_2$ receptors has anti-inflammatory effects (Klein and Newton, 2007; Romero-Sandoval et al., 2009; Correa et al., 2010; Hsieh et al., 2011). In particular, activation of $CB_2$ receptors expressed in brain microglia during neuroinflammation (Benito et al., 2008; Atwood and Mackie, 2010) reduced NO production and TNF-α in primary microglia (Ehrhart et al., 2005). Furthermore, it protected against human microglial neurotoxicity by enhancing IL-10 production (Klegeris et al., 2003; Correa et al., 2005; 2010; Eljaschewitsch et al., 2006).

However, the specific intracellular mechanism of action by which $CB_2$ receptor activation alters the microglial phenotype still remains to be elucidated. Hence, building on previous studies of the role of $CB_2$ receptors in microglial cells, the rationale behind this study was to confirm and further explore the role of this receptor subtype in immune modulation within the CNS. In particular, we set out to characterize $CB_2$ receptor cell signalling, to verify whether the $CB_2$ receptor is coupled to the activation of MAPKs and to determine its role in NO production. In this way, we aimed to provide a comprehensive description of the signal transduction mechanisms coupled to $CB_2$ receptor activation.

To this end, we examined the effect of stimulating $CB_2$ receptors in quiescent and LPS-activated murine microglial cell line N9 and primary murine microglia. We found that $CB_2$ receptors exerted different effects on ERK activation in microglial cells, depending on the duration of cannabinoid challenge and the state of cell activation. We observed reversal of ERK phosphorylation in the LPS-treated microglial cells following 30 min of $CB_2$ receptor activation, a negative feed-back loop dependent on NO. This phenomenon was shown to diminish the response of microglial cells to LPS, by reducing NO synthesis and thereby regulating neuroinflammation. Hence, our findings suggest that $CB_2$ receptor agonists may promote therapeutic anti-inflammatory responses in activated microglia.

# Materials and Methods

## Drugs and materials

Tissue culture media and growth supplements were acquired from Cambrex (Bergamo, Italy). U0126 (MEK-1 and MEK-2 inhibitor, soluble in DMSO), human anti-ACTIVE®MAPK (phosphorylated $Thr^{183}/Tyr^{185}$) and human anti-ERK 1/2 pAb were purchased from Promega (Milan, Italy). Phosphorylated ($Thr^{180}/Tyr^{182}$) and total p38, phosphorylated ($Thr^{183}/Tyr^{185}$) and total JNK-1/2, anti-iNOS and phosphorylated $Ser^{338}$ Raf antibodies were from Cell Signaling Technology (Celbio, Milan, Italy). JWH-015 (1-propyl-2-methyl-3-(1-naphthoyl)indole) (soluble in ethanol) and anti-$CB_2$ receptor rabbit polyclonal antibody (ALX-210–198) were provided by Enzo Life Sciences (Vinci-Biochem, Vinci, Florence, Italy).

The immunogen for the $CB_2$ receptor antibody was a synthetic peptide corresponding to residues 20–33 of the human $CB_2$ receptor N-terminal. Anti-TLR4 (sc-30002), small interfering RNA (siRNA) for TLR4 (sc-40261) and siRNA for the $CB_2$ receptor (sc-39913) were from Santa Cruz Biotechnology (DBA, Milan, Italy). AM 251, N-(piperidin-1-yl)-1-(2,4-dichlorophenyl)-5-(4 iodophenyl)-4-methyl-1H-pyrazole-3-carboxamide and AM 630 (AM 630, 6-iodo-2-methyl-1-[2-(4-morpholinyl)ethyl]-1H-indol-3-yl](4-methoxyphenyl)methanone(6-iodopravadoline) (both soluble in DMSO) were from Tocris Bioscience (Bristol, UK).

RNAiFect ™ Transfection Kit was from Qiagen (Milan, Italy). Unless otherwise stated, all other chemicals were purchased from Sigma (Milan, Italy). L-NAME (L-$N^G$-nitroarginine methyl ester (hydrochloride)) was dissolved in DMSO, and Pertussis toxin (PTX) and sodium nitroprusside (SNP) were dissolved in distilled water. Drug and molecular target nomenclature conforms to Alexander et al., 2013.

## Animals

All animal care and experimental procedures conformed to the guidelines issued by the European Council (86/609/EEC) and were approved by the local Animal Care and Ethics Committee. One-day-old Balb/c mice were obtained from Charles River (Calco, Italy).

## Cell lines

The N9 murine microglial cell line (kindly donated by Dr P Ricciardi-Castagnoli, University of Milan, Milan, Italy) was generated by infecting primary mouse microglial cultures with the J2 retrovirus carrying v-raf/v-myc oncogenes (Corradin et al., 1993). CHO cells transfected with the human recombinant $CB_2$ receptor cDNA (CHO-h$CB_2$) were obtained from PerkinElmer (Milan, Italy).

## Primary microglial cell cultures

Primary glial cultures were prepared as described in a previous study (Molina-Holgado et al., 2002). Briefly, after anesthesia (Zoletil 100, 30 mg·kg$^{-1}$, Virbac Laboratories, France) and decapitation, forebrains from newborn Balb/c mice were excised, meninges were removed and tissue was dissociated mechanically. Cells were re-suspended in Dulbecco's modified Eagle medium (DMEM) supplemented with 10% heat-inactivated fetal bovine serum (FBS) and 1% penicillin/streptomycin, then plated on poly-D-lysine-coated (5 μg·mL$^{-1}$) 75 cm$^2$ flasks (Falcon; Celbio, Milan, Italy). After 15 days, the flasks were shaken vigorously to remove loosely adherent microglia. The supernatant was plated on multi-well culture plates for 2 h, and the medium was changed to remove non-adherent cells. Cells were grown in a humidified environment containing 5% $CO_2$ at a constant temperature of 37°C. The purity of microglial cultures was assessed by examining cell morphology under phase-contrast microscopy and was confirmed by flow cytometry with Mac-1 anti-CD11b antibody (BD Pharmingen, Milan, Italy).

## Cell cultures

Cells were maintained in DMEM (primary and N9) or Ham's (CHOh-$CB_2$) medium containing 10% fetal calf serum, penicillin (100 U·mL$^{-1}$), streptomycin (100 μg·mL$^{-1}$) and L-glutamine (2 mM) at 37°C in 5% $CO_2$/95% air. Geneticin (G418, 0.4 mg·mL$^{-1}$) was added to CHO-h$CB_2$ cells. Cells were split two or three times weekly at a ratio of 1:5 and 1:10.

## Flow cytometry of primary microglial cells

Aliquots of 0.5 x$10^6$ cells were incubated for 40 min at 4°C with either specific phycoerythrin (PE)-labelled antibodies (Abs) or isotype-matched irrelevant IgG-PE (Beckman Coulter, Fullerton, CA) as negative control. Cells were washed with PBS and characterized for expression of CD11b and the glial fibrillary acidic protein (GFAP) by flow cytometry with PE-labelled anti-CD11b monoclonal antibody (MoAb) (BD Pharmingen, Milan, Italy) and the fluorescein isothiocyanate (FITC)-labelled anti-GFAP MoAb (BD Pharmingen). In particular, GFAP immunophenotyping was performed in permeabilized cells, using IntraPrep™ fixing/permeabilization reagent (Beckman Coulter) (Gobbi et al., 2003). Analysis was performed on an Epics XL flow cytometer (Beckman Coulter) using Expo ADC software (Beckman Coulter).

## Primary and N9 microglial cell exposure to cannabinoids and LPS treatment

LPS, a cell wall component of Gram-negative bacteria, is a potent activator of glia. Hence, microglial cells were treated with 1 $\mu g \cdot mL^{-1}$ LPS (from Escherichia coli, serotype 055:B5, dissolved in cell culture medium) before commencing incubation with cannabinoid ligands. Microglia were then maintained in DMEM containing cannabinoids or their vehicle and harvested after treatment at the indicated times.

## Nitrite assay for primary microglial cells

NOS activity was assessed indirectly by measuring nitrite ($NO_2^-$) accumulation in the cell culture media using a colorimetric kit (Calbiochem, Milan, Italy). At the end of the treatment period, the nitrite concentration in the conditioned media was determined according to a modified Griess method (Merighi et al, 2012). Briefly, the NADH-dependent enzyme nitrate reductase was used to convert the nitrate to nitrite prior to quantification of the absorbance, measured at 540 nm by a spectrophotometric microplate reader (Fluoroskan Ascent, Labsystems, Sweden). Sodium nitrite was used as the standard compound.

## Western blotting in primary and N9 microglial cells

Western blot assay was performed as previously described (Merighi et al., 2009). Aliquots of total protein sample (50 μg) were analyzed using antibodies specific for phosphorylated or total p44/p42 MAPK (1:5000 dilution), phosphorylated or total p38 (1:1000 dilution), phosphorylated or total JNK 1/2 (1:1000 dilution) and for anti-$CB_2$ receptor and anti-TLR4 sera. Specific reactions were revealed with Enhanced Chemiluminescence Western blotting detection reagent (Amersham Corp., Arlington Heights, IL). The membranes were then stripped and re-probed with tubulin (1:250) to ensure equal protein loading.

## Densitometry analysis

The intensity of each immunoblot assay band was quantified using a VersaDoc Imaging System (Bio-Rad, Milan, Italy). Mean densitometric data from independent experiments were normalized to the results obtained with control cell cultures. The ratio of phospho-protein to total protein was reported in a densitometric analysis. In particular, MAPK phosphorylation was expressed as ratios between phosphorylated and total MAPK intensity (pMAPK/MAPK).

## siRNA transfection of N9 microglial cells

Microglial cells were plated in six-well plates and grown to 50–70% confluence before transfection. Transfection of siR-$NA_{CB2}$ or $siRNA_{TLR4}$ was performed at a concentration of 100 nM using RNAiFect™ Transfection Kit (Qiagen). Cells were cultured in complete media, and total proteins were isolated at 24, 48 and 72 h for Western blot analysis of $CB_2$ and TLR4 receptor protein. A randomly chosen non-specific siRNA was used under identical conditions as control (Merighi et al., 2005; 2007).

## Immunocytochemistry in cultured N9 microglial cells

Immunostaining was performed directly on cells seeded on glass coverslips. ERK-1 and ERK-2 were detected by anti-ACTIVE MAPK pAb, an affinity-purified rabbit serum that specifically

recognizes the dual-phosphorylated active forms of MAP (also known as p44/ERK-1 and p42/ERK-2) enzymes. Microglial cells were seeded on glass coverslips in 24-well plates overnight at 37°C in a humidified atmosphere containing 5% $CO_2$. Microglial cells were treated with 1μg·mL$^{-1}$ LPS alone or in combination with JWH-015. After 15 or 30 min, the medium was removed, and cells were washed twice with PBS, mixed in 10% paraformaldehyde for 30 min, permeabilized in a PBS solution containing 0.1% Triton X-100 and incubated for 30 min with PBS-plus 5% goat serum and 0.5% BSA. Cells were then stained (for 24 h at 4°C in a humidified chamber) with a 1:200 dilution of anti-ACTIVE MAPK pAb in 0.5% of goat serum and 0.5% BSA PBS solution. Excess antibody was washed away with PBS, and rabbit antibodies were detected with FITC-labelled goat anti-rabbit IgG. Coverslips were stained with 4′,6′-diamino-2-phenyl-indole (DAPI), mounted in DABCO glycerol-PBS and observed with a Nikon fluorescent microscope.

## Data analysis

All values in the figures and text are expressed as mean ± SE of n observation ($n \geq 3$). For the primary cell work, n is equal to the number of mice from which the cells were derived. Data sets were examined by ANOVA and Dunnett's test (when necessary). A P-value of less than 0.05 was considered statistically significant.

# Results

## $CB_2$ receptor expression in primary and N9 mouse microglial cells

Expression of the myeloid cell surface antigen CD11b was analyzed in primary microglial cells by flow cytometry. Cells were treated with specific MoAbs or isotype-matched irrelevant MoAbs. Microglia were negative for the astrocyte-specific protein GFAP but showed significant positive staining for CD11b, as compared with the isotype control, thereby indicating high expression levels of the microglial cell marker CD11b (Figure 3A).

The expression of $CB_2$ cannabinoid receptor in CHO-h$CB_2$ (used as positive control) in quiescent and LPS-activated primary and N9 mouse microglial cells is illustrated in Figure 3. The molecular weight of the protein detected in these cells was 50 kDa, comparable with the calculated molecular weight of $CB_2$ receptors. Expression of $CB_2$ receptor protein was not modified by 30 min treatment with LPS ($1 \mu g \cdot mL^{-1}$; Figure 3B).

To evaluate the previously reported effect of LPS-induced up-regulation of $CB_2$ receptors, we assayed $CB_2$ receptors over 4 h of LPS treatment. In agreement with published data (Mukhopadhyay et al., 2006), no significant increase in $CB_2$ receptor immunoreactivity was observed by Western blot in 4 h after LPS treatment (data not shown).

## Effects of activating $CB_2$ receptors on MAPKs in quiescent N9 microglial cells

The effects of $CB_2$ cannabinoid receptor stimulation were studied using JWH-015, a cannabinoid receptor agonist known to bind more readily to $CB_2$ than $CB_1$ receptors (Merighi et al., 2010), to test whether $CB_2$ receptors could induce ERK-1/2, p38 and JNK-1/2 phosphorylation in murine N9 microglial cells. As shown in Figure 4A, JWH-015 (10 nM) induced a rapid and sustained (up to 60 min) stimulation of ERK-1/2 and JNK-1/2. Conversely, p38 phosphorylation levels were not affected.

We then set out to evaluate the concentration-dependent effects of JWH-015 on N9 cells treated for 10 min. As shown in Figure 4B, JWH-015 (10–1000 nM) increased p-ERK-1/2 and p-JNK-1/2 expression levels but did not modulate p-p38. Furthermore, addition of the antagonist AM 630 (0.1–1 μM) blocked the JWH-015-induced (10–1000 nM) increase in ERK-1/2 and JNK-1/2 phosphorylation (Figure 5A,B). The $CB_1$ receptor antagonist AM 251 (1 μM), on the other hand,

had no effect on the increase in ERK-1/2 and JNK-1/2 phosphorylation levels induced by JWH-015 (1 μM; Figure 5B).

To further investigate the possible involvement of the $G_i/G_o$-proteins in the signal transduction pathway responsible for ERK-1/2 and JNK-1/2 modulation, N9 cells were treated with PTX (50 $ng \cdot mL^{-1}$). Blockade of $G_i/G_o$-protein dissociation with PTX abolished the JWH-015-induced activation of ERK-1/2 and JNK-1/2 in N9 cells (Figure 5C).

## Effects of activating $CB_2$ receptors on MAPKs in activated N9 and primary microglial cells

We went on to investigate how the activation of microglial cells interferes with the signalling pathways modulated by $CB_2$ receptors by maintaining microglial N9 cells in LPS-supplemented (1 $\mu g \cdot mL^{-1}$) DMEM; the ability of JWH-015 (10 and 100 nM) to modulate MAPKs was evaluated after 15 and 30 min. As shown in Figure 6A, LPS significantly increased all kinases under investigation. In contrast, the $CB_2$ receptor agonist JWH-015 failed to modulate the activity of LPS on p38 and JNK-1/2 at any time, but p-ERK-1/2 levels in LPS-treated cells were increased at 15 min. Conversely, JWH-015 significantly decreased ERK-1/2 phosphorylation levels in LPS-activated cells after 30 min of treatment (Figure 6A).

These results were confirmed in primary microglial cells, which yielded similar results to those observed in N9 cells. In particular, as shown in Figure 6B, JWH-015 (100 nM) significantly decreased ERK-1/2 phosphorylation levels in LPS-activated primary cells (after 30 min of treatment).

Figure 6C shows that, in LPS-treated primary microglial cells, the $CB_2$ antagonist AM 630 (1 μM) abolished the effect of JWH-015 on ERK-1/2 phosphorylation, thereby confirming $CB_2$ receptor involvement. In contrast, the $CB_1$ antagonist AM 251 (1 μM) did not reverse the ability of JWH-015 to down-regulate the LPS-induced increase in p-ERK-1/2 (Figure 6C).

We then studied the time-course of the effects of the $CB_2$ receptor agonist on LPS signalling. As shown in Figure 6D, LPS stimulation of microglial cells resulted in a rapid (after 15 min) increase in ERK-1/2 phosphorylation, which was maximal at 30 min and declined towards basal levels within 60 min. In the presence of the $CB_2$ agonist JWH-015 (100 nM), on the other hand, ERK-1/2 phosphorylation was significantly higher at 15 min than with LPS alone. In contrast, ERK-1/2 phosphorylation levels were significantly reduced by LPS + JWH-015 at the 30 min incubation time

point, as compared with LPS alone. Activation of ERK-1/2 returned to baseline levels within 120 min.

Finally, we studied the intracellular distribution of activated ERK-1 and ERK-2 MAPKs in N9 cells during LPS (1 μg·mL$^{-1}$) and JWH-015 (100 nM) treatment, alone and in combination, at 15 and 30 min. As seen in Figure 7, faint fluorescence caused by anti-ERK-1 and anti-ERK-2-activated isoforms was detected in the cytoplasm of cells treated with drug vehicle, contrasting with the strong fluorescence present in the nuclei of LPS- and JWH-015-treated cells after 15 and 30 min of treatment. Activated ERKs were also detected in the nuclei of N9 cells after 15 min of treatment with LPS in combination with JWH-015, but not after 30 min of combined treatment.

## $CB_2$ receptors modulate Raf-1 and MEK-1/2 kinases in quiescent N9 microglial cells

We investigated the levels of p-ERK upstream effectors, namely, p-Raf-1 and p-MEK-1/2, after $CB_2$ receptor stimulation in N9 cells. A significant increase in p-Raf expression levels was noted after 5 min of treatment with JWH-015 in the range 1–1000 nM (Figure 8A). The increase in Raf phosphorylation was marked until 30 min but had disappeared entirely by 60 min. Interestingly, the kinetics of Raf phosphorylation were comparable with those of ERK-1/2 phosphorylation. Furthermore, the JWH-015-induced increase of Raf activity was blocked by the addition of the selective $CB_2$ antagonist AM 630 (0.1–1 μM) (Figure 8A).

An increase in MEK-1/2 phosphorylation in N9 cells was promptly (5 min) induced by JWH-015 (10–100 nM; Figure 8B), an effect that was prevented by the $CB_2$ receptor antagonist AM 630 (0.1–1μM) (Figure 8B).

p-Raf and p-MEK-1/2 levels were then evaluated in N9 cells treated with 1mg·mL$^{-1}$ LPS for 5 and 20 min. LPS increased p-Raf and p-MEK-1/2 levels at 5 and 20 min of treatment, JWH-015 had no effect on LPS activity at 5 min (Figure 8C), while $CB_2$ receptor activation inhibited LPS stimulation of Raf and MEK-1/2 after 20 min of treatment (Figure 8D). Moreover, the antagonist AM 630 (1 μM) blocked the ability of JWH-015 to decrease the LPS-modulated p-Raf and p-MEK-1/2 expression levels at 20 min (Figure 8D). Figure 8E shows that blockade of $G_i/G_o$-protein dissociation by PTX (50 ng·mL$^{-1}$) abolished the ability of JWH-015 (10 and 100 nM) to impair LPS-induced Raf, MEK-1/2 and ERK-1/2 phosphorylation.

## $CB_2$ receptors modulate ERK-1/2 kinases by a NO-dependent pathway in activated primary microglial cells

To define the signalling responsible for ERK-1/2 activation, downstream of $CB_2$ receptors, in microglia, quiescent and activated primary microglial cells were treated for 30 min with JWH-015 (100 nM) in the presence of the NOS inhibitor L-NAME (100 μM). Figure 9A shows that L-NAME failed to alter the increased p-ERK-1/2 levels provoked by JWH-015, indicating that activation of the $CB_2$ receptor increased ERK activation in quiescent microglia cells in a NO-independent manner. In contrast, L -NAME blocked the ability of JWH-015 to down-regulate LPS-induced ERK activation in activated microglial cells, suggesting that $CB_2$ receptor stimulation reduced the effects of LPS on ERK-1/2 phosphorylation via a NO-mediated mechanism (Figure 9B).

To investigate the potential role of NO in LPS-mediated up-regulation of p-ERK-1/2, primary microglial cells were treated with either LPS alone, LPS + JWH-015 (100 nM) or LPS + the NO donor SNP (2.5 mM) for 30 min. As shown in Figure 9C, LPS significantly increased ERK-1/2 phosphorylation levels in primary microglial cells, an effect that was attenuated by JWH-015 and also by SNP, thereby confirming that an excess of intracellular NO is sufficient to impair p-ERK expression levels in primary microglial cells activated by LPS. In order to analyze iNOS protein expression, primary microglial cells were then stimulated with LPS, with or without JWH-015, and Western blotting was performed. As shown in Figure 9D, iNOS protein was induced after 4 h of stimulation with LPS ($1 \mu g \cdot mL^{-1}$). This induction was reduced by co-treatment with either JWH-015 or U0126 (0.5–1 μM).

Temporal conditions and concentrations of LPS required for optimal production of NO in primary microglial cells were then defined. Nitrite levels were measured at 30 min and 4 h in culture supernatants of microglial cells maintained in DMEM supplemented with LPS ($1 \mu g \cdot mL^{-1}$; Figure 9E,F).

Primary microglial cultures were incubated with JWH-015 (0.5–1 μM) before and after LPS activation. Different effects of $CB_2$ receptor stimulation on nitrite levels were seen in quiescent versus LPS-activated microglial cells. In the former, JWH-015 increased LPS-induced nitrite levels at 30 min of treatment, when this increase was particularly significant (Figure 9E). In contrast, at 4 h, nitrite levels induced by LPS were decreased by $CB_2$ receptor stimulation (Figure 9F). Subsequently, the effect on nitrite release of pre-treatment of microglial cells with the $CB_2$ antagonist AM 630 administered before exposure to JWH-015 was examined. 1 μM AM 630 alone had no effect on microglial cell release of nitrite but did reverse the activity of JWH-015 (Figure 9E,F).

The effect on nitrite release of pre-treatment of microglial cells with U0126 (1 μM), a specific inhibitor of MEK-1/2, the upstream regulator of ERK-1/2 phosphorylation, before exposure to LPS and JWH-015 was investigated; U0126 administered alone had no effect on nitrite release by microglial cells. Furthermore, in cells pre-treated with U0126, LPS for 30 min induced no significant increase in nitrite levels, as compared with cells treated with LPS alone (Figure 9E), indicating that LPS increased nitrite in an ERK-1/2-dependent manner. In contrast, the potentiating effect of JWH-015 on LPS seen at 30 min was not abolished by U0126. There, unlike LPS, $CB_2$ receptor activation must increase NO production in microglial cells by ERK-independent signalling. These data are in agreement with those reported in Figure 9B, which apparently shows p-ERK downstream of NO in $CB_2$-mediated signalling. At 4 h, JWH-015 reduced LPS-mediated NO accumulation; this activity was mimicked by U0126, which suggests that, at 4 h, the effects of $CB_2$ receptor stimulation in LPS-stimulated cells are consequent to the down-regulation of ERK-1/2 activation (Figure 9F).

Similar results were obtained with the MEK-1 inhibitor PD98059 in LPS- and JWH-015-treated cell cultures (30 min and 4 h, data not shown).

## $CB_2$ and TLR4 receptor gene silencing in N9 cells

To confirm the apparent role of $CB_2$ receptors and to investigate the involvement of TLR4, we reduced $CB_2$ and TLR4 receptor expression in N9 cells by siRNA transfection, in order to cause transient knockdown of the $CB_2$ and TLR4 receptor genes. N9 cells were transfected with non-specific random control ribonucleotides (siRNA scrambled, $siRNA_{ctr}$) or with small interfering RNAs that targeted $CB_2$ or TLR4 receptor mRNAs ($siRNA_{CB2}$ or $siRNA_{TLR4}$, respectively) for degradation.

As seen in Figure 10A, $CB_2$ receptor protein expression was strongly reduced after 48 and 72 h of treatment with $siRNA_{CB2}$. Therefore, 48 h after $siRNA_{CB2}$ transfection, N9 cells were exposed to LPS (1 $\mu g \cdot mL^{-1}$) and JWH-015 (100 nM) for 30 min, after which ERK-phosphorylated protein levels were measured. This revealed that inhibition of $CB_2$ receptor expression was sufficient to block the JWH-015-induced inhibition of ERK-1/2 phosphorylation levels increased by LPS (Figure 10B). These results clearly show the connection between $CB_2$ receptor stimulation and ERK signalling in activated microglial cells.

Likewise, Figure 10C shows that TLR4 receptor expression was reduced after 48 and 72 h of treatment with $siRNA_{TLR4}$. Therefore, 72 h post-$siRNA_{TLR4}$ transfection, N9 cells were exposed to

LPS (1μg·mL$^{-1}$) and JWH-015 (100 nM) for 30 min. Inhibition of TLR4 receptor expression blocked LPS-induced ERK-1/2 activation (Figure 10D). In contrast, JWH-015 significantly increased ERK-1/2 phosphorylation levels even in the absence of TLR4, indicating that this agonist acted in a TLR4-independent manner.

# Discussion and Conclusions

As microglial differentiation and immune function is regulated by activation of $CB_2$ receptors (Stella, 2010), we set out to characterize the signalling pathways modulated by these receptors expressed in microglial cells. $CB_2$ receptor ligands (agonist and antagonist) and $CB_2$-receptor-knockout microglial cells were thus used to determine the role of the cannabinoid system in in-vitro models, using N9 and primary microglial cells. By this means we described the mechanism by which $CB_2$ cannabinoid receptors modulated the MAPK signalling in response to LPS, an agent widely used experimentally to create inflammation in the brain (Lehnardtet al.,2002).

Multiple signalling molecules are activated in response to LPS in microglia (Aloisi, 2001). In particular, while microglial cells display a quiescent phenotype in the normal brain, they become highly activated upon insult, altering their phagocytic and antigen presentation functions, as well as the production of cytokines and NO release (Lehnardt et al., 2002; Hanisch and Kettenmann, 2007). Pathways associated with the induction of pro-inflammatory mediators of microglia include reactive oxygen species, PI3K/Akt, MAPKs and NF-kB (Aloisi, 2001; Hanisch and Kettenmann, 2007).

The discrepancies between physiological microglia and microglial cell cultures, including primary cultured microglia, have been much discussed (Horvathet al., 2008), and N9, being an artificially immortalized cell line, may not entirely reflect the physiological functions of microglia. In an attempt to clarify this situation, we compared mouse primary microglial and N9 cells in experiments assessing the phosphorylation of ERKs and production and release of NO. As N9 cells responded in a similar fashion to primary microglia, the cell line did, in our system, provide an adequate model of primary microglia.

Moreover, in this study, we showed that $CB_2$ cannabinoid receptors had different effects on ERK activation in microglial cells, depending on the duration of cannabinoid exposure and the state of cell activation. In particular, $CB_2$ receptor stimulation increased ERK-1/2 phosphorylation levels in quiescent and LPS-treated cells for 15 min, while, surprisingly, in the presence of both stimuli (LPS and JWH-015), phosphorylation of ERK-1/2 was reduced following 30 min of treatment.

The signalling revealed in the presence of $siRNA_{CB2}$ confirmed the role of $CB_2$ receptors in microglial cells. Thus, we demonstrated that $CB_2$ receptor stimulation provoked a state of activation in microglial cells by rapid MAPK-phosphorylation but prevented over-activation in the presence of a second stimulus.

It has been previously observed that $CB_2$ receptor stimulation leads to ERK-mediated cellular activation and anti-inflammatory effects in monocytes/macrophages and microglia (Gertsch et al.,

2008; Correa et al., 2010). Furthermore, the endocannabinoid AEA has been shown to protect neurones from inflammatory damage during CNS inflammation by rapid $CB_{1/2}$-receptor-mediated induction of MKP-1 in microglial cells (Eljaschewitsch et al., 2006). Hence, rapid AEA-induced MKP-1 expression switches off MAPK signal transduction in activated microglial cells. Similarly, a more recent study has demonstrated that $CB_2$ receptor stimulation in microglial cells induces an anti-inflammatory phenotype and reduces migration via MKP-induced ERK dephosphorylation (Romero-Sandoval et al., 2009). Interestingly, here we show that the signalling observed in ERK-1/2 kinase is reflected in Raf and MEK-1/2, thereby indicating that the $CB_2$ receptor is coupled to the activation of the ERK-1/2 kinase cascade through a classical upstream mechanism involving $G_i/G_o$-protein, Raf and MEK-1/2.

It has been reported that CB receptor agonists inhibit the production of pro-inflammatory molecules, which can be induced by LPS, in CNS glial cells (Molina-Holgado et al., 2002; Fachinetti et al., 2003; Ortega-Gutiérrez et al., 2005; Sheng et al., 2005; Correa et al., 2008; 2009). In particular, $CB_2$ receptors affect the production of the potent inflammatory mediator NO, released from quiescent and, to a greater extent, from activated microglia (Stella, 2010). Here we characterized, for the first time, the events occurring when quiescent microglia are exposed to LPS and $CB_2$ receptor agonist for 30 min, showing that $CB_2$ receptor stimulation increased their response to LPS without involving the TLR-4 pathway. Interestingly, at 15 and 30 min, the increase in ERK activation and nitrite levels in response to LPS plus $CB_2$ receptor stimulation was found to be additive rather than synergistic. However, at 30 min, $CB_2$ receptor stimulation was shown to reduce LPS-induced ERK-1/2 increase in LPS activated microglia through modulation of NO production. These data suggest that $CB_2$ receptor stimulation alone activates the MAPK pathway but switches off MAPK signal transduction by rapid induction of NO, in the presence of a second microglial stimulus. Therefore, $CB_2$ receptors expressed in microglia may participate in regulating neuroinflammation and provide neuro-protection by tempering LPS-induced NO synthesis.

In agreement with previous reports that all three MAPK pathways are involved in iNOS gene regulation in response to inflammatory stimuli in astrocytes and microglia (Bhat et al., 1998; Bodles and Barger, 2005; Wang et al., 2006), we showed that $CB_2$ receptor stimulation specifically reduced iNOS activation via inhibition of ERK-1/2 phosphorylation. This indicates that inhibition of MAPK pathways, and hence reduction in iNOS expression and NO production, is an important cellular signalling cascade in glial cell activation, suggesting a functional inhibitory role for the cannabinoid system in NO production. This accords with previous observations describing cannabinoid responses in activated microglia and in macrophage-like cells (Stefano et al., 1996; Ross et al., 2000; Walter et al., 2003; Ehrhart et al., 2005; Cabral et al., 2008; Kreitzer and Stella, 2009; Pietr et

al., 2009; Oh et al., 2010). Indeed, endogenous or synthetic cannabinoids are known to inhibit LPS-induced inducible NOS expression (mRNA and protein) through $CB_1$ receptors in astrocyte cultures. In addition, $\Delta^9$-tetrahydrocannabinol has been reported to produce a marked inhibition of NO release in the macrophage cell line RAW 264.7 by inhibiting NF-kB/Rel activation and increasing iNOS transcription (Jeon et al., 1996). Moreover, the $CB_1$ receptor has been implicated in the regulation of neuronal NOS in cerebellar granule neurons (Hillard et al., 1999). In cultured rat microglial cells, on the other hand, inhibition of LPS/IFN-γ-induced NO release by the agonist CP-55940 has been shown to act via a $CB_1$ receptor-mediated pathway (Waksman et al.,1999). However, in macrophages, the inhibition of LPS-mediated NO release by WIN-55212 occurs after activation of $CB_2$ receptors (Ross et al., 2000).

In addition, it has been recently reported that pharmacological stimulation of $CB_2$ receptors and manipulation of endocannabinoid tone, via inhibition of AEA hydrolysis in microglia, could result in modification of the cytokine milieu, contributing to the accumulation of anti-inflammatory microglia at lesion sites, in this case in multiple sclerosis (Correa et al., 2010). In particular, it has been demonstrated that AEA inhibits the production of biologically active IL-12p70 and IL-23. These cytokines play a crucial role in the pathogenesis of multiple sclerosis by activating human (and murine) microglial cultures, acting through the ERK-1/2 and JNK pathways to down-regulate IL-12p70 and IL-23 and up-regulate IL-10, effects that are partially mediated by $CB_2$ receptor activation (Correa et al., 2009; 2010).

Furthermore, it is well known that NO has an influence on critical signalling proteins; indeed, exposure of cells to NO and NOS inhibitors has revealed their complex effects on the production of cytokines. Precursors of IL-1β and IL-18 are not cleaved in the presence of NO, which also inhibits the expression of IL-8 and MCP-1. In contrast, NO increased the release of TNF-α and IL-6 acting simultaneously as a pro-inflammatory and anti-inflammatory agent (Murphy, 2000). Therefore, the modulation of NO mediated by $CB_2$ receptors may affect important target proteins in the CNS.

In conclusion, our results indicate a regulatory role for the $CB_2$ receptor in preventing excessive microglial cell response to injury in activated microglial cells. Hence, the development of selective $CB_2$ receptor agonists may open new avenues of therapeutic intervention, with the aim of reducing the release of pro-inflammatory mediators, especially in chronic neuropathologies. This is particularly exciting because selective $CB_2$ receptor agonists are devoid of the psychoactive side effects, characteristic of $CB_1$ receptor activation in the CNS (Fernández-Ruiz et al., 2007; Dhopeshwarkar et al, 2014).

# Figure Legends

**Figure 3:** Detection of $CB_2$ cannabinoid receptors. (A) Cell surface expression of CD11b and intracellular expression of GFAP by flow cytometry analysis. Primary microglial cells were treated with specific MoAbs (grey histograms) or with isotype-matched irrelevant MoAbs (empty histograms, controls). (B) $CB_2$ receptor detection by Western blot assay in CHO-h$CB_2$ cells, in quiescent and LPS-activated (1 $\mu g \cdot mL^{-1}$ for 30 min) primary and N9 microglial cells. Tubulin shows equal loading of protein.

**Figure 4:** Effects of stimulating $CB_2$ cannabinoid receptors in N9 cells. (A) N9 cells were incubated with 10 nM JWH-015 for the indicated time and ERK-1/2, p38 and JNK-1/2 phosphorylation levels were analyzed by Western blot. (B) Western blot analysis of ERK-1/2, p38 and JNK-1/2 phosphorylation in N9 cells incubated for 30 min with JWH-015 (1–1000 nM). The immunoblot signals were quantified using a VersaDoc Imaging System (Bio-Rad). MAPK phosphorylation was expressed as ratios between phosphorylated and total MAPK intensity (pMAPK/MAPK). The mean values of three independent experiments (one of which is shown) were normalized to the result obtained with JWH-015-untreated cell cultures. Densitometric analysis is reported. The unstimulated control (0, cells in the absence of JWH-015) was set to 100 %. *$P < 0.05$, significantly different from unstimulated control; ANOVA followed by Dunnett's test.

**Figure 5:** The $CB_2$ cannabinoid receptor and the $G_i/G_o$-protein pathway in N9 cells. (A) Western blot analysis of p-ERK-1/2 and p-JNK-1/2 expression levels. N9 cells were incubated with JWH-015 (10 and 100 nM) and AM 630 (0.1 and 1 μM) alone or in combination. (B) Western blot analysis of p-ERK-1/2 and p-JNK-1/2 expression levels. N9 cells were incubated with JWH-015 (1 μM), AM 630 (1 μM) and AM 251 (1 μM), alone or incombination. (C) N9 cells were incubated with or without PTX (50 $ng \cdot mL^{-1}$ for 14 h) and then with or without JWH-015 (10 and 100 nM) for additional 10 min. The immunoblot signals were quantified using a VersaDoc Imaging System (Bio-Rad). MAPK phosphorylation was expressed as ratios between phosphorylated and total MAPK intensity (pMAPK/MAPK). Densitometric analysis is reported. The unstimulated control (0, cells in the absence of JWH-015) was set to 100%. *$P < 0.05$, significantly different from unstimulated control; ANOVA followed by Dunnett's test.

**Figure 6:** Effect of $CB_2$ cannabinoid receptor stimulation in activated microglia cells. (A) JWH-015 effect on ERK-1/2, JNK-1/2 and p38 phosphorylation in N9 cells treated with LPS. N9 cells were incubated with DMSO vehicle (lane 0) or with JWH-015 (10 and 100 nM) in the presence of LPS (1 $\mu g \cdot mL^{-1}$) for 15 and 30 min. (B) JWH-015 effect on ERK-1/2 phosphorylation in primary microglia cells treated with LPS. Microglial cells were incubated with DMSO vehicle (lane 0) or with JWH-015 (100 nM) in the presence of LPS (1 $\mu g \cdot mL^{-1}$ for 15 and 30 min). (C) Primary microglial cells were incubated with DMSO vehicle (lane 1, control), LPS (1 $\mu g \cdot mL^{-1}$, lane 2), LPS + JWH-015 (100 nM), LPS + AM630 (1 μM; upper panel)/AM 251 (1 μM; lower panel) (lanes 3 and 4, respectively), and with LPS + JWH-015 + AM 630/AM 251 (lane 5) for 30 min. (D) Time-dependent pERK-1/2/MAPK phosphorylation induced by LPS (1 $\mu g \cdot mL^{-1}$) and LPS + JWH-015 (100 nM) after 0, 15, 30, 60 and 120 min. The mean values of three independent experiments (one of wich is shown) were normalized to the result obtained in cells in the absence of LPS. Plots are mean ± SE values (n = 3). The unstimulated control (0) was set to 100%. The immunoblot signals were quantified using a VersaDoc Imaging System (Bio-Rad). Densitometric analysis of MAPK activation is shown as the ratio of phospho-protein to total protein. $^{*}P < 0.05$ significantly different from untreated cells; $^{\#}P < 0.05$ significantly different from cells treated with LPS alone; ANOVA followed by Dunnet's test.

**Figure 7:** Intracellular localization of pERK-1/2. N9 cells (untreated cells, ctr) were treated with LPS (1 $\mu g \cdot mL^{-1}$) alone or in combination with JWH-015 (100 nM) for 15 or 30 min. Cells were then stained with antibody to ERK-1/2 phosphorylated isoforms and detected by goat FITC anti-rabbit IgG. The fluorescent dye DAPI (blue panel) was used to stain the nuclei of all microglial cells. Overlap of DAPI and FITC is shown (right panels). Original magnification, 40x.

**Figure 8:** $CB_2$ cannabinoid receptors modulate Raf and MEK-1/2 phosphorylation in quiescent (A–B) and activated (C–E) N9 cells. Cells were incubated with 10 nM JWH-015 for the indicated time (from 0 to 60 min) or for 30 min with different concentrations of JWH-015 (1–1000 nM). Raf (A) and MEK-1/2 (B) kinase phosphorylation levels were quantified by Western blot analysis. Furthermore, N9 cells were incubated with JWH-015 (10 and 100 nM). AM 630 (0.1 and 1 μM) was added alone or in the presence of JWH-015 (10 and 100 nM) before determination of Raf (A) and MEK-1/2 (B) phosphorylation. N9 cells were treated with LPS (1 $\mu g \cdot mL^{-1}$) for 5 (C) or 20 (D) min. The effect of the antagonist AM 630 (1 μM) is shown. (E) N9 cells were incubated with or without

PTX (50 ng·mL$^{-1}$ for 14 h) and then with or without LPS (1 μg·mL$^{-1}$) alone or in combination with JWH-015 (10 and 100 nM) for additional 30 min. The immunoblot signals were quantified using a VersaDoc Imaging System (Bio-Rad). The mean values of three independent experiments (one of which is shown) were normalized to the result obtained in cells in the absence of JWH-015. Densitometric analysis is shown as the ratio of phospho-protein to total protein. The unstimulated control (0, cells in the absence of JWH-015) was set to 100%. *P < 0.05, significantly different from unstimulated control; analysis was by ANOVA followed by Dunnett's test.

**Figure 9**: The $CB_2$ cannabinoid receptor and the NO pathway in primary microglial cells. (A) Primary microglial cells were incubated with DMSO vehicle (lane 1, control), L-NAME (100 μM; lanes 2, 4) and with JWH-015 (100 nM; lanes 3–4). (B) Primary microglial cells were incubated with DMSO vehicle (lane 1, control), LPS (1 μg·mL$^{-1}$; lane 2) and with JWH-015 (100 nM; lanes 4–5) or L-NAME (100 μM lanes 3, 5) for 30 min. (C) Primary microglial cells were incubated for 30 min with DMSO vehicle (lane 1) or LPS (1 μg·mL$^{-1}$; lanes 2–4), JWH-015 (100 nM; lane 3) or SNP (2.5 mM; lane 4). The immunoblot signals were quantified using a VersaDoc Imaging System (Bio-Rad). The mean values of three independent experiments (one of which is shown) were normalized to the result obtained in cells in the absence of LPS. Densitometric analysis is reported as the ratio of phospho-protein to total protein. The unstimulated control was set to 100%. *P < 0.05 with respect to unstimulated control; $^{\#}$P < 0.05, significantly different from cells treated with LPS alone; **P < 0.05, significantly different from LPS + JWH-015; ANOVA followed by Dunnett's test. (D) Primary microglial cells were treated with LPS (1 μg·mL$^{-1}$) for 4 h without and with JWH-015 (0.5 and 1 μM) to assess the effect on iNOS levels. These cells were harvested for Western analysis of iNOS expression. The mean values of three independent experiments (one of which is shown) were normalized to the result obtained in cells in the absence of LPS. The unstimulated control was set to 100%. *P < 0.05, significantly different from unstimulated control; $^{\#}$P < 0.05, significantly different from cells treated with LPS alone; ANOVA followed by Dunnett's test. (E–F) Effect of LPS and $CB_2$ receptor stimulation on nitrite levels in microglial cells. Primary microglial cells were treated with JWH-015 (0.5 and 1 μM), with or without LPS (1 μg·mL$^{-1}$) and culture supernatants were assayed for nitrite after 30 min (E) and 4 h (F) of treatment. The effects of U0126 (1 μM) and of AM 630 (1 μM) are shown. *P < 0.01, significantly different from untreated cells; $^{\#}$P < 0.05, significantly different from LPS-treated cells. *P < 0.01, significantly different from untreated cells; $^{\#}$P < 0.05, significantly different from LPS-treated cells; ANOVA followed by Dunnett's test.

**Figure 10:** $CB_2$ and TLR4 receptor expression silencing. (A) N9 microglial cells were treated with scrambled (-) (control) or with $siRNA_{CB2}$ (+) and cultured for 24, 48 and 72 h. Tubulin shows equal loading of protein. Densitometric quantification of $CB_2$ receptors by Western blot; plots are mean ± SE values (n = 3); *P < 0.01, significantly different from the control (scrambled transfected cells). (B) N9 microglial cells were treated with $siRNA_{CB2}$ or without (control) $siRNA_{CB2}$ for 48 h and cultured with LPS (1 $\mu g \cdot mL^{-1}$) alone or in combination with JWH-015 (100 nM) for 30 min. Densitometric analysis of phosphorylated isoform is shown as the ratio of phospho-protein to total protein. The immunoblot signals were quantified using a VersaDoc Imaging System (Bio-Rad). The mean values of three independent experiments (one of which is shown) were normalized to the result obtained in cells in the absence of LPS. The unstimulated control was set to 100%. *P < 0.05, significantly different from unstimulated control; $^{\#}P < 0.05$, significantly different from cells treated with LPS alone; ANOVA followed by Dunnett's test. (C) N9 microglial cells were treated with scrambled (-) (control) or with $siRNA_{TLR4}$ (+) and cultured for 24, 48 and 72 h. Tubulin shows equal loading of protein. Densitometric quantification of TLR4 receptor by Western blot; plots are mean ± SE values (n = 3); *P < 0.01 compared with the control (scramble transfected cells). (D) N9 microglial cells were treated with $siRNA_{TLR4}$ or without (control) $siRNA_{TLR4}$ for 72 h and cultured with LPS (1 $\mu g \cdot mL^{-1}$) alone or in combination with JWH-015 (100 nM) for 30 min. Densitometric analysis of phosphorylated isoform is reported as the ratio of phospho-protein to total protein is used. The immunoblot signals were quantified using a VersaDoc Imaging System (Bio-Rad). The mean values of three independent experiments (one of which is shown) were normalized to the result obtained in cells in the absence of LPS. The unstimulated control was set to 100%. *P < 0.05, significantly different from unstimulated control; $^{\#}P < 0.05$, significantly different from cells treated with LPS alone; ANOVA followed by Dunnett's test.

**Figure 3**

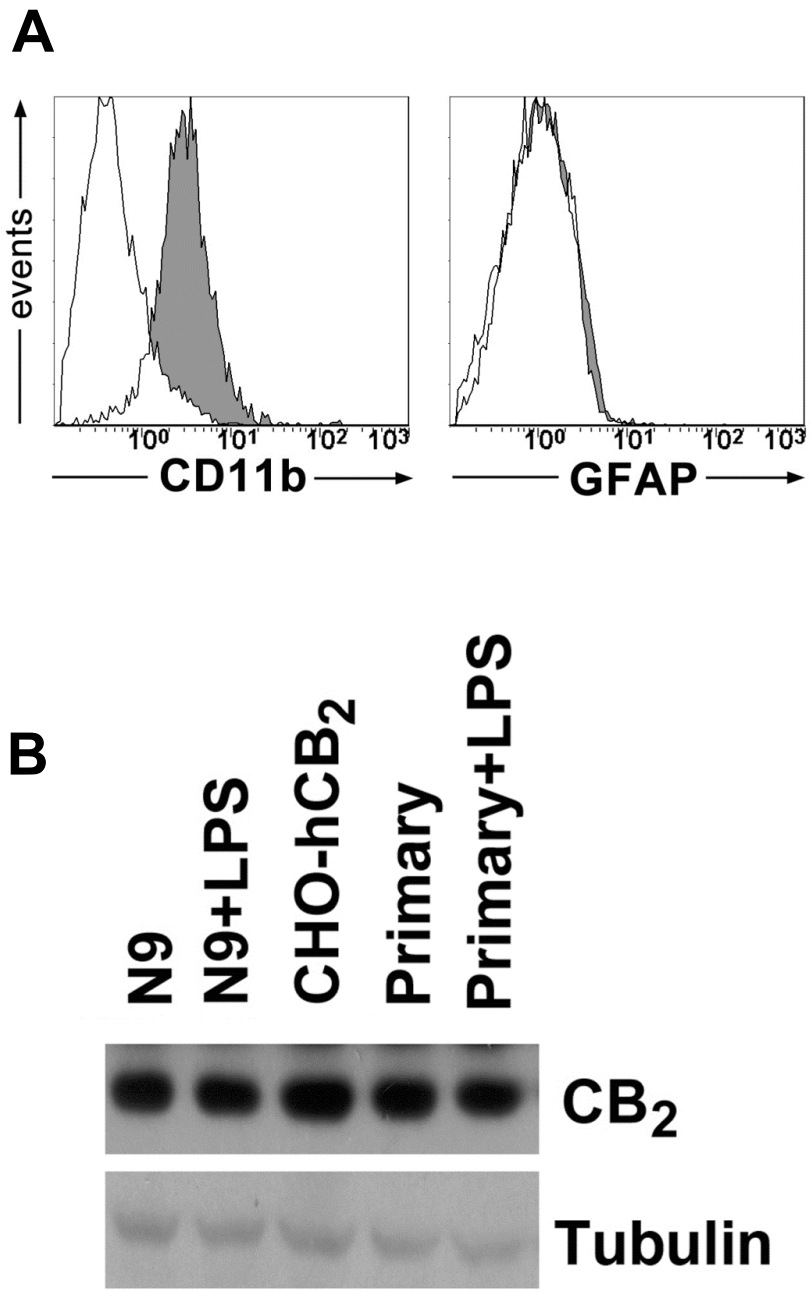
A
events
CD11b
GFAP
B
N9
N9+LPS
CHO-hCB2
Primary
Primary+LPS
CB2
Tubulin

**Figure 4**

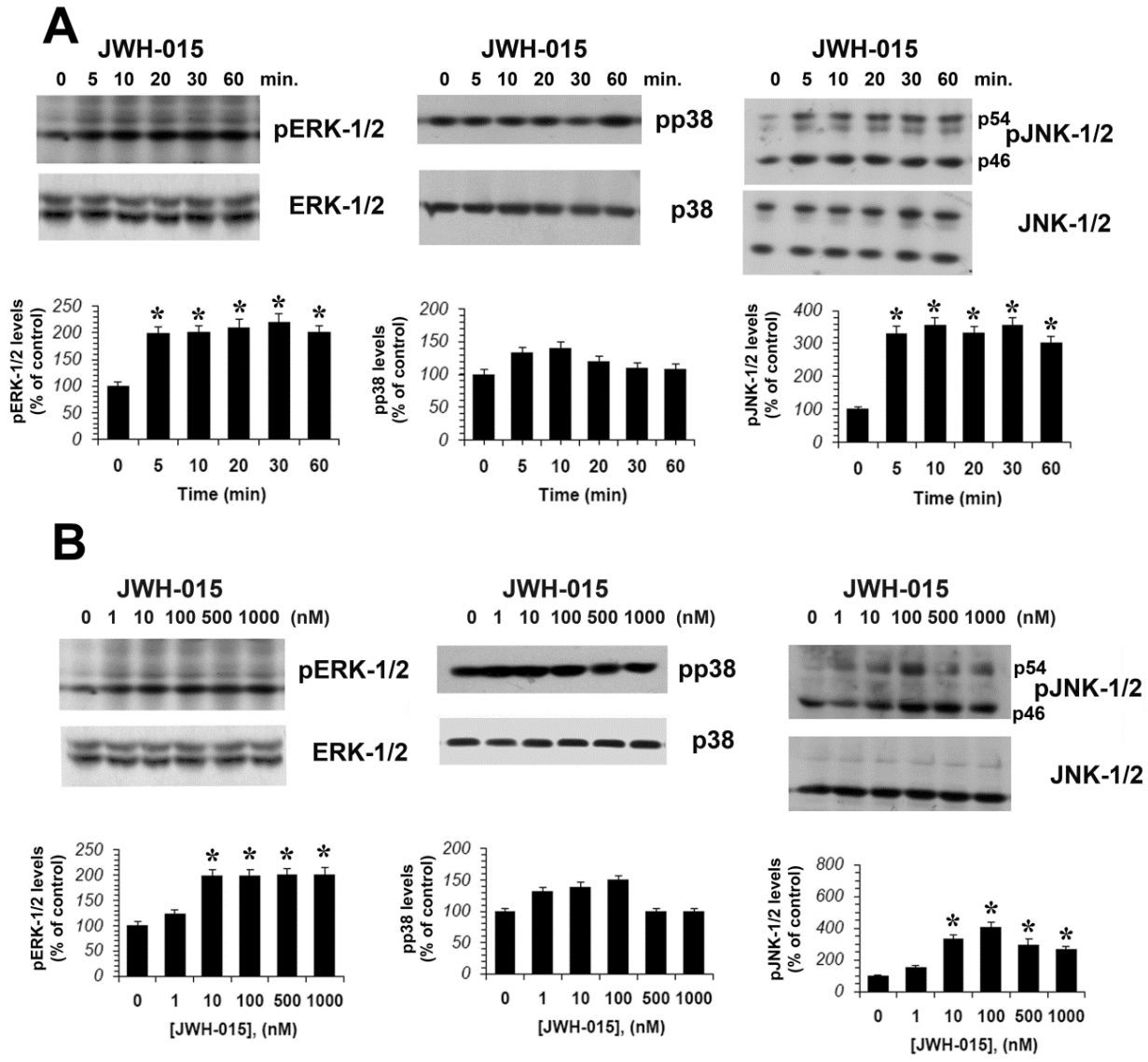
A
JWH-015
0 5 10 20 30 60 min.
pERK-1/2
ERK-1/2
pp38
p38
p54
p46
pJNK-1/2
JNK-1/2
pERK-1/2 levels (% of control)
pp38 levels (% of control)
pJNK-1/2 levels (% of control)
Time (min)
B
JWH-015
0 1 10 100 500 1000 (nM)
[JWH-015], (nM)

**Figure 5**

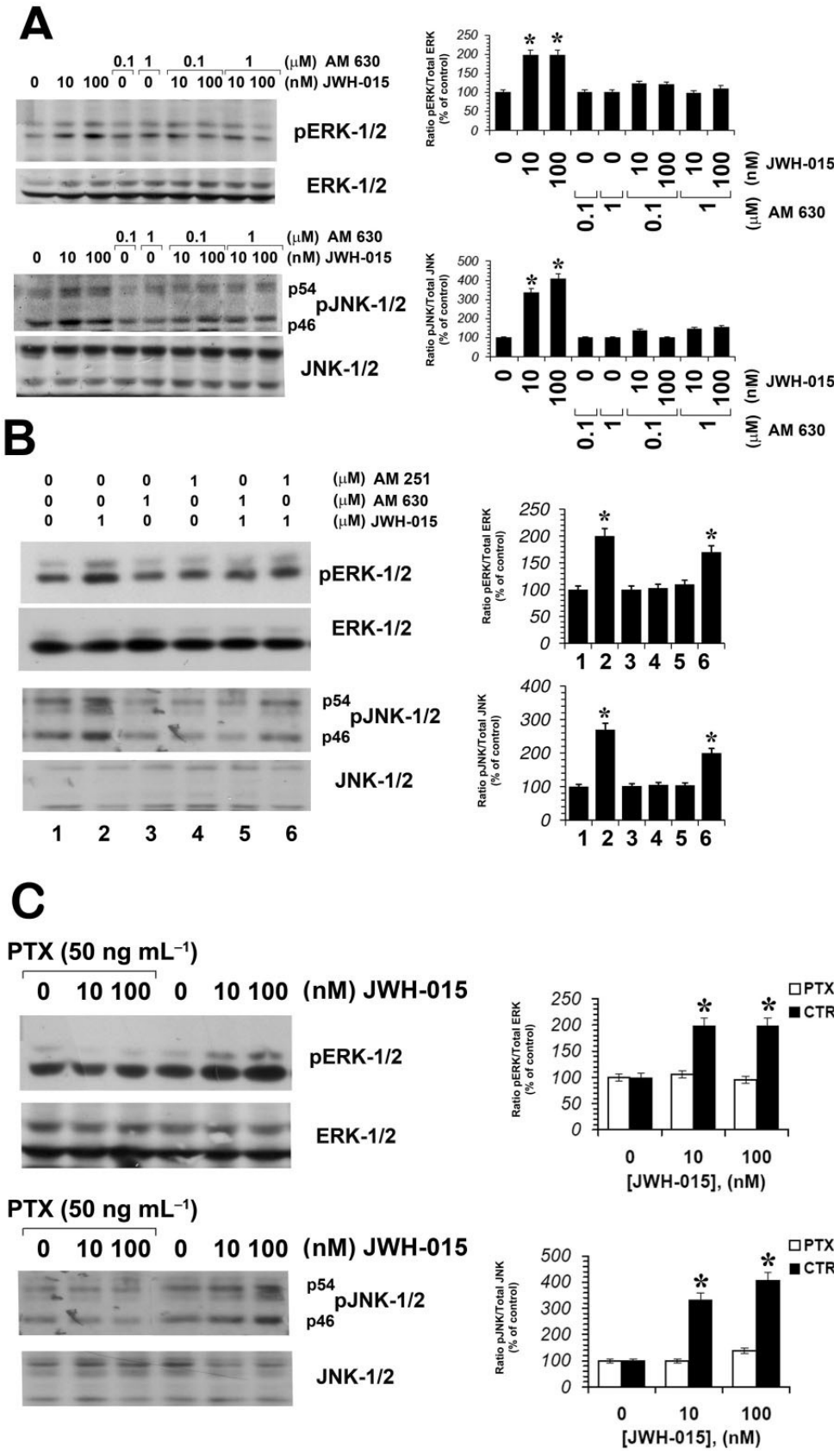
A
0.1 1 0.1 1 (μM) AM 630
0 10 100 0 0 10 100 10 100 (nM) JWH-015
pERK-1/2
ERK-1/2
p54
pJNK-1/2
p46
JNK-1/2
Ratio pERK/Total ERK (% of control)
Ratio pJNK/Total JNK (% of control)
JWH-015 (nM)
AM 630 (μM)
B
0 0 0 1 0 1 (μM) AM 251
0 0 1 0 1 0 (μM) AM 630
0 1 0 0 1 1 (μM) JWH-015
1 2 3 4 5 6
C
PTX (50 ng mL⁻¹)
0 10 100 0 10 100 (nM) JWH-015
PTX
CTR
[JWH-015], (nM)

**Figure 6**

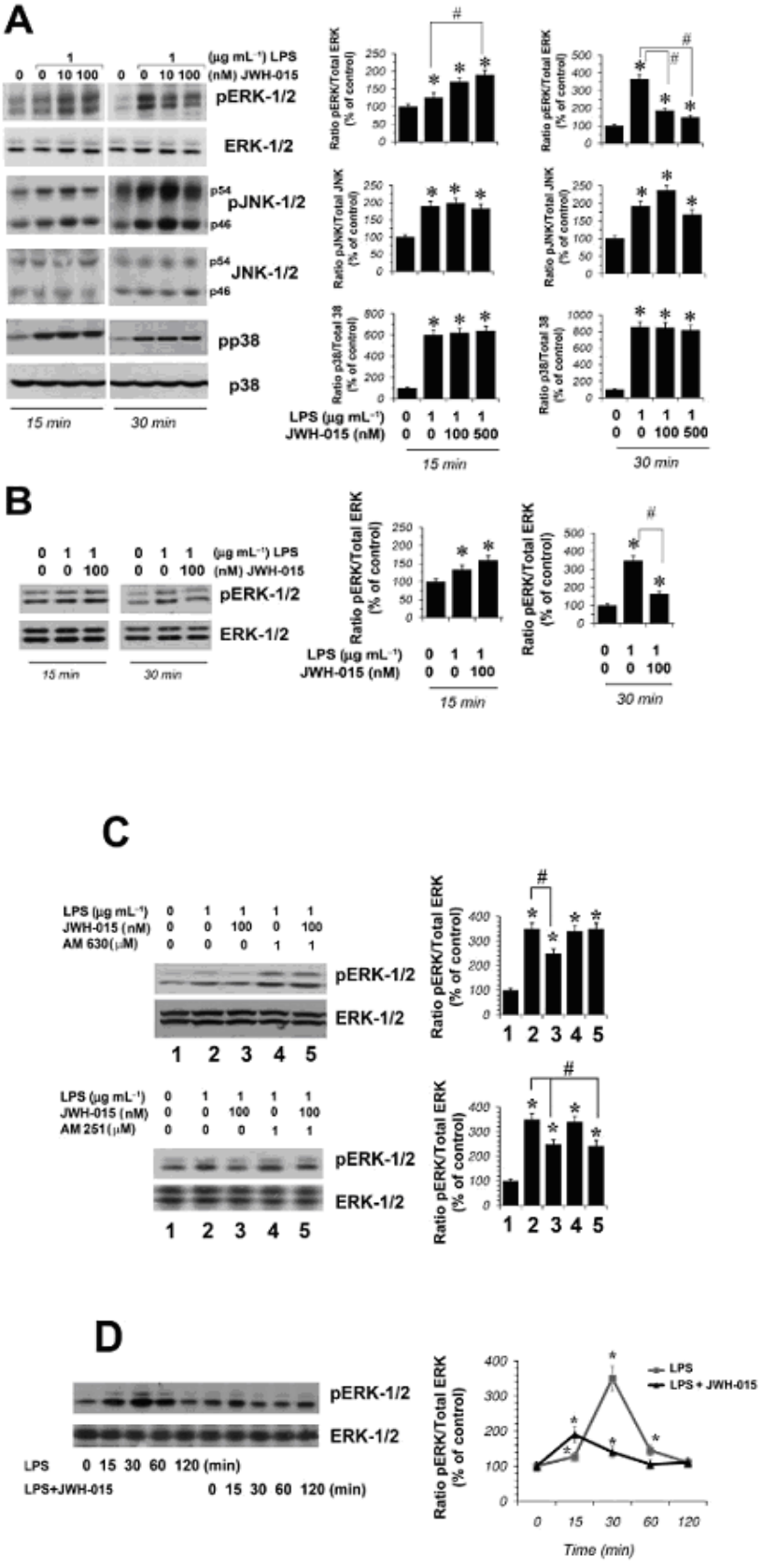
A
(μg mL⁻¹) LPS
(nM) JWH-015
pERK-1/2
ERK-1/2
pJNK-1/2
JNK-1/2
pp38
p38
15 min
30 min
Ratio pERK/Total ERK (% of control)
Ratio pJNK/Total JNK (% of control)
Ratio p38/Total 38 (% of control)
LPS (μg mL⁻¹)
JWH-015 (nM)
B
C
LPS (μg mL⁻¹)
JWH-015 (nM)
AM 630 (μM)
AM 251 (μM)
D
LPS
LPS+JWH-015
0 15 30 60 120 (min)
LPS
LPS + JWH-015
Time (min)

**Figure 7**

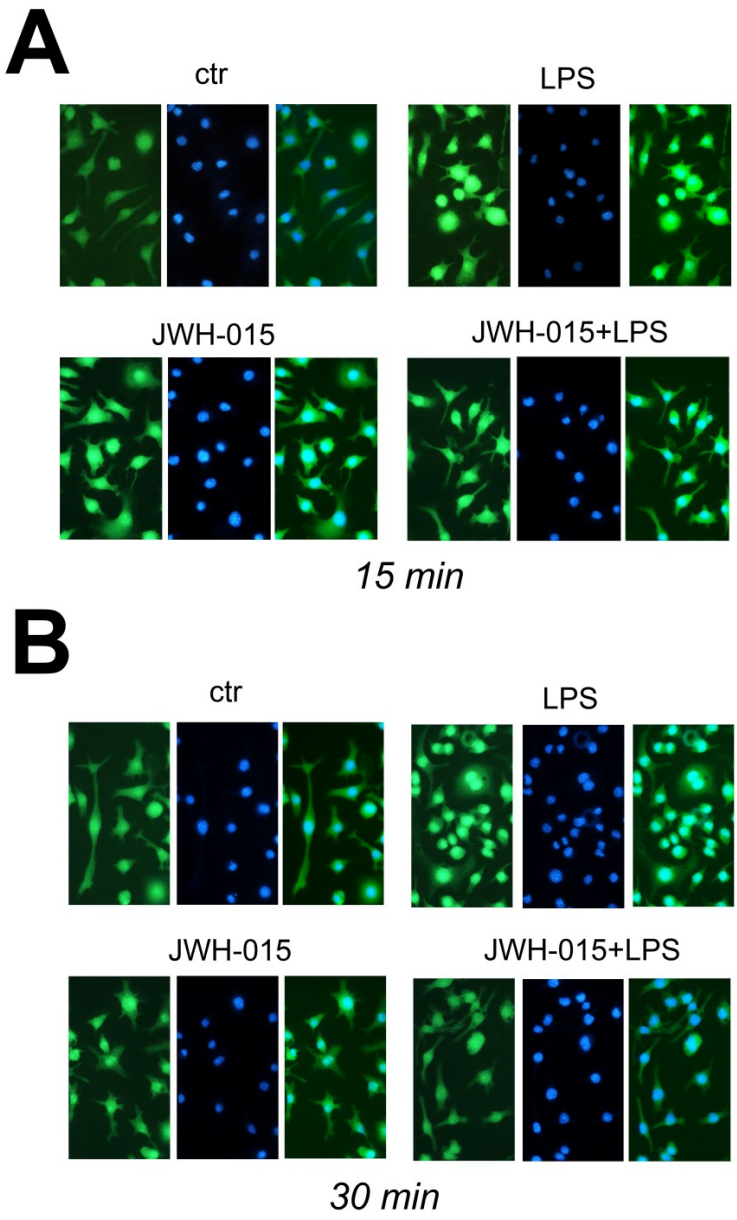
A
ctr
LPS
JWH-015
JWH-015+LPS
15 min
B
ctr
LPS
JWH-015
JWH-015+LPS
30 min

# Figure 8

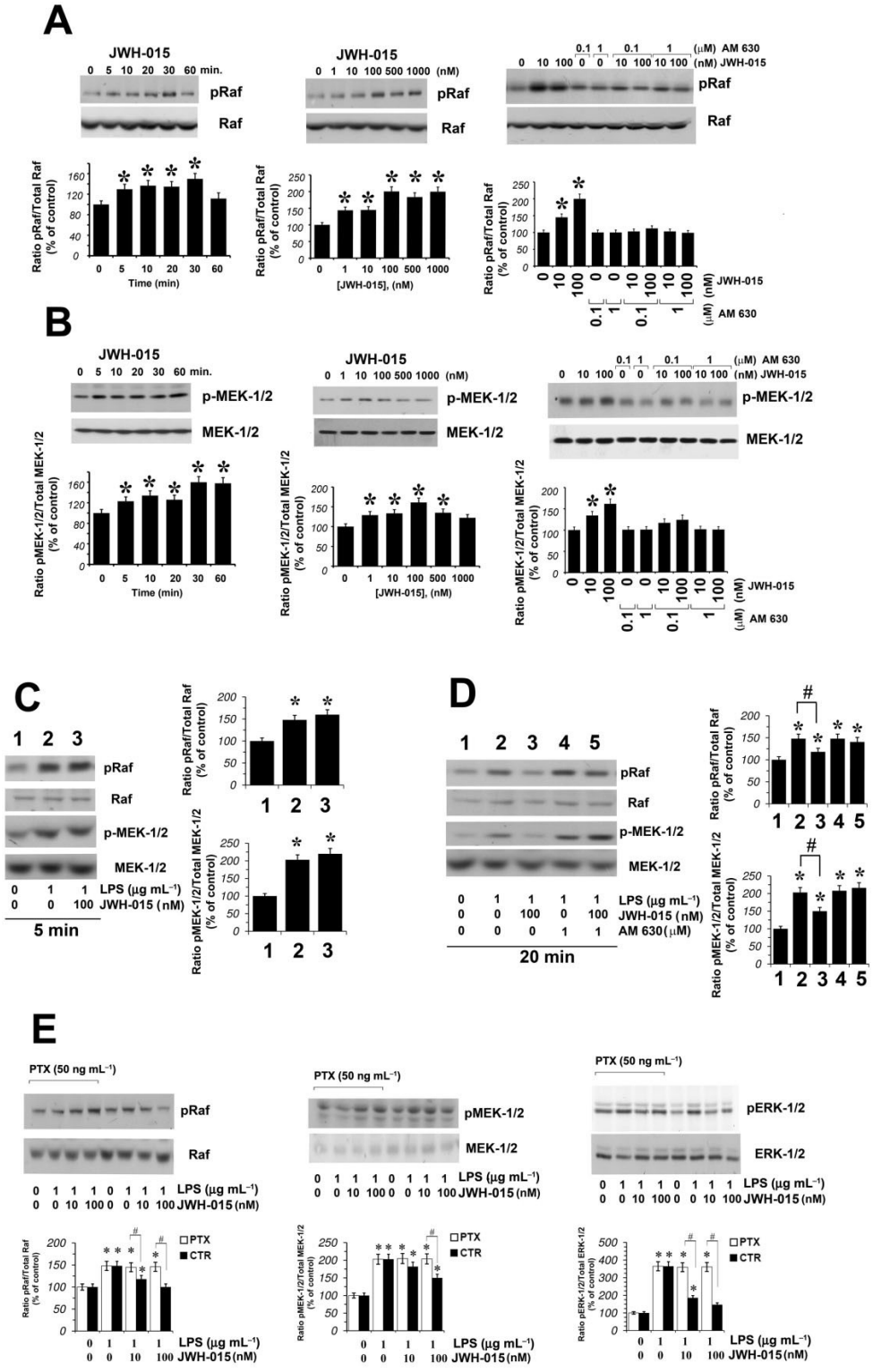
A
JWH-015
0 5 10 20 30 60 min.
pRaf
Raf
Ratio pRaf/Total Raf (% of control)
Time (min)
JWH-015
0 1 10 100 500 1000 (nM)
[JWH-015], (nM)
0.1 1 0.1 1 (μM) AM 630
0 10 100 0 0 10 100 10 100 (nM) JWH-015
B
p-MEK-1/2
MEK-1/2
Ratio pMEK-1/2/Total MEK-1/2 (% of control)
C
1 2 3
LPS (μg mL⁻¹)
JWH-015 (nM)
5 min
D
1 2 3 4 5
AM 630 (μM)
20 min
E
PTX (50 ng mL⁻¹)
pMEK-1/2
pERK-1/2
ERK-1/2
Ratio pERK-1/2/Total ERK-1/2 (% of control)
PTX
CTR

# Figure 9

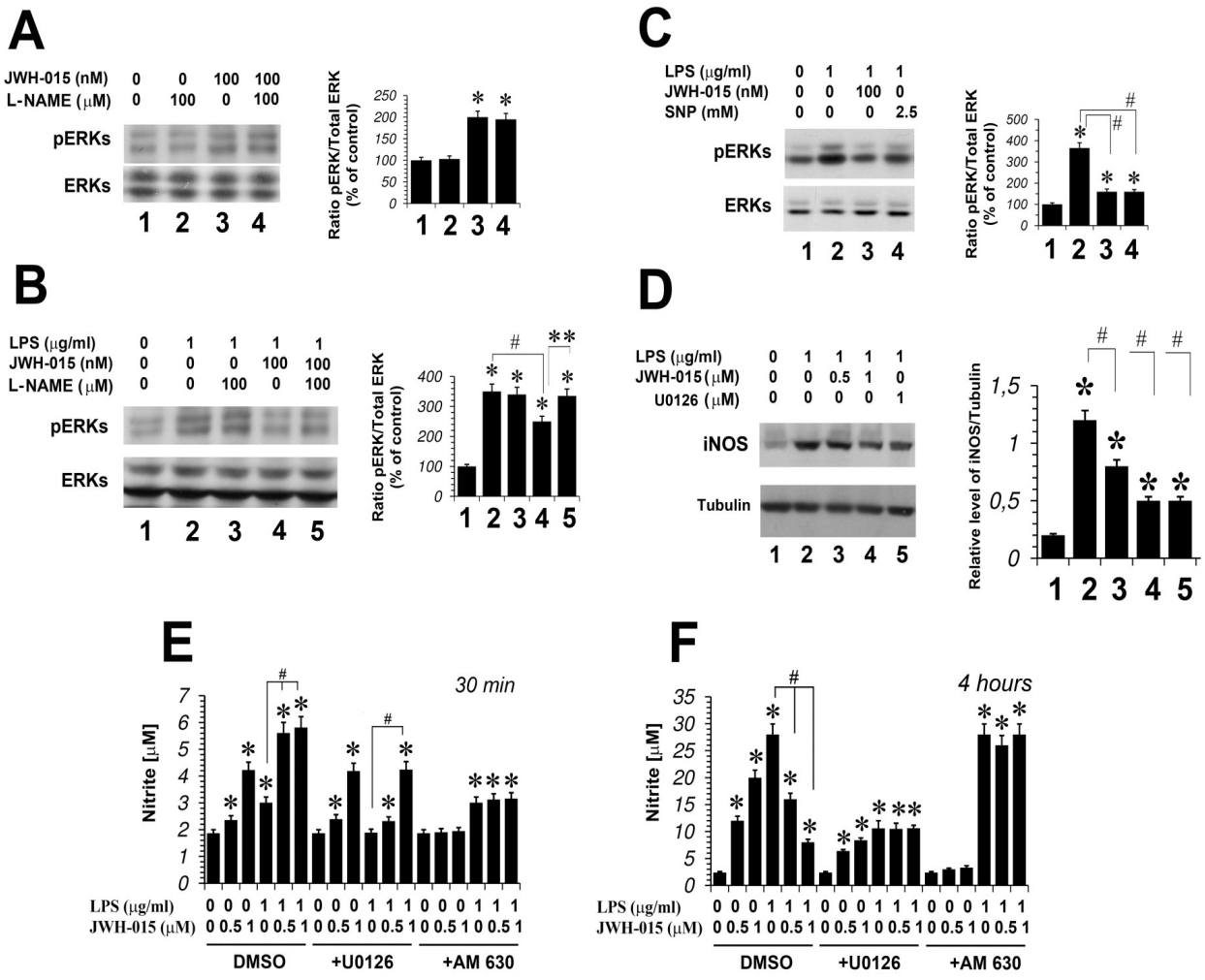
A
JWH-015 (nM) 0 0 100 100
L-NAME (μM) 0 100 0 100
pERKs
ERKs
1 2 3 4
Ratio pERK/Total ERK (% of control)
B
LPS (μg/ml) 0 1 1 1 1
JWH-015 (nM) 0 0 0 100 100
L-NAME (μM) 0 0 100 0 100
pERKs
ERKs
1 2 3 4 5
Ratio pERK/Total ERK (% of control)
C
LPS (μg/ml) 0 1 1 1
JWH-015 (nM) 0 0 100 0
SNP (mM) 0 0 0 2.5
pERKs
ERKs
1 2 3 4
Ratio pERK/Total ERK (% of control)
D
LPS (μg/ml) 0 1 1 1 1
JWH-015 (μM) 0 0 0.5 1 0
U0126 (μM) 0 0 0 0 1
iNOS
Tubulin
1 2 3 4 5
Relative level of iNOS/Tubulin
E
30 min
Nitrite [μM]
LPS (μg/ml) 0 0 0 1 1 1 0 0 0 1 1 1 0 0 0 1 1 1
JWH-015 (μM) 0 0.5 1 0 0.5 1 0 0.5 1 0 0.5 1 0 0.5 1 0 0.5 1
DMSO +U0126 +AM 630
F
4 hours
Nitrite [μM]
LPS (μg/ml) 0 0 0 1 1 1 0 0 0 1 1 1 0 0 0 1 1 1
JWH-015 (μM) 0 0.5 1 0 0.5 1 0 0.5 1 0 0.5 1 0 0.5 1 0 0.5 1
DMSO +U0126 +AM 630

**Figure 10**

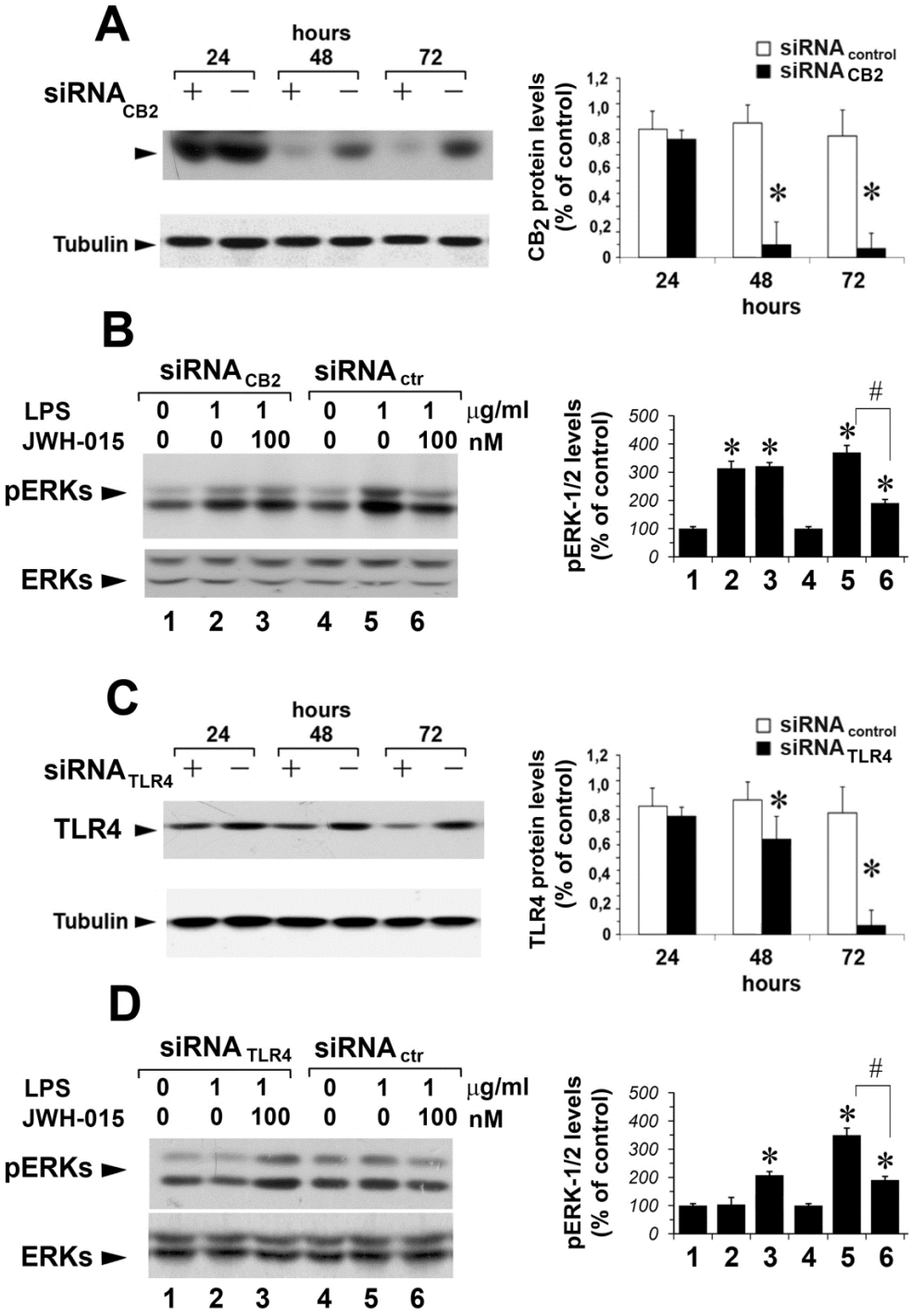
A
hours
24
48
72
siRNA CB2
+ − + − + −
Tubulin
siRNA control
siRNA CB2
CB2 protein levels (% of control)
1,2
1,0
0,8
0,6
0,4
0,2
0
24
48
72
hours
B
siRNA CB2
siRNA ctr
LPS 0 1 1 0 1 1 µg/ml
JWH-015 0 0 100 0 0 100 nM
pERKs
ERKs
1 2 3 4 5 6
pERK-1/2 levels (% of control)
500
400
300
200
100
0
C
hours
24
48
72
siRNA TLR4
+ − + − + −
TLR4
Tubulin
siRNA control
siRNA TLR4
TLR4 protein levels (% of control)
24
48
72
hours
D
siRNA TLR4
siRNA ctr
LPS 0 1 1 0 1 1 µg/ml
JWH-015 0 0 100 0 0 100 nM
pERKs
ERKs
1 2 3 4 5 6
pERK-1/2 levels (% of control)

# References


Alexander SPH, Mathie A, Peters JA (2011). Guide to Receptors and Channels (GRAC), 5th Edition. Br J Pharmacol 164 (Suppl. 1): S1–S324.

Alexander SPH, Benson HE, Faccenda E, Pawson AJ, Sharman JL, Catterall WA, Spedding M, Peters JA, Harmar AJ, CGTP collaborators (2013). The Concise Guide to PHARMACOLOGY 2013/2014: Overview . Br J Pharmacol 170: 1449-1458.

Aloisi F (2001). Immune function of microglia. Glia 36: 165–179.

Atwood BK, Mackie K (2010). $CB_2$: a cannabinoid receptor with an identity crisis. Br J Pharmacol 160: 467–479.

Benito C, Tolón RM, Pazos MR, Núñez E, Castillo AI, Romero J (2008). Cannabinoid $CB_2$ receptors in human brain inflammation. Br J Pharmacol 153: 277–285.

Bhat NR, Zhang P, Lee JC, Hogan EL (1998). Extracellular signal-regulated kinase and p38 subgroups of mitogen-activated protein kinases regulate inducible nitric oxide synthase and tumor necrosis factor-alpha gene expression in endotoxin-stimulated primary glial cultures. J Neurosci 18: 1633–1641.

Bondarenko AI (2014). Endothelial atypical cannabinoid receptor: do we have enough evidence? Br J Pharmacol 171: 5573-5588.

Bodles AM, Barger SW (2005). Secreted beta-amyloid precursor protein activates microglia via JNK and p38-MAPK. Neurobiol Aging 26: 9–16.

Bosier B, Muccioli GG, Hermans E, Lambert DM (2010). Functionally selective cannabinoid receptor signaling: therapeutic implications and opportunities. Biochem Pharmacol 80: 1–12.

Cabral GA, Raborn ES, Griffin L, Dennis J, Marciano-Cabral F (2008). $CB_2$ receptors in the brain: role in central immune function. Br J Pharmacol 153: 240–251.

Corradin SB, Mauel J, Donini SD, Quattrocchi E, Castagnoli PR (1993). Inducible nitric oxide synthase activity of cloned murine microglial cells. Glia 7: 255–262.

Correa F, Mestre L, Docagne F, Guaza C (2005). Activation of cannabinoid $CB_2$ receptor negatively regulates IL-12p40 production in murine macrophages: role of IL-10 and ERK1/2 kinase signaling. Br J Pharmacol 145: 441–448.

Correa F, Docagne F, Clemente D, Mestre L, Becker C, Guaza C (2008). Anandamide inhibits IL-12p40 production by acting on the promoter repressor element GA-12: possible involvement of the COX-2 metabolite prostamide E(2). Biochem J 409: 761–770.

Correa F, Docagne F, Mestre L, Clemente D, Hernangómez M, Loría F, Guaza C (2009). A role for $CB_2$ receptors in anandamide signalling pathways involved in the regulation of IL-12 and IL-23 in microglial cells. Biochem Pharmacol 77: 86–100.

Correa F, Hernangómez M, Mestre L, Loría F, Spagnolo A, Docagne F, Di Marzo V, Guaza C (2010). Anandamide enhances IL-10 production in activated microglia by targeting $CB_2$ receptors: roles of ERK1/2, JNK, and NF-kappaB. Glia 58: 135–147.

Correa F, Hernangómez-Herrero M, Mestre L, Loría F, Docagne F, Guaza C (2011). The endocannabinoid anandamide downregulates IL-23 and IL-12 subunits in a viral model of multiple sclerosis: evidence for a cross-talk between IL-12p70/IL-23 axis and IL-10 in microglial cells. Brain Behav Immun 25: 736–749.

Dhopeshwarkar A, Mackie K (2014). $CB_2$ cannabinoid receptors as a therapeutic target - what does the future hold? Mol Pharmacol 86(4):430-437.

Ehrhart J, Obregon D, Mori T, Hou H, Sun N, Bai Y, Klein T, Fernandez F, Tan J, Shytle RD (2005). Stimulation of cannabinoid receptor 2 ($CB_2$) suppresses microglial activation. J Neuroinflammation 2: 29.

Eljaschewitsch E, Witting A, Mawrin C, Lee T, Schmidt PM, Wolf S, Hoertnagl H, Raine CS, Schneider-Stock R, Nitsch R, Ullrich O (2006). The endocannabinoid anandamide protects neurons during CNS inflammation by induction of MKP-1 in microglial cells. Neuron 49: 67–79.

Fachinetti F, Del Giudice G, Furegato S, Passarotto M, Leon M (2003). Cannabinoids ablate release of TNFα in rat microglial cells stimulated with lypopolysaccharide. Glia 41: 161–168.

Fernández-Ruiz J (2009). The endocannabinoid system as a target for the treatment of motor dysfunction. Br J Pharmacol 156: 1029–1040.

Fernández-Ruiz J, Romero J, Velasco G, Tolón RM, Ramos JA, Guzmán M (2007). Cannabinoid $CB_2$ receptor: a new target for controlling neural cell survival? Trends Pharmacol Sci 28: 39–45.

Fricker M, Oliva-Martin MJ, Brown GC (2012). Primary phagocytosis of viable neurons by microglia activated with LPS or Aβ is dependent on calreticulin/LRP phagocytic signalling. J Neuroinflam 9:196-208.

Gertsch J, Leonti M, Raduner S, Racz I, Chen JZ, Xie XQ, Altmann KH, Karsak M, Zimmer A (2008). Beta-caryophyllene is a dietary cannabinoid. Proc Natl Acad Sci USA 105: 9099–9104.

Gobbi G, Mirandola P, Tazzari PL, Ricci F, Caimi L, Cacchioli A, Papa S, Conte R, Vitale M (2003). Flow cytometry detection of serotonin content and release in resting and activated platelets. Br J Haematol 121: 892–896.

González-Scarano F, Baltuch G (1999). Microglia as mediators of inflammatory and degenerative diseases. Annu Rev Neurosci 22: 219–240.

Grace PM, Hutchinsons MR, Maier SF, Watkins LR (2014). Pathological pain and the neuroimmune interface. Nat Rev Immunol 14: 217-231.

Hanisch UK, Kettenmann H (2007). Microglia: active sensor and versatile effector cells in the normal and pathologic brain. Nat Neurosci 10: 1387–1394.

Hillard CJ, Shanmugam M, Kearn CS (1999). Effects of $CB_1$ cannabinoid receptor activation on cerebellar granule cell nitric oxide synthase activity. FEBS Lett 459: 277–281.

Horvath RJ, Nutile-McMenemy N, Alkaitis MS, Deleo JA (2008). Differential migration, LPS-induced cytokine, chemokine, and NO expression in immortalized BV-2 and HAPI cell lines and primary microglial cultures. J Neurochem 107: 557–569.

Howlett AC (2005). Cannabinoid receptor signaling. Handb Exp Pharmacol 168: 53–79.

Howlett AC, Barth F, Bonner TI, Cabral G, Casellas P, Devane WA, Felder CC, Herkenham M, Mackie K, Martin BR, Mechoulam R, Pertwee RG (2002). International Union of Pharmacology. XXVII. Classification of cannabinoid receptors. Pharmacol Rev 54: 161–202.

Hsieh GC, Pai M, Chandran P, Hooker BA, Zhu CZ, Salyers AK, Wensink EJ, Zhan C, Carroll WA, Dart MJ, Yao BB, Honore P, Meyer MD (2011). Central and peripheral sites of action for $CB_2$ receptor mediated analgesic activity in chronic inflammatory and neuropathic pain models in rats. Br J Pharmacol 162: 428–440.

Jeon YJ, Yang KH, Pulaski JT, Kaminsky ND (1996). Attenuation of inducible nitric oxide synthase gene expression by delta 9-tetrahydrocannabinol is mediated through the inhibition of nuclear factor-kappa B/Rel activation. Mol Pharmacol 50: 334–341.

Jung WK, Lee DY, Park C, Choi YH, Choi I, Park SG, Seo SK, Lee SW, Yea SS, Ahn SC, Lee CM, Park WS, Ko JH, Choi IW (2010). Cilostazol is anti-inflammatory in BV2 microglial cells by inactivating nuclear factor-kappaB and inhibiting mitogen-activated protein kinases. Br J Pharmacol 159: 1274–1285.

Klegeris A, Bissonnette CJ, McGeer PL (2003). Reduction of human monocytic cell neurotoxicity and cytokine secretion by ligands of the cannabinoid-type $CB_2$ receptor. Br J Pharmacol 139: 775–786.

Klein TW, Newton CA (2007). Therapeutic potential of cannabinoid-based drugs. Adv Exp Med Biol 601: 395–413.

Kreitzer FR, Stella N (2009). The therapeutic potential of novel cannabinoid receptors. Pharmacol Ther 122: 83–96.

Lehnardt S, Lachance C, Patrizi S, Lefebvre S, Follett PL, Jensen FE, Rosenberg PA, Volpe JJ, Vartanian T (2002). The toll-like receptor TLR4 is necessary for lipopolysaccharide-induced oligodendrocyte injury in the CNS. J Neurosci 22: 2478–2486.

Ma L, Jia J, Liu X, Bai F, Wang Q, Xiong L (2015). Cannabinoid $CB_2$ receptor agonist AM1241 attenuates microglial activation by modulating the activated state in N9 microglia exposed to LPS plus IFNγ. Biochem and Biophysic Res Com in press.

Lourbopoulos A, Grigoriadis N, Lagoudaki R, Touloumi O, Polyzoidou E, Mavromatis I, Tascos N, Breuer A, Ovadia H, Karussis D, Shohami E, Mechoulam R, Simeonidou C (2011). Administration of 2-arachidonoylglycerol ameliorates both acute and chronic experimental autoimmune encephalomyelitis. Brain Res 1390: 126–141.

Marrs WR, Blankman JL, Horne EA, Thomazeau A, Lin YH, Coy J, Bodor AL, Muccioli GG, Hu SS, Woodruff G, Fung S, Lafourcade M, Alexander JP, Long JZ, Li W, Xu C, Möller T, Mackie K, Manzoni OJ, Cravatt BF, Stella N (2010). The serine hydrolase ABHD6 controls the accumulation and efficacy of 2-AG at cannabinoid receptors. Nat Neurosci 13: 951–957.

Massi P, Solinas M, Cinquina V, Parolaro D (2013). Cannabidiol as potential anticancer drug. Br J Clin Pharmacol 75(2): 303-312.

Merighi S, Benini A, Mirandola P, Gessi S, Varani K, Leung E, Maclennan S, Borea PA (2005). $A_3$ adenosine receptor activation inhibits cell proliferation via phosphatidylinositol 3-kinase/Akt-dependent inhibition of the extracellular signal-regulated kinase 1/2 phosphorylation in A375 human melanoma cells. J Biol Chem 280: 19516–19526.

Merighi S, Benini A, Mirandola P, Gessi S, Varani K, Simioni C, Leung E, Maclennan S, Baraldi PG, Borea PA (2007). Caffeine inhibits adenosine-induced accumulation of hypoxia-inducible factor-1alpha, vascular endothelial growth factor, and interleukin-8 expression in hypoxic human colon cancer cells. Mol Pharmacol 72: 395–406.

Merighi S, Simioni C, Gessi S, Varani K, Mirandola P, Tabrizi MA, Baraldi PG, Borea PA (2009). $A_{2B}$ and $A_3$ adenosine receptors modulate vascular endothelial growth factor and interleukin-8

expression in human melanoma cells treated with etoposide and doxorubicin. Neoplasia 11: 1064–1073.

Merighi S, Simioni C, Gessi S, Varani K, Borea PA (2010). Binding thermodynamics at the human cannabinoid $CB_1$ and $CB_2$ receptors. Biochem Pharmacol 79: 471–477.

Merighi S, Gessi S, Varani K, Fazzi D, Borea PA (2012). Hydrogen sulfide modulates the release of nitric oxide and VEGF in human keratinocytes. Pharmacol Res 66:428-436.

Molina-Holgado F, Molina-Holgado E, Guaza C, Rothwell NJ (2002). Role of $CB_1$ and $CB_2$ receptors in the inhibitory effects of cannabinoids on lipopolysaccharide-induced nitric oxide release in astrocyte cultures. J Neurosci Res 67: 829–836.

Mukhopadhyay S, Das S, Williams EA, Moore D, Jones JD, Zahm DS, Ndengele MM, Lechner AJ, Howlett AC (2006). Lipopolysaccharide and cyclic AMP regulation of $CB_2$ cannabinoid receptor levels in rat brain and mouse RAW 264.7 macrophages. J Neuroimmunol 181: 82–92.

Murphy S (2000). Production of nitric oxide by glial cells: regulation and potential roles in the CNS. Glia 29: 1–13.

Oh YT, Lee JY, Lee J, Lee JH, Kim JE, Ha J, Kang I. (2010). Oleamide suppresses lipopolysaccharide-induced expression of iNOS and COX-2 through inhibition of NF-kappaB activation in BV2 murine microglial cells. Neurosci Lett 474: 148–153.

Ortega-Gutiérrez S, Molina-Holgado E, Guaza C (2005). Effect of anandamide uptake inhibition in the production of nitric oxide and in the release of cytokines in astrocyte cultures. Glia 52: 163–168.

Pertwee RG, Howlett AC, Abood ME, Alexander SP, Di Marzo V, Elphick MR, Greasley PJ, Hansen HS, Kunos G, Mackie K, Mechoulam R, Ross RA (2010). International Union of Basic and Clinical Pharmacology. LXXIX. Cannabinoid receptors and their ligands: beyond $CB_1$ and $CB_2$. Pharmacol Rev 62: 588–631.

Pietr M, Kozela E, Levy R, Rimmerman N, Lin YH, Stella N, Vogel Z, Juknat A (2009). Differential changes in GPR55 during microglial cell activation. FEBS Lett 583: 2071–2076.

Romero-Sandoval EA, Horvath R, Landry RP, DeLeo JA (2009). Cannabinoid receptor type 2 activation induces a microglial anti-inflammatory phenotype and reduces migration via MKP induction and ERK dephosphorylation. Mol Pain 5: 25.

Ross RA, Brockie HC, Pertwee RG (2000). Inhibition of nitric oxide production in RAW 264.7 macrophages by cannabinoids and palmitoylethanolamide. Eur J Pharmacol 401: 121–130.

Sheng WS, Hu S, Min X, Cabral GA, Lokensgard JR, Peterson PK (2005). Synthetic cannabinoid WIN55,212-2 inhibits generation of inflammatory mediators by IL-1beta-stimulated human astrocytes. Glia 49: 211–219.

Stefano GB, Liu Y, Goligorsky MS (1996). Cannabinoid receptors are coupled to nitric oxide release in invertebrate immunocytes, microglia, and human monocytes. J Biol Chem 271: 19238–19242.

Stella N (2010). Cannabinoid and cannabinoid-like receptors in microglia, astrocytes, and astrocytomas. Glia 58: 1017–1030.

Waksman Y, Olson JM, Carlisle SJ, Cabral GA (1999). The central cannabinoid receptor $CB_1$ mediates inhibition of nitric oxide production by rat microglial cells. J Pharmacol Exp Ther 288: 357–366.

Walter L, Franklin A, Witting A, Wade C, Xie Y, Kunos G, Mackie K, Stella N (2003). Nonpsychotropic cannabinoid receptors regulate microglial cell migration. J Neurosci 23: 1398–1405.

Wang MJ, Kuo JS, Lee WW, Huang HY, Chen WF, Lin SZ (2006). Translational event mediates differential production of tumor necrosis factor-alpha in hyaluronan-stimulated microglia and macrophages. J Neurochem 97: 857–871.

# Cannabinoid $CB_2$ receptor attenuates morphine-induced inflammatory responses in activated microglial cells

# Introduction

## Interactions between opioids and cannabinoids

Opioids and cannabinoids are two classes of drugs that share numerous similar pharmacological effects, including sedation, analgesia, euphoria, inhibition of the intestinal motility, locomotor activity, and suppression of immune function. However, the most important interactions were found in antinociception and, to lesser extent, in drug reinforcement (Manzanares et al., 1999).

Opioids constitute a large family of compounds with different chemical natures (from peptides to alkaloids). They produce their pharmacological effects by acting mainly through three types of receptors, namely μ, δ and κ (Satoh and Minami, 1995; receptor nomenclature follows Alexander et al., 2011). They bind endogenous opioid peptides including enkephalins, endorphins and dynorphins. In clinical practice, opioids are considered mainly as analgesics; however, they play an important role as neuroregulators of a number of central and peripheral tissues, including immunomodulation, respiration, behavior, and gastrointestinal motility. Pharmacological overdosing may result in side effects that include respiratory depression, miosis, serenity, urinary retention, vomiting, pruritus, dyspnea, sedation, euphoria, dysphoria, or psychomimetic effects (Lazarczyk et al., 2010). Opioids are the drugs of choice for treating severe pain, despite the development of tolerance, dependence and hyperalgesia (da Fonseca Pacheco et al., 2008). The cellular and molecular mechanisms involved in this phenomenon are complex and may involve receptor desensitization and endocytosis, intracellular signalling hyperactivity, secondary activation of excitatory amino acid receptors, and subsequent intracellular cascades as well as glial activation and the release of proinflammatory mediators (Mayer et al., 1999; Watkins et al., 2005). Glial activation by opioids is an important phenomenon to understand, as it opposes opioid analgesia and enhances opioid tolerance, dependence and other negative side-effects, such as respiratory depression (Watkins et al., 2009). In particular, there is good evidence that glia and glia-derived proinflammatory mediators, such as IL-1β, TNF-α, and IL-6, could be involved in tolerance to anti-nociceptive properties of morphine. Glial cells are also considered to be crucial sources of nitric oxide (NO), responsible for morphine tolerance (Mayer et al., 1999; Chen and Sommer, 2009). Repeated morphine treatment can activate glia and hence up-regulate these various mediators (Raghavendra et al., 2002; 2004; Johnston et al., 2004; Watkins et al., 2005) through the MAPK, PKC and PI3K/Akt pathways, key players in the intracellular signalling cascade leading to the

development of morphine tolerance (Mayer et al., 1999; Watkins et al., 2001; Raghavendra et al., 2002, 2004; Galeotti et al., 2006; Cunha et al., 2010).

In the nervous system, neurotransmission and neuroinflammation are mediated by the endocannabinoid signalling system (Fernández-Ruiz, 2009; Marrs et al., 2010). To date, two cannabinoid receptors have been identified by molecular cloning - $CB_1$ and $CB_2$ receptors. The $CB_1$ receptors are expressed by the neurons and regulate the release of neurotransmitters, while $CB_2$ receptors are expressed by the microglia, regulating their motility and immunomodulator production (Atwood and Mackie, 2010; Pertwee et al., 2010). In the nervous system, activation of $CB_1$ and $CB_2$ receptors is induced by the endocannabinoids, arachidonoylethanolamide (anandamide, AEA) and 2-arachidonoylglycerol produced by the neurons and glia (Massi et al., 2013). However, ample evidence suggests that additional receptors may contribute to the behavioral, vascular and immunological actions of $\Delta^9$-tetrahydrocannabinol (THC), the major psychoactive constituent of marijuana, and endocannabinoids (Begg et al., 2005). In particular, it has been established that GPR55 is an additional novel cannabinoid receptor (Lauckner et al., 2008; Bondarenko 2014).

Microglia, a specialized population of macrophages found in the CNS, are quiescent in normal brain. However, after CNS injury or after interaction of LPS with toll-like receptor (TLR)-4 during bacterial infection (González-Scarano and Baltuch, 1999), these cells can be activated by cytokines produced by infiltrating immune effector cells. Activated microglia can promote neuroinflammatory response throught the release of inflammatory mediators, including IL-1β, TNF-α, prostaglandin $E_2$ ($PGE_2$), and NO (Grace et al., 2014). Thus, LPS stimulation of the microglia is a useful model for the study of mechanisms underlying neuronal injury by various proinflammatory and neurotoxic factors released by activated microglia (Jung et al., 2010).

CB receptor agonists produce pain relief in a variety of animal models (Richardson, 2000). Cannabinoids act on glia and neurons to inhibit the release of proinflammatory molecules, including IL-1β, TNF-α, and NO (Molina-Holgado et al., 1997; 2002; Shohami et al., 1997; Puffenbarger et al., 2000; Cabral et al., 2001), and enhance the release of the anti-inflammatory cytokines IL-4, IL-10 (Klein et al., 2000), and IL-1 receptor antagonist (Molina-Holgado et al., 2003). It is known that the anti-inflammatory properties of CB receptor agonists are expressed through the activation of $CB_2$ receptors (Klein and Newton, 2007; Romero-Sandoval et al., 2009; Correa et al., 2010; Hsieh et al., 2011). In particular, the activation of $CB_2$ receptors expressed in brain microglia during neuroinflammation (Benito et al., 2008; Atwood and Mackie, 2010) reduced NO production and TNF-α in primary microglia (Ehrhart et al., 2005; Merighi et al., 2012a). Furthermore, such activation protects against human microglial neurotoxicity by enhancing IL-10 production (Klegeris et al., 2003; Correa et al., 2005; 2010; Eljaschewitsch et al., 2006). The activation of $CB_2$ receptors

also reduces the release of proinflammatory factors in animal models of peritoneal hypoxia-ischemia and Huntington's disease (Benito et al., 2008). In the periphery, both $CB_1$ and $CB_2$ receptors participate in pain control (Malan et al., 2001).

Interestingly, receptors for opioids and cannabinoids are coupled to similar intracellular signalling mechanisms, leading to a decrease in cAMP production through the activation of $G_i$ proteins (Satoh and Minami, 1995; Pertwee et al., 2010). Therefore, following the discovery that opioids and cannabinoids produce not only similar biochemical effects but also similar pharmacological effects, the interaction between these two classes of drugs has been studied (Manzaneres et al., 1999). Cannabinoids can enhance the antinociceptive properties of opioids (Cichewicz, 2004; Wilson et al., 2008; Parolaro et al., 2010) and adolescent exposure to chronic THC blocks opiate dependence in maternally deprived rats (Morel et al., 2009). However, the molecular signalling underlying the participation of cannabinoids in the side effects induced by opioids is still unknown. Nevertheless, it is possible that cannabinoids may interfere with the tolerance and dependence effects induced by opioids because the administration of low-dose combinations of cannabinoids and opioids seems to be an alternative regimen that reduces the need to escalate opioid dose, while increasing opioid potency.

Therefore, the aim of the present study was to explore whether and how $CB_2$ receptor stimulation affected opioid actions on activated microglia, with a view to improving pain control by increasing the clinical efficacy of opioids.

# Materials and Methods

## Animals

All animal care and experimental procedures conformed to the guidelines issued by the European Council (86/609/EEC) and were approved by the local Animal Care and Ethics Committee. The results of all studies involving animals are reported in accordance with the ARRIVE guidelines for reporting experiments involving animals (McGrath et al., 2010). One-day-old Balb/c mice (50 in total) were obtained from Charles River (Calco, Italy).

## Cell line, reagents and antibodies

CHO cells transfected with the human recombinant $CB_2$ receptor cDNA (CHO-hCB2) were purchased from PerkinElmer (Milan, Italy). Tissue culture media and growth supplements were obtained from Cambrex, Bergamo, Italy. U0126 (MEK-1 and MEK-2 inhibitor, soluble in DMSO); human anti-ACTIVE®MAPK (phosphorylated $Thr^{183}/Tyr^{185}$) and human anti-ERK1/2 pAb were provided by Promega (Milan, Italy). Phosphorylated ($Thr^{180/}Tyr^{182}$) and total p38, phosphorylated ($Thr^{183}/Tyr^{185}$) and total JNK1/2 antibodies were from Cell Signalling Technology (Celbio, Milan, Italy). JWH-015 (1-propyl-2-methyl-3-(1-naphthoyl)indole) (soluble in ethanol), SH5 (inhibitor of Akt), blocking peptide for pAb to $CB_2$ receptor (ALX-153-027) and anti-$CB_2$ receptor rabbit polyclonal antibody (ALX-210-198) were from Enzo Life Sciences (Vinci-Biochem, Florence, Italy). The immunogen for the $CB_2$ receptor antibody was a synthetic peptide corresponding to aa 20–33 of the human $CB_2$ receptor N-terminal. Anti-MOR-1 (H80) (sc-15310), small interfering RNA (siRNA) for the $CB_2$ receptor (sc-39913) and MOR-1 siRNA (sc-35958) were from Santa Cruz Biotechnology (DBA, Milan, Italy). AM 251 (*N*-(piperidin-1-yl)-1-(2,4-dichlorophenyl)-5-(4-iodophenyl)-4-methyl-1H-pyrazole-3-carboxamide) and AM 630 (6-iodo-2-methyl-1-[2-(4-morpholinyl)ethyl]-1H-indol-3-yl](4-methoxyphenyl)methanone (6-iodopravadoline) (both soluble in DMSO) were from Tocris Bioscience (Bristol, UK). RNAiFect™ Transfection Kit was from Qiagen (Milan, Italy). Unless otherwise stated, all other chemicals were purchased from Sigma (Milan, Italy). Drug and molecular target nomenclature conforms to Alexander et al., 2013.

## Primary microglial cell cultures

Primary glial cultures were prepared as described in a previous study (Molina-Holgado et al., 2002). Briefly, after anesthesia (Zoletil 100, 30 $mg \cdot kg^{-1}$, Virbac Laboratories, Carros, France) and decapitation, forebrains from newborn Balb/c mice were excised, meninges removed and tissue dissociated mechanically. Cells were re-suspended in DMEM supplemented with 10% heat-inactivated FBS and 1% penicillin/streptomycin, then plated on poly-D-lysine-coated (5 $\mu g \cdot mL^{-1}$) 75 $cm^2$ flasks (Falcon; Celbio, Milan, Italy). After 15 days, the flasks were shaken vigorously to remove loosely adherent microglia. The supernatant was plated on multi-well culture plates for 2 h, and the medium was changed to remove non-adherent cells. Cells were grown in a humidified environment containing 5% $CO_2$ at a constant temperature of 37°C. The purity of microglial cultures was assessed by examining cell morphology under phase-contrast microscopy, and was confirmed by flow cytometry with Mac-1 anti-CD11b antibody (BD Pharmingen, Milan, Italy).

## Cell cultures

Cells were maintained in DMEM (primary microglia) or Ham's (CHOh-$CB_2$ cells) medium containing 10% fetal calf serum, penicillin (100 $U \cdot mL^{-1}$), streptomycin (100 $\mu g \cdot mL^{-1}$), and L-glutamine (2 mM) at 37°C in 5% $CO_2$/95% air. Geneticin (G418, 0.4 $mg \cdot mL^{-1}$) was added to CHO-h$CB_2$ cells. Cells were split two or three times weekly at a ratio between 1:5 and 1:10.

## Flow cytometry of primary microglial cells

Aliquots of 0.5 x $10^6$ cells were incubated for 40 min at 4°C with either specific phycoerythrin (PE)-labelled antibodies, or isotype-matched irrelevant IgG-PE (Beckman Coulter, Fullerton, CA, USA) as negative control. Cells were washed with PBS and characterized for CD11b and glial fibrillary acidic protein (GFAP) expression by flow cytometry with PE-labelled anti-CD11b MoAb (BD Pharmingen) and the fluorescein isothiocyanate (FITC)-labelled anti-GFAP MoAb (BD Pharmingen). In particular, GFAP immunophenotyping was performed in permeabilized cells, using IntraPrep™ fixing/permeabilization reagent (Beckman Coulter) (Gobbi et al., 2003). Analysis was performed on an Epics XL flow cytometer (Beckman Coulter) using Expo ADC software (Beckman Coulter).

## Primary microglial cell exposure to cannabinoids, opioids and LPS treatment

LPS, a cell wall component of Gram-negative bacteria, is a potent activator of glia. Hence, microglial cells were treated with 1 $\mu g \cdot mL^{-1}$ LPS (from *Escherichia coli*, serotype 055:B5) (soluble in cell culture medium) before commencing incubation with CB and opioid receptor ligands. Unless otherwise stated, the concentration of morphine (Salars, Como, Italy), naloxone, Tyr-DAla-Gly-[NMePhe]-$NH(CH_2)_2$ (DAMGO), cyc[$DPen^2$, $DPen^5$]enkephalin (DPDE), 5α,7α, 8β- (-) -N-methyl-N-(7-[1-pyrrolidinyl]-1-oxasipro(4,5)dec-8-yl)benzeneacetamide (U69593), D-Phe-cyc[Cys-Tyr-D-Trp-Arg-Thr-Pen]-Thr-$NH_2$ (CTAP), JWH-015 (Enzo Life Sciences, Vinci-Biochem, Vinci, Florence, Italy), AM 630 and AM 251 was 100 nM, which is the ligand concentration able to occupy 99% of the receptors at equilibrium. Microglia were then maintained in DMEM containing cannabinoids, opioids or their vehicle, and harvested after treatment at the indicated times.

## Nitrite assay for primary microglial cells

NO synthase activity was assessed indirectly by measuring nitrite ($NO_2^-$) accumulation in the cell culture media using a colorimetric kit (Calbiochem, Milan, Italy). At the end of the treatment period, the nitrite concentration in the conditioned media was determined according to a modified Griess method (Merighi et al., 2012b). Briefly, the NADH-dependent enzyme nitrate reductase was used to convert the nitrate to nitrite prior to quantification of the absorbance, measured at 540 nm by a spectrophotometric microplate reader (Fluoroskan Ascent Labsystems, Stockholm, Sweden). Values were obtained by comparison with reference concentrations of sodium nitrite.

## ELISA

The levels of IL-1β, TNF-α and IL-6 protein secreted by the cells in the medium were determined by ELISA kits (R&D Systems). In brief, subconfluent cells were changed into fresh medium in the presence of solvent or various concentrations of drugs. The medium was collected, and IL-1β, TNF-α and IL-6 protein concentrations were measured by ELISA according to the manufacturer's instructions. The results were normalized to the number of cells per plate. The data are presented as mean ± SE from four independent experiments performed in triplicate.

## Western blotting for primary microglial cells

Western blot assay was performed as previously described (Merighi et al., 2009). Aliquots of total protein sample (50 μg) were analysed using antibodies specific for phosphorylated or total p44/p42 MAPK (1:5000 dilution), phosphorylated or total p38 (1:1000 dilution), phosphorylated or total JNK1/2 (1:1000 dilution), phosphorylated or total Akt (1:1000 dilution), for $CB_2$ and μ-opioid receptors. Specific reactions were revealed with enhanced chemiluminescence Western blotting detection reagent (Amersham Corp., Arlington Heights, IL, USA). The membranes were then stripped and re-probed with tubulin (1:250) to ensure equal protein loading.

## Densitometry analysis

The intensity of each immunoblot assay band was quantified using a VersaDoc Imaging System (Bio-Rad, Milan, Italy). Mean densitometric data from independent experiments was normalized to the results obtained with control cell cultures. The ratio of phospho-protein to total protein was reported in a densitometric analysis.

## Treatment of primary microglial cells with siRNA

Microglial cells were plated in six-well plates and grown to 50–70% confluence before transfection. Transfection of $siRNA_{CB2}$ or $siRNA_{\mu}$ was performed at a concentration of 100 nM using RNAiFect™ Transfection Kit (Qiagen). Cells were cultured in complete media and total proteins were isolated at 24, 48 and 72 h for Western blot analysis of $CB_2$ and μ-opioid receptor protein. A randomly chosen non-specific siRNA was used under identical conditions as control (Merighi et al., 2005; 2007).

## Statistical analysis

All data are reported as mean ± SEM of independent experiments and are indicated in the figure legends. Each experiment was performed by using the microglial cells derived from one single mouse, and was performed in triplicate. The experiments were repeated at least four times as

indicated from n values that represent the number of mice used. Data sets were examined by ANOVA for comparisons between multiple groups and Dunnett's test for comparing a control group to all other groups (when necessary). A P value $< 0.05$ was considered statistically significant.

# Results

## $CB_2$ and μ-opioid receptor expression in primary mouse microglial cells

The expression of the myeloid cell surface antigen CD11b was analyzed in primary microglial cells by flow cytometry. Cells were treated with specific MoAbs or isotype-matched irrelevant MoAbs. Microglia were negative for the astrocyte-specific protein GFAP but showed significant positive staining for CD11b, as compared to the isotype control, thereby indicating high expression levels of the microglial cell marker CD11b (Figure 11A).

The expression of $CB_2$ receptors in CHO-h$CB_2$ cells (used as positive control), in quiescent and LPS-activated primary microglial cells is shown in Figure 11B. The molecular weight of the protein detected in these cells was 50 kDa, comparable with the calculated molecular weight of $CB_2$ receptors. To ascertain the specificity of the $CB_2$ receptor antibody used in Western blots, antigen preabsorption experiments were carried out with the corresponding blocking peptide. Co-incubation with the immunizing peptide completely prevented the signal (data not shown). $CB_2$ receptor protein expression was not modified by 30-min treatment with 1 $\mu g \cdot mL^{-1}$ LPS (Figure 11B). Similarly, the expression of μ-opioid receptors in mouse brain extracts (used as positive control) in quiescent and LPS-activated primary microglial cells is shown in Figure 11B. Therefore, $CB_2$ and μ-opioid receptors were expressed in primary mouse microglial cells. To evaluate whether LPS induced changes in $CB_2$ receptor expression, we assayed $CB_2$ receptors over 24 h of LPS treatment. In agreement with published data (Carlisle et al., 2002), LPS 1 $\mu g \cdot mL^{-1}$ produced a time-dependent increase in $CB_2$ receptor expression over the period from 6 to 24 h (Figure 11C).

## Effect of opioid receptor ligands on cytokine and nitrite production in primary microglial cells

To investigate the effect of opioid receptor ligands on microglial activation, the ability of morphine to induce inflammatory mediator production, such as IL-1β, TNF-α, IL-6 and nitrite, was examined in LPS-stimulated microglial cells. The TLR-4 agonist LPS was used to induce IL-1β, TNF-α, IL-6 and NO (as nitrite) release from primary microglial cells. Preliminary studies in our laboratory demonstrated that LPS induced release of these mediators from primary microglial cells in a

concentration-dependent manner, with maximum release occurring at a concentration of 1 $\mu g \cdot mL^{-1}$ (data not shown). As shown in Figure 12, non-stimulated microglial cells showed a very low level of IL-1β, TNF-α, IL-6 and nitrite but LPS triggered a robust increase in the release of these mediators into the culture media. Then, we went on to investigate how the activation of opioid receptors interferes with the signaling pathways modulated by LPS by maintaining primary microglial cells in LPS-supplemented (1 $\mu g \cdot mL^{-1}$) DMEM in combination with the opioid receptor agonist morphine (100 nM) for 24 h. As shown in Figure 12, LPS-induced cytokine and nitrite release was significantly increased in the presence of morphine in primary microglial cells. The stimulatory response of morphine on cytokine and nitrite production was reversed in the presence of the broad-range opioid receptor-antagonist naloxone (Figure 12). Furthermore, DAMGO (100 nM), a μ-opioid receptor-selective agonist, mimicked the effects of morphine on microglial cytokine and nitrite induction (Figure 12). Conversely, DPDPE and U-69593, δ- and κ-receptor-selective agonists, respectively, had no effect on LPS-induced microglial cytokine and nitrite production (Figure 12). Finally, pretreatment of microglial cells with CTAP (100 nM), a selective antagonist of μ-opioid receptors, before treatment with morphine (100 nM) or DAMGO (100 nM), abolished the effects of opioid receptor agonists on LPS-induced cytokine and nitrite production by microglia (Figure 12).

## Influence of $CB_2$ receptors on μ-opioid receptor-induced cytokine and nitrite production in primary microglial cells

The effect of $CB_2$ receptor stimulation on μ-opioid receptor induced cytokine and nitrite production in primary microglial cells was studied using JWH-015, a CB receptor agonist known to bind more readily to $CB_2$ than $CB_1$ receptors (Merighi et al., 2010). By this means we tested whether $CB_2$ receptors can modulate cytokine and nitrite production in activated microglial cells. As shown in Figure 13, JWH-015 (100 nM) significantly decreased LPS-induced IL-1β, TNF-α, IL-6 and nitrite levels. Furthermore, co-administration of LPS (1 $\mu g \cdot mL^{-1}$), morphine (100 nM) and JWH-015 (100 nM) significantly attenuated the morphine-induced increases in cytokine and nitrite production (Figure 13). The anti-inflammatory response of JWH-015 in LPS-activated microglial cells treated with morphine was reversed in the presence of the $CB_2$ receptor antagonist AM 630 (100 nM) (Figure 13). In contrast, the $CB_1$ antagonist AM 251 (100 nM) did not affect the ability of JWH-015 to down-regulate the increase in IL-1β, TNF-α, IL-6 and nitrite induced by morphine in LPS-activated microglial cells (Figure 13).

## Signalling induced by morphine on quiescent and activated microglial cells

We went on to investigate whether the stimulatory effect of morphine on cytokine and nitrite release induced by LPS is mediated via the MAPK and Akt pathways. We tested whether morphine could induce ERK1/2, p38, JNK1/2 and Akt phosphorylation in primary murine microglial cells, treated for 30 min at 37°C, in a concentration-dependent manner. As shown in Figure 14A, morphine (1–1000 nM) increased p-ERK1/2 and pAkt expression levels but did not modulate pp38 and pJNK1/2. In particular, morphine (100 nM) induced a rapid and sustained (up to 60 min) stimulation of ERK1/2 and pAkt (Figure 14B). Furthermore, we have investigated how the activation of microglial cells interferes with the signalling pathways modulated by morphine. Thus, microglial cells were maintained in DMEM containing LPS (1 $\mu g \cdot mL^{-1}$), and the ability of morphine (100 nM) to modulate ERK1/2 and Akt phosphorylation was evaluated at 15, 30 and 60 min. As shown in Figure 14B, LPS stimulation of microglial cells resulted in a rapid (15 min) increase in ERK1/2 and Akt phosphorylation, which was maximal at 30 min and declined towards basal levels within 60 min. In the presence of morphine (100 nM), ERK1/2 and Akt phosphorylation were significantly higher than LPS alone. To evaluate whether the morphine-induced changes in ERK1/2 and Akt phosphorylation levels were μ-opioid receptor-dependent, we used the selective antagonist of μ-opioid receptors, CTAP. Primary microglial cells were pretreated with CTAP, then exposed to morphine for 30 min. Morphine-induced p-ERK1/2 and p-Akt increased levels were reduced with CTAP pretreatment (Figure 14C), indicating that the effect of morphine was mediated via the μ-opioid receptor subtype.

## Signalling induced by morphine and JWH-015 on LPS-activated microglial cells

Primary microglial cells were treated with either LPS alone, LPS + JWH-015 (100 nM) or LPS + morphine (100 nM) for 30 min. As shown in Figure 15, LPS significantly increased all kinases measured. Furthermore, while the $CB_2$ receptor agonist JWH-015 failed to modulate the activity of LPS on p38 and JNK1/2, it significantly decreased ERK1/2 and Akt phosphorylation levels in LPS-activated cells (Figure 15). Similarly, the phosphorylation of ERK1/2 and Akt were significantly increased by morphine (100 nM) added LPS-activated cells, compared with treatment with LPS alone. In contrast, morphine did not modulate LPS-induced phosphorylation of p38 and JNK (Figure 15). Finally, when microglial cells were treated with LPS (1 $\mu g \cdot mL^{-1}$) plus morphine (100 nM) in combination with JWH-015 (100 nM), we found that JWH-015 decreased ERK1/2 and Akt

activation induced by LPS plus morphine, without affecting pp38 and pJNK1/2 levels (Figure 15). The effect of morphine and JWH-015 on ERK1/2 and Akt activation was reversed in the presence of the antagonists naloxone and AM 630 respectively (Figure 16). In contrast, the $CB_1$ receptor antagonist AM 251 (100 nM) did not reverse the ability of JWH-015 to down-regulate the increase in p-ERK1/2 and p-Akt induced by morphine (Figure 16).

## Akt and MEK-1/2 inhibition decreases LPS-induced inflammatory effects in microglial cells

To elucidate the mechanisms involved in the effects of morphine and JWH-015 on citokine and nitrite production by activated microglial cells, we investigated the effects of inhibiting ERK1/2 or Akt signalling pathways, with the MEK1/MEK2 inhibitor U0126 (1 μM) or the Akt inhibitor SH-5 ( 1 μM). To confirm the activity of these inhibitors, primary microglial cells were treated with U0126 (1 μM) and with SH-5 (1 μM) for 30 min and ERK-1/2 or Akt activation were measured. We observed that 30 min incubations of microglial cells with either U0126 or SH-5 resulted in significant decreases in active ERK-1/2 or Akt respectively, when compared with control cells incubated for 30 min with DMSO (U0126 = 32 ± 5% of control; n = 3; SH-5 = 28 ± 3% of control; n = 3). As shown in Figure 17, U0126 significantly reduced the production of TNF-α, IL-6 and nitrite induced by LPS-stimulated microglial cells. Similarly, the inhibition of the Akt pathway, by SH-5 (1 μM), resulted in a significant reduction of TNF-α, IL-6 and nitrite levels (Figure 17). However, while LPS-induced expression of IL-1β was significantly reduced by addition of SH-5, IL-1β expression was not affected by U0126 in LPS-treated microglia (Figure 17). These results suggest that ERK and Akt could mediate the enhancing effects of LPS on TNF-α, IL-6 and nitrite induction. In contrast, while the Akt pathway was involved in LPS-induced IL-1β production, the ERK pathway was not implicated.

## $CB_2$ and μ-opioid receptor gene silencing in microglial cells

To confirm the apparent role of $CB_2$ receptors and to investigate the involvement of μ-opioid receptors, we reduced $CB_2$ and μ-opioid receptor expression in primary microglial cells by siRNA transfection, in order to cause transient knockdown of the $CB_2$ and μ-opioid receptor genes. Primary microglial cells were transfected with non-specific random control ribonucleotides (siRNA

scramble, $siRNA_{ctr}$) or with small interfering RNAs that target $CB_2$ or μ-opioid receptor mRNAs ($siRNA_{CB2}$ or $siRNA_{\mu}$, respectively) for degradation.

As shown in Figure 18, $CB_2$ and μ-opioid receptor protein expression were strongly reduced after 48 and 72 h of treatment with $siRNA_{CB2}$ and $siRNA_{\mu}$ respectively. Therefore, 48 h after $siRNA_{CB2}$ or $siRNA_{\mu}$ transfection, primary microglial cells were treated with either LPS (1 $\mu g \cdot mL^{-1}$), JWH-015 (100 nM) or morphine (100 nM), alone and in combination, for 30 min, after which ERK1/2- and Akt-phosphorylated protein levels were measured. This revealed that inhibition of $CB_2$ receptor expression was sufficient to block the JWH-015 induced inhibition of ERK1/2 and Akt phosphorylation levels, increased by morphine in LPS-treated microglia (Figure 19). Furthermore, inhibition of the expression of μ-opioid receptors blocked morphine-induced increases in pERK1/2 and pAkt in microglia (Figure 19). These results clearly show the connection between $CB_2$ receptor stimulation, morphine, ERKs and Akt signalling in activated primary microglial cells.

We also measured cytokine and nitrite levels in microglial cells in which $CB_2$ or μ-opioid receptors were down-regulated. We found that, in microglial cells with μ-opioid receptors down-regulated, morphine did not significantly increase IL-1β, TNF-α, IL-6 and nitrite protein levels when compared to LPS. Similarly, the $CB_2$ agonist JWH-015 did not significantly reduce cytokine and nitrite levels in microglial cells with down-regulated $CB_2$ receptors, compared with those after LPS alone (Figure 20).

# Discussion and Conclusions

The presence of opioid receptors on glia and the ability of morphine to prime microglia for enhanced production of proinflammatory cytokines supports a possible direct interaction of morphine with glial cells (Chao et al., 1994). As microglial differentiation and immune function is regulated by activation of $CB_2$ receptors (Stella, 2010), we set out to characterize the signalling pathways modulated by both μ-opioid and $CB_2$ receptors expressed in microglial cells. $CB_2$ and μ-opioid receptor ligands (agonist and antagonist) and $CB_2$- and μ-opioid receptor-knockout microglial cells were used to determine the role of the CB and opioid system in primary microglial cells. We have described the mechanisms by which $CB_2$ and opioid receptors modulate the MAPK signal response to LPS, an agent widely used experimentally to create inflammation in the brain (Lehnardt et al., 2002).

In this study, we demonstrated that (1) morphine enhanced the release of NO and the proinflammatory cytokines, IL-1β, IL-6, TNF-α, from activated microglial cells; (2) $CB_2$ receptor stimulation attenuated morphine-induced microglial proinflammatory mediator increases; (3) morphine-induced microglial proinflammatory mediator increases were μ-opioid receptor dependent; and (4) $CB_2$ receptor stimulation interfered with morphine action by acting on Akt-ERK1/2 signalling. Together, these results suggest that $CB_2$ receptors are critical to the activity of microglia, opposing the morphine-induced release of NO and cytokines from microglial cells. Therefore, we suggest a novel interaction between μ-opioid- and $CB_2$-receptor systems in microglia, which is likely to be mediated via the Akt/ERK1/2 pathways.

The influence of $CB_2$ receptor stimulation on μ-opioid receptor-induced cytokine and nitrite production in primary microglial cells was studied using JWH-015, a CB receptor agonist known to bind more readily to $CB_2$ than $CB_1$ receptors (Merighi et al., 2010). However, JWH-015 also stimulates GPR55 (Lauckner et al., 2008). Similarly, different studies have demonstrated that the $CB_1$ receptor antagonist AM 251 induces GPR55 activity (Lauckner et al., 2008; Henstridge et al., 2010; Anavi-Goffer et al., 2012). Therefore, even if the activity of CB receptor ligands at GPR55 is influenced by the assay used to assess receptor-mediated downstream signaling (Henstridge et al., 2010), a role for GPR55 activation needs to be considered in further pharmacological studies of cannabinoid actions. Furthermore, a non-selective CB agonist enhanced morphine antinociception via the $CB_1$ receptor, pointing to the involvement of $CB_1$ receptors in cannabinoid antinociception produced by CB receptor ligands (Wilson et al., 2008).

The first report linking glia to morphine tolerance demonstrated that chronic systemic morphine increased glia activation in the spinal cord (Song and Zhao, 2001). Other authors have also shown that chronic morphine administration activated astroglia and microglia (Raghavendra et al., 2002; Cui et al., 2006). Activated microglial cells in the spinal cord may release proinflammatory cytokines and other substances thought to facilitate pain transmission (Watkins et al., 2001; 2003). Therefore, pharmacological attenuation of glial activation represents a novel approach for controlling neuropathic pain (Watkins et al., 2005). Neuropathic hyperalgesia could lead to lowered morphine efficacy and quicker development of morphine tolerance (Mayer et al., 1999), and some authors have suggested that uncontrolled activation of microglial cells after nerve injury can lead to altered activities of opioid systems or opioid specific signalling (Watkins et al., 2005; 2007). It is already known that microglia release neuroexcitatory substances in response to morphine, thereby opposing its effects (Watkins et al., 2001; 2005; 2007). This raises an older hypothesis that suppression of glial activation and the resulting blockade of proinflammatory cytokine synthesis can improve morphine efficacy (Song and Zhao, 2001; Raghavendra et al., 2002; Watkins et al., 2007). The mechanism underlying the involvement of glial cells in morphine tolerance is unclear. It is possible that morphine can act directly on glial cells, triggering alterations in their morphology and functions (Raghavendra et al., 2002; 2004). Additionally, glial cells are also considered to be crucial sources of NO, cytokines and cyclooxygenase products that influence synaptic transmission in the CNS. Inhibition of these factors may delay morphine tolerance (Powell et al., 1999).

Many current studies aim to find substances inhibiting the biosynthesis of proinflammatory cytokines. Propentofylline, minocycline and ibudilast inhibit cytokines and decrease astroglia and microglia activation, thereby suppressing the development of neuropathic pain (Romero-Sandoval et al., 2008). The beneficial effects of minocycline are associated with a reduction of inducible NO synthase and cyclooxygenase-2 expression and a decrease in cytokine and prostaglandin release in microglia (Yrjanheikki et al., 1998; 1999). Further studies have shown that minocycline reduced microglial activation by inhibiting p38 MAPK in microglia and, in this way, delayed morphine tolerance (Romero-Sandoval et al., 2008). Ibudilast may counteract opioid tolerance by blocking the activation of glial cells in the spinal cord in rodents (Romero-Sandoval et al., 2008). In the present work, we found that in activated microglial cells, morphine increased Akt and ERK kinase phosphorylation. ERK1/2 kinases are known to regulate the production of proinflammatory mediators from glial cells (Watkins et al., 2001). Furthermore, p38 and ERK kinases have been implicated in the development of morphine-induced hyperalgesia and antinociceptive tolerance (Cuiet al., 2006; Wang et al., 2009). Therefore, it is of interest that $CB_2$ receptor stimulation was able to downregulate Akt and ERK1/2 activation induced by morphine in activated microglial cells.

Our data indicate that the $CB_2$ receptor did not mediate its effects through p38 and JNK1/2 kinases. However, β-caryophyllene, a $CB_2$ receptor selective agonist, modulates JNK1/2 in LPS-stimulated monocytes (Gertsch et al., 2008). As microglia are considered as the resident macrophage-like cells in the brain, we suggest that this contrasting behavior may be due to the different experimental conditions, for example, time of ligand incubation (30 min vs. 3 h for microglia and monocytes respectively) or LPS concentration (1 $\mu g \cdot mL^{-1}$ vs. 0.313 $\mu g \cdot mL^{-1}$ for microglia and monocytes respectively). As for ERK1/2 signalling, it has been previously observed that $CB_2$ receptor stimulation leads to ERK-mediated cellular activation and anti-inflammatory effects in monocytes/macrophages and microglia (Gertsch et al., 2008; Correa et al., 2010). Similarly, a more recent study has demonstrated that $CB_2$ receptor stimulation in microglial cells induced an anti-inflammatory phenotype and reduced migration via MKP-induced ERK dephosphorylation (Romero-Sandoval et al., 2009). Agonist at CB receptors inhibited the production of proinflammatory molecules, which were induced by LPS, in CNS glial cells (Molina Holgado et al., 2002; Fachinetti et al., 2003; Ortega-Gutiérrez et al., 2005; Sheng et al., 2005; Correa et al., 2008; 2009). In particular, $CB_2$ receptors influence the production of the potent inflammatory mediator NO, released from quiescent, and, to a greater extent, from activated microglia (Stella, 2010). In this work, we have described the activation of the ERK1/2 and Akt pathways by LPS leading to an increment in TNF-α, IL-6 and nitrite production. In contrast, while Akt is engaged as the signalling pathway generating IL-1β in LPS-activated microglia, the ERK pathway was not implicated. The involvement of the ERK-MAPK pathway in IL-1β production by LPS is controversial. Some reports show that the ERK cascade is important for LPS-stimulated production of IL-1β in macrophage cell lines and monocytes (Scherle et al., 1998; Caivano and Cohen, 2000). However, it has also been reported that the ERK pathway is not essential for IL-1β production in BV-2 microglia (Watters et al., 2002). Consistent with findings on BV-2 microglia cell lines, our study indicates that the regulation of LPS-stimulated IL-1β production is ERK-independent also in primary microglia.

According to previous studies showing that $CB_2$ receptor mRNA and protein are modulated in vitro differentially in relation to cell activation state (Carlisle et al., 2002; Cabral et al., 2008), we have demonstrated that LPS increases $CB_2$ receptor expression level in primary microglial cells. It is important to mention that $CB_2$ receptors, identified in the healthy brain, mainly in glial elements, and, to a lesser extent, in certain subpopulations of neurons, are dramatically up-regulated in response to damaging stimuli, which supports the idea that the cannabinoid system behaves as an endogenous neuroprotective system. This $CB_2$ receptor up-regulation has been found in many neurodegenerative disorders, which supports the beneficial effects found for $CB_2$ receptor agonists

in these pathologies (Fernández-Ruiz et al., 2011). Now, we have characterized, for the first time, the events occurring in LPS-activated microglia via $CB_2$ receptor stimulation, which reduces not only ERK1/2- but also Akt-phosphorylation increases induced by LPS. Therefore, $CB_2$ receptors expressed in microglia may participate in regulating neuroinflammation and provide neuroprotection by tempering morphine-induced cytokine and NO synthesis through ERK1/2 and Akt signalling in activated microglia. Interestingly, in microglia, we showed that the effects of morphine were mediated by the μ-opioid receptor subtype. This accords with previous observations describing the involvement of endocannabinoids in the peripheral antinociception induced by the μ-opioid receptor agonist morphine. In contrast, the release of endocannabinoids appears not to be involved in the peripheral antinociceptive effect induced by κ- and δ-opioid receptor agonists (da Fonseca Pacheco et al., 2008). At the same time, it would be possible that certain effects of $CB_2$ receptor agonists in different models for inflammation and possibly their analgesic effects previously reported, actually reflect their interaction with endogenous opioids. In particular, it has been demonstrated that morphine is present in human gliomas (Olsen et al., 2005) and that it increases the proliferation of human glioblastoma cells (Lazarczyk et al., 2010). Because morphine is used to alleviate pain associated with cancers, this study suggests that a combination of $CB_2$ receptor agonists to prevent morphine-induced proliferation may have clinically important implications.

In conclusion, the novel finding of this study is the existence of a receptor–receptor interaction when the receptors are co-expressed in the same cells leading to the interaction of their intracellular pathways. In particular, $CB_2$ receptor stimulation counteracts the ability of morphine to upregulate Akt and ERK1/2 activation induced by LPS, thus reducing NO and proinflammatory cytokine release, a process which is ERK- and Akt-dependent. The studies presented here are the first to assess the signalling mechanisms through which $CB_2$ receptor stimulation modulates morphine effects on microglia and MAPK activation. The ability to modulate microglia and MAPK is very interesting because their activation in the central and peripheral nervous system contributes to morphine tolerance and dependence (Mayer et al., 1999; Watkins et al., 2001; Raghavendra et al., 2002; 2004; Galeotti et al., 2006; Cunha et al., 2010). Our results indicate a regulatory role for $CB_2$ receptors in preventing excessive microglial cell response to injury in activated microglia. Based on the findings obtained in the present study, we will advance our research to reinforce the idea that the cannabinoid system exerts an important control on the tolerance and dependence effects induced by opioids. In particular, it will be interesting to evaluate the impact of low-dose combinations of cannabinoids and opioids to effectively treat acute and chronic pain, especially pain that may be resistant to opioids alone. It is well known that the use of cannabinoids, like that of the opioids, has

liability for abuse potential. The use of marijuana as a therapeutic pain management tool has generated a great deal of publicity and controversy. However, it should be noted that $CB_2$ receptor agonists, in comparison with $CB_1$ agonists, lack the undesirable CNS side effects, like sedation and psychotomimetic effects (Fernández-Ruiz et al., 2011; Dhopeshwarkar et al, 2014). Therefore, the development of selective $CB_2$ receptor agonists might open new avenues of therapeutic intervention to reduce the release of proinflammatory mediators especially during morphine therapy. Accordingly, $CB_2$ receptors may be potential targets for reducing morphine tolerance and dependence.

# Figure Legends

**Figure 11**: Detection of $CB_2$ and μ-opioid receptors in primary microglial cells. (A), Cell surface expression of CD11b and intracellular expression of GFAP by flow cytometry analysis. Primary microglial cells were treated with specific monoclonal antibodies (black histograms) or with isotype-matched irrelevant monoclonal antibodies (empty histograms, controls). (B), $CB_2$ and μ-opioid receptor detection by Western blot assay in quiescent and LPS-activated (1 $\mu g \cdot mL^{-1}$ for 30 min) primary microglial cells. Tubulin shows equal loading of protein. The expression of $CB_2$ receptors in CHO-h$CB_2$ cells and of μ-opioid receptors in mouse brain extracts, used as positive controls (Control), is shown. (C), $CB_2$ receptor detection by Western blot assay in quiescent and LPS-activated (1 $\mu g \cdot mL^{-1}$ for 6, 12 and 24 h) primary microglial cells. Tubulin shows equal loading of protein.

**Figure 12**: Effect of opioid receptor ligands on LPS-induced production of proinflammatory cytokines and nitrite in primary microglial cells. Microglial cells were treated with either LPS alone, LPS + morphine 100 nM (MOR), LPS + naloxone, a non-selective opioid receptor antagonist (Nal; 100 nM), LPS + DAMGO, a selective μ-opioid receptor agonist (100 nM), LPS + DPDPE, a selective δ-opioid receptor agonist (100 nM), LPS + U69593, a selective κ-opioid receptor agonist (100 nM) or LPS + CTAP, a selective μ-opioid receptor antagonist (100 nM) for 24 h. The antagonists were added 30 min before morphine. Data shown are mean ± SEM values of four separate experiments performed in triplicate (n = 4). *$P < 0.01$ significantly different from control conditions (absence of drugs, CTR); $^{\#}P < 0.01$ significantly different from LPS conditions (0); $^{\S}P < 0.01$ significantly different from LPS + MOR; $^{\dagger}P < 0.01$ significantly different from LPS + DAMGO; analysis was by ANOVA followed by Dunnett's test.

**Figure 13**: Effect of opioid and CB receptor ligands on LPS-induced production of proinflammatory cytokine and nitrite in primary microglial cells. Microglial cells were treated with either LPS alone, LPS + morphine (MOR; 100 nM), LPS + JWH-015 a $CB_2$ receptor agonist (JWH; 100 nM), LPS + DAMGO (100 nM), LPS + AM 251 a selective $CB_1$ receptor antagonist (100 nM) or LPS + AM 630 a selective $CB_2$ receptor antagonist (100 nM) for 24 h. The antagonists were added 30 min before morphine. Data shown are mean ± SE values of four separate experiments

performed in triplicate (n = 4). *P < 0.01 significantly different from control conditions (absence of drugs, CTR); #P < 0.01 significantly different from LPS conditions (0); §P < 0.01 significantly different from LPS + MOR; †P < 0.01 significantly different from LPS + MOR + JWH; analysis was by ANOVA followed by Dunnett's test.

**Figure 14**: Morphine-enhanced Akt and ERK1/2 phosphorylation in a μ-opioid receptor-dependent manner. (A), Western blot analysis of Akt, ERK1/2, p38, and JNK1/2 phosphorylation in primary microglial cells incubated for 30 min with morphine (MOR) (1–1000 nM). The immunoblot signals were quantified using a VersaDoc Imaging System (Bio-Rad). The ratio of phospho-protein to total protein is used. The mean values of four independent experiments (one of which is shown) were normalized to the result obtained with morphine-untreated cell cultures (0). Densitometric analysis is shown. The unstimulated control (0, cells in the absence of morphine) was set to 100%. Data shown are mean ± SE values of four separate experiments performed in triplicate (n = 4). *P < 0.05 significantly different from unstimulated control; analysis was by ANOVA followed by Dunnett's test. (B), Primary microglial cells were treated with morphine (100 nM) for 0, 15, 30 and 60 min, subjected to Western blot analysis and probed with anti-pERK1/2, anti-pAkt, then Akt and ERK1/2 antibody. The ratio of phospho-protein to total protein is used. Data shown are mean ± SE values of four separate experiments performed in triplicate (n = 4). *P < 0.01 significantly different from control conditions (0); #P < 0.01 significantly different from LPS conditions; analysis was by ANOVA followed by Dunnett's test. (C), Image of Western blot membrane probed with anti-pERK1/2, anti-pAkt, then Akt and ERK1/2 antibody of primary microglial cells pre-treated for 30 min with 0 or 100 nM of the μ-opioid receptor antagonist CTAP, then treated for 30 min with 0 or 100 nM morphine. The ratio of phospho-protein to total protein is used. Data shown are mean ± SEM values of four separate experiments performed in triplicate (n = 4). *P < 0.01 significantly different from untreated cells; analysis was by ANOVA followed by Dunnett's test.

**Figure 15:** Effect of $CB_2$ receptor stimulation in morphine-treated activated primary microglial cells. JWH-015 and morphine (MOR) effect on Akt, ERK1/2, p38 and JNK1/2 phosphorylation in primary microglial cells treated with LPS. Microglial cells were incubated with DMSO vehicle (CTR), with MOR (100 nM), or with JWH-015 (100 nM) alone and in combination in the presence of LPS 1 $\mu g \cdot mL^{-1}$ for 30 min. The mean values of four independent experiments (one of which is shown) were normalized to the result obtained in cells in the absence of LPS (CTR). Data shown

are mean ± SEM values of four separate experiments performed in triplicate (n = 4). CTR was set to 100%. The immunoblot signals were quantified using a VersaDoc Imaging System (Bio-Rad). Densitometric analysis of kinase activation is shown. The ratio of phospho-protein to total protein is used. *P < 0.05 significantly different from CTR; $^{\#}$P < 0.05 significantly different from cells treated with LPS; $^{\S}$P < 0.05 significantly different from cells treated with LPS + morphine; analysis was by ANOVA followed by Dunnett's test.

**Figure 16:** Effect of CB and opioid receptor blockade in morphine-treated activated primary microglial cells. Primary microglial cells were incubated with either DMSO vehicle (lane 1), morphine (MOR; 100 nM), naloxone a non-selective opioid receptor antagonist (Nal; 100 nM), JWH-015 100 nM, AM 251 a selective $CB_1$ receptor antagonist (100 nM) or AM 630 a selective $CB_2$ receptor antagonist (100 nM) in the presence of LPS (1$\mu g \cdot mL^{-1}$) for 30 min. The mean values of four independent experiments (one of which is shown) were normalized to the result obtained in cells in the absence of LPS (lane 1). Data shown are mean ± SEM values of four separate experiments performed in triplicate (n = 4). The unstimulated control (lane 1) was set to 100%. The immunoblot signals were quantified using a VersaDoc Imaging System (Bio-Rad). Densitometric analysis of kinase activation is shown. The ratio of phospho-protein to total protein is used. *P < 0.05 significantly different from untreated cells (lane 1); $^{\#}$P < 0.05 significantly different from cells treated with LPS (lane 2); $^{\S}$P < 0.05 significantly different from cells treated with LPS + morphine (lane 5); $^{\dagger}$P < 0.05 significantly different from LPS + morphine + JWH-015 (lane 6); analysis was by ANOVA followed by Dunnett's test.

**Figure 17:** Effect of kinase inhibitors on LPS-induced production of proinflammatory cytokines and nitrite in primary microglial cells. Microglial cells were treated with LPS with either the MEK-1/2 inhibitor U0126 (1 μM) or the Akt inhibitor SH-5 (1 μM) for 24 h. The inhibitors were added 30 min before LPS. Data shown are mean ± SEM values of four separate experiments performed in triplicate (n = 4); *P < 0.01 significantly different from control conditions (CTR); #P < 0.01 significantly different from LPS conditions; analysis was by ANOVA followed by Dunnett's test.

**Figure 18:** $CB_2$ and μ-opioid receptor expression silencing. (A), Primary microglial cells were treated with either scrambled (-) ($siRNA_{control}$), with $siRNA_{CB2}$ (+) or with $siRNA_{\mu}$ and cultured for 24, 48 and 72 h. Tubulin shows equal loading of protein. Densitometric quantification of $CB_2$ and μ-opioid receptor by Western blot is shown; the immunoblot signals were quantified using a

VersaDoc Imaging System (Bio-Rad). Plots are mean ± SEM values of four separate experiments performed in triplicate (n = 4); *P < 0.01 significantly different from control (scrambled siRNA transfected cells); analysis was by ANOVA followed by Dunnett's test.

**Figure 19:** Primary microglial cells were treated with either $siRNA_{ctr}$, $siRNA_{CB2}$ or $siRNA_{\mu}$ for 48 h and cultured with LPS (1 $\mu g \cdot mL^{-1}$) alone or plus morphine (MOR; 100 nM), JWH-015 (JWH; 100 nM) alone and in combination for 30 min. Densitometric analysis of phosphorylated isoform is shown. The ratio of phospho-protein to total protein is used. The immunoblot signals were quantified using a VersaDoc Imaging System (Bio-Rad). The mean values of four independent experiments (one of which is shown) were normalized to the result obtained in cells in the absence of LPS. The unstimulated control was set to 100%. *P < 0.05 significantly different from unstimulated control (CTR); $^{\#}P < 0.05$ significantly different from cells treated with LPS; $^{\S}P < 0.05$ significantly different from LPS + MOR; analysis was by ANOVA followed by Dunnett's test.

**Figure 20:** Primary microglial cells were treated with either $siRNA_{ctr}$, $siRNA_{CB2}$ or with $siRNA_{\mu}$ for 48 h and cultured with LPS (1 $\mu g \cdot mL^{-1}$) alone or plus morphine (MOR; 100 nM) or JWH-015 (JWH; 100 nM) alone and in combination for 24 h. The unstimulated control (CTR) was set to 100%. Data shown are mean ± SEM values of four separate experiments performed in triplicate (n = 4); *P < 0.05 significantly different from CTR; $^{\#}P < 0.05$ significantly different from LPS; $^{\S}P < 0.05$ significantly different from LPS + MOR; analysis was by ANOVA followed by Dunnett's test.

**Figure 11**

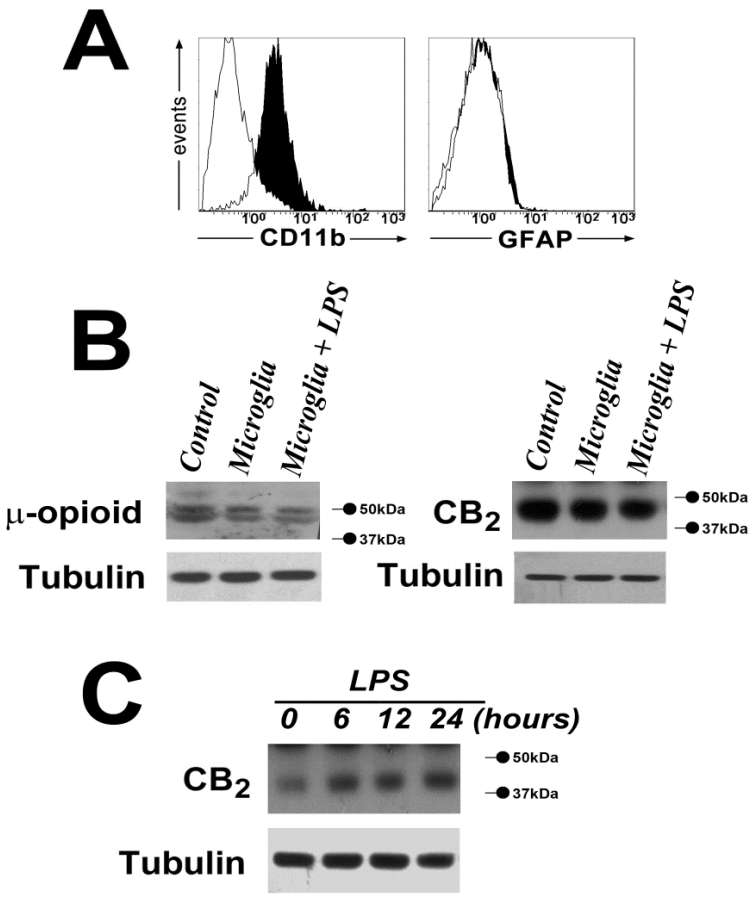
A
events
CD11b
GFAP
B
Control
Microglia
Microglia + LPS
μ-opioid
Tubulin
50kDa
37kDa
CB2
C
LPS
0 6 12 24 (hours)

**Figure 12**

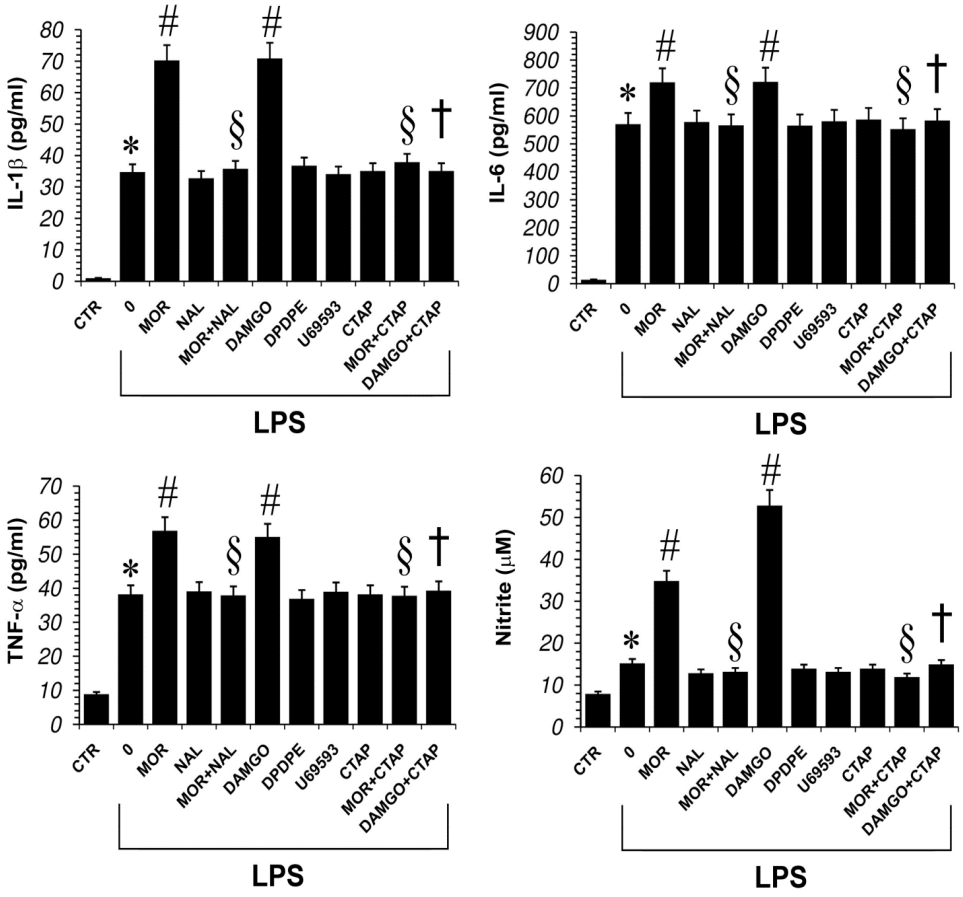
IL-1β (pg/ml)
IL-6 (pg/ml)
TNF-α (pg/ml)
Nitrite (μM)
CTR
0
MOR
NAL
MOR+NAL
DAMGO
DPDPE
U69593
CTAP
MOR+CTAP
DAMGO+CTAP
LPS

**Figure 13**

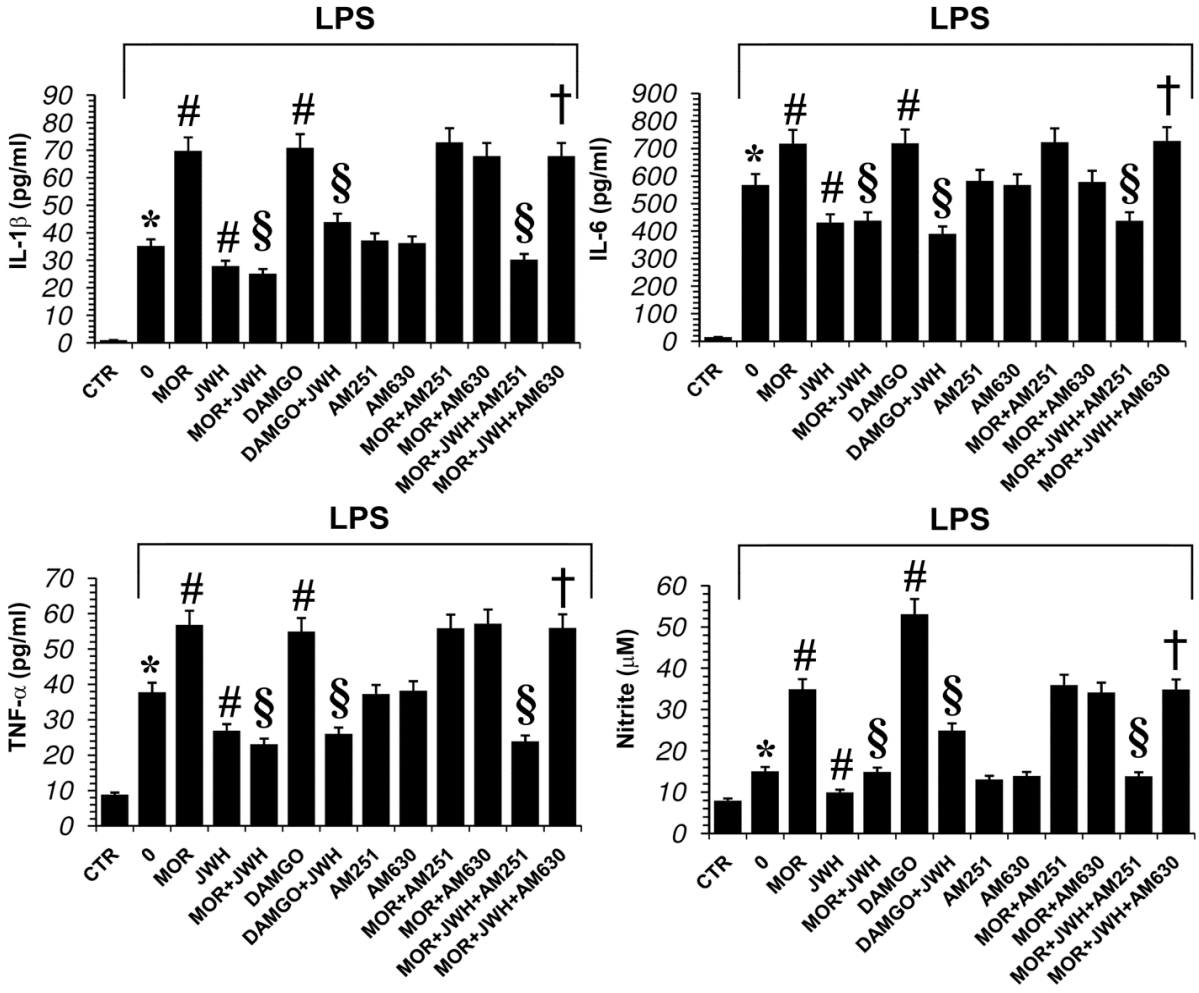
LPS
IL-1β (pg/ml)
IL-6 (pg/ml)
TNF-α (pg/ml)
Nitrite (μM)
CTR
0
MOR
JWH
MOR+JWH
DAMGO
DAMGO+JWH
AM251
AM630
MOR+AM251
MOR+AM630
MOR+JWH+AM251
MOR+JWH+AM630

**Figure 14**

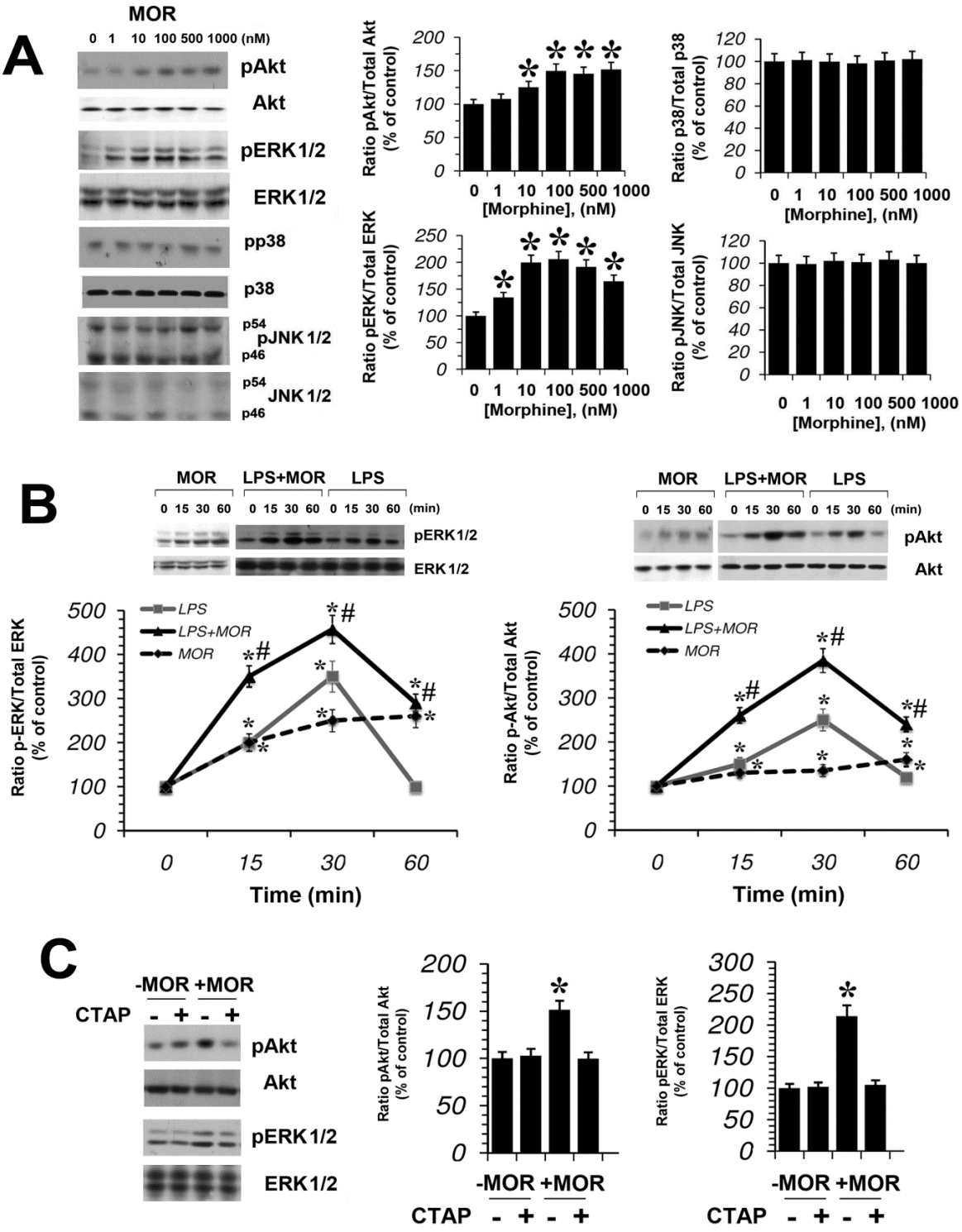
A
MOR
0 1 10 100 500 1000 (nM)
pAkt
Akt
pERK1/2
ERK1/2
pp38
p38
p54 pJNK 1/2 p46
p54 JNK 1/2 p46
Ratio pAkt/Total Akt (% of control)
Ratio p38/Total p38 (% of control)
Ratio pERK/Total ERK (% of control)
Ratio pJNK/Total JNK (% of control)
[Morphine], (nM)
B
MOR
LPS+MOR
LPS
0 15 30 60 (min)
pERK1/2
ERK1/2
pAkt
Akt
LPS
LPS+MOR
MOR
Ratio p-ERK/Total ERK (% of control)
Ratio p-Akt/Total Akt (% of control)
Time (min)
C
-MOR +MOR
CTAP - + - +
pAkt
Akt
pERK1/2
ERK1/2
Ratio pAkt/Total Akt (% of control)
Ratio pERK/Total ERK (% of control)

**Figure 15**

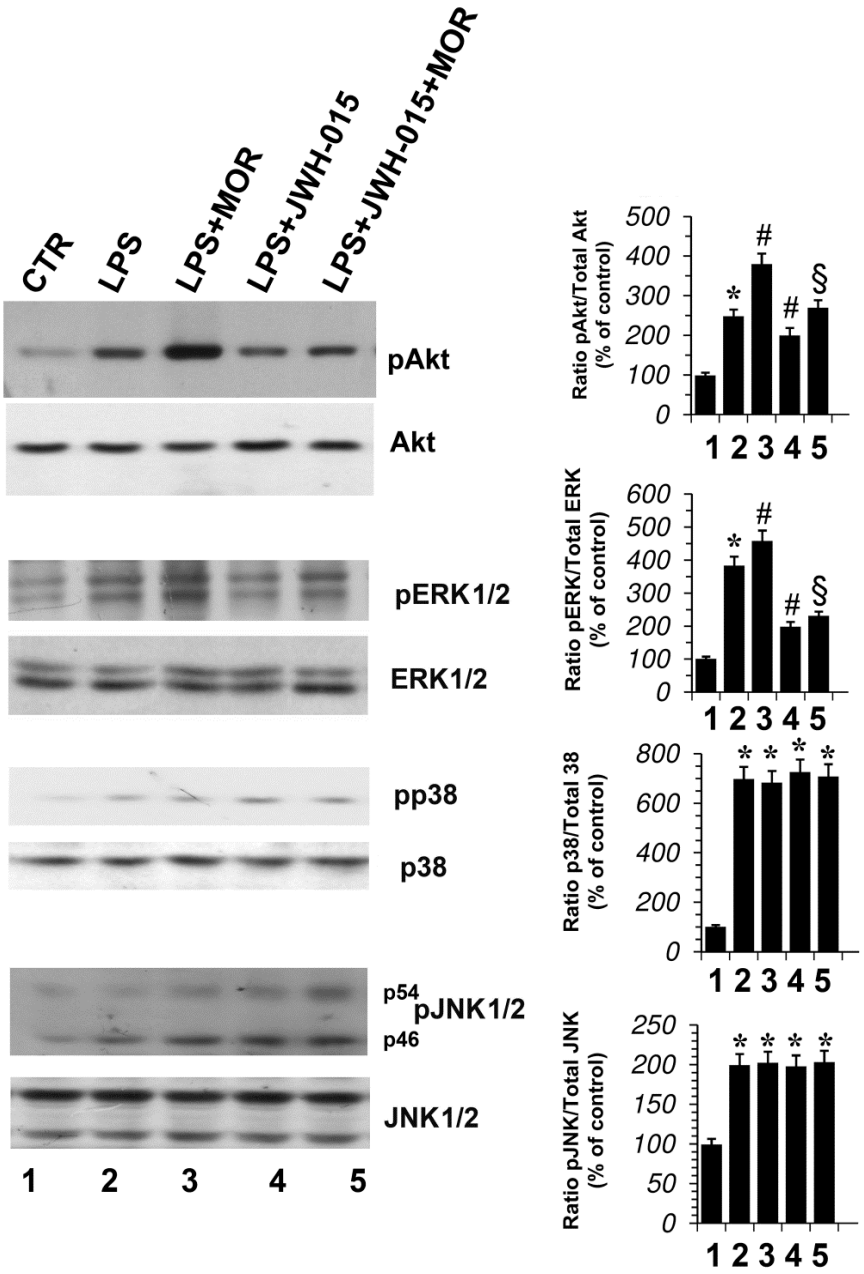
CTR
LPS
LPS+MOR
LPS+JWH-015
LPS+JWH-015+MOR
pAkt
Akt
pERK1/2
ERK1/2
pp38
p38
p54
pJNK1/2
p46
JNK1/2
1 2 3 4 5
Ratio pAkt/Total Akt (% of control)
Ratio pERK/Total ERK (% of control)
Ratio p38/Total 38 (% of control)
Ratio pJNK/Total JNK (% of control)

## Figure 16

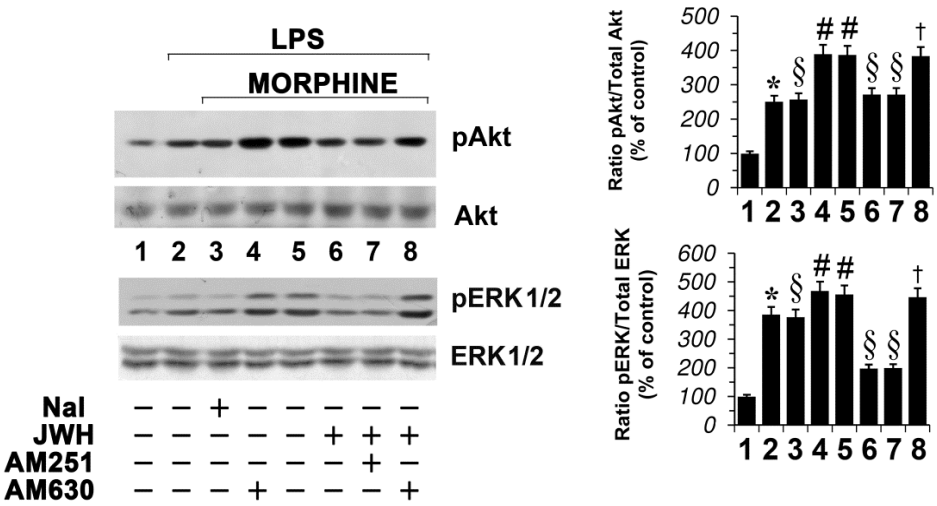


## Figure 17

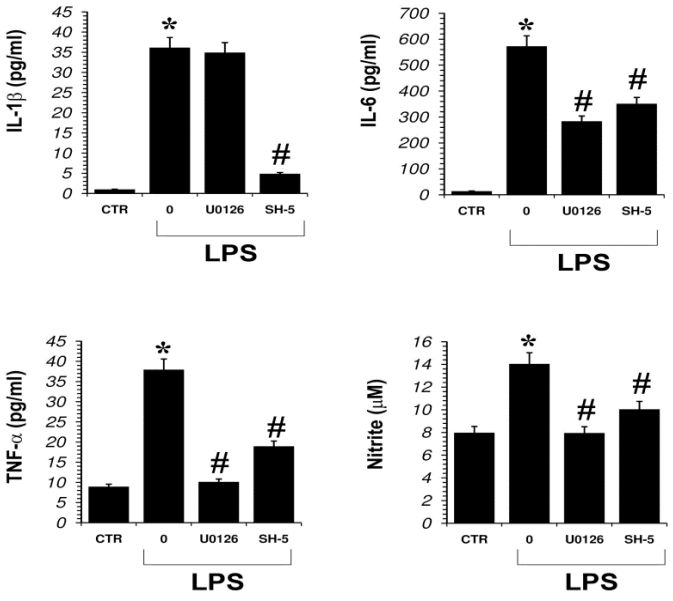

**Figure 18**

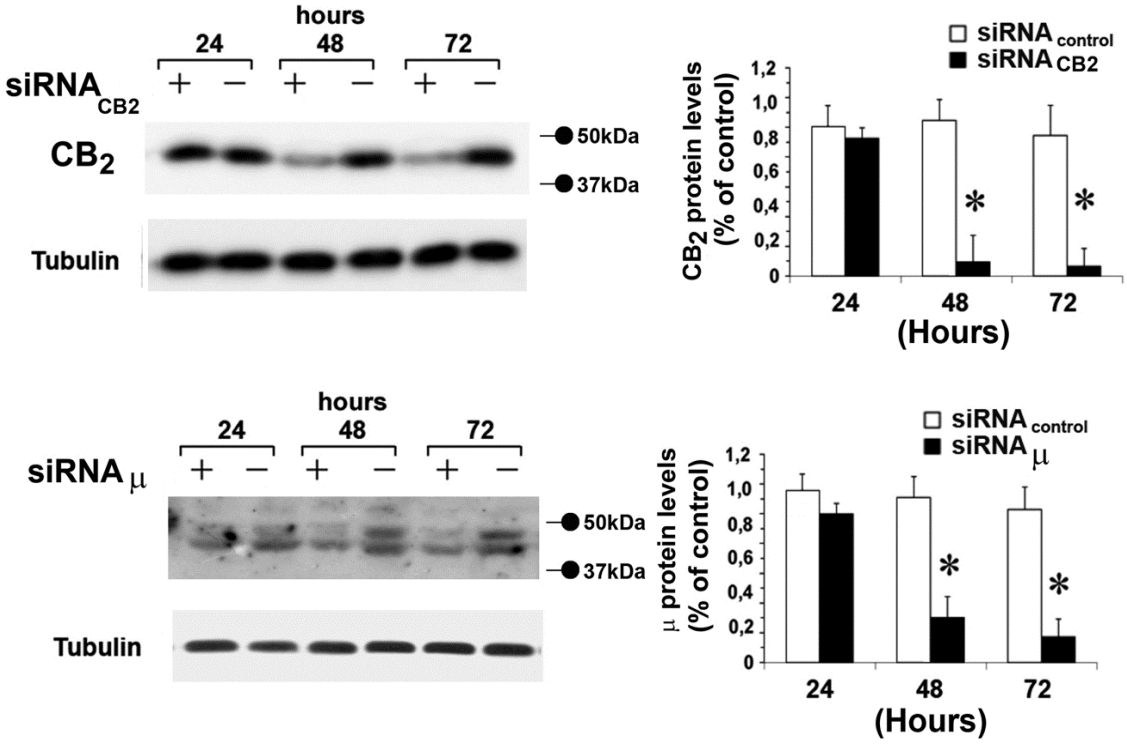
hours
24
48
72
siRNA CB2
+ − + − + −
CB2
50kDa
37kDa
Tubulin
siRNA control
siRNA CB2
CB2 protein levels (% of control)
1,2
1,0
0,8
0,6
0,4
0,2
0
*
*
24
48
72
(Hours)
hours
24
48
72
siRNA μ
+ − + − + −
50kDa
37kDa
Tubulin
siRNA control
siRNA μ
μ protein levels (% of control)
1,2
1,0
0,8
0,6
0,4
0,2
0
*
*
24
48
72
(Hours)

**Figure 19**

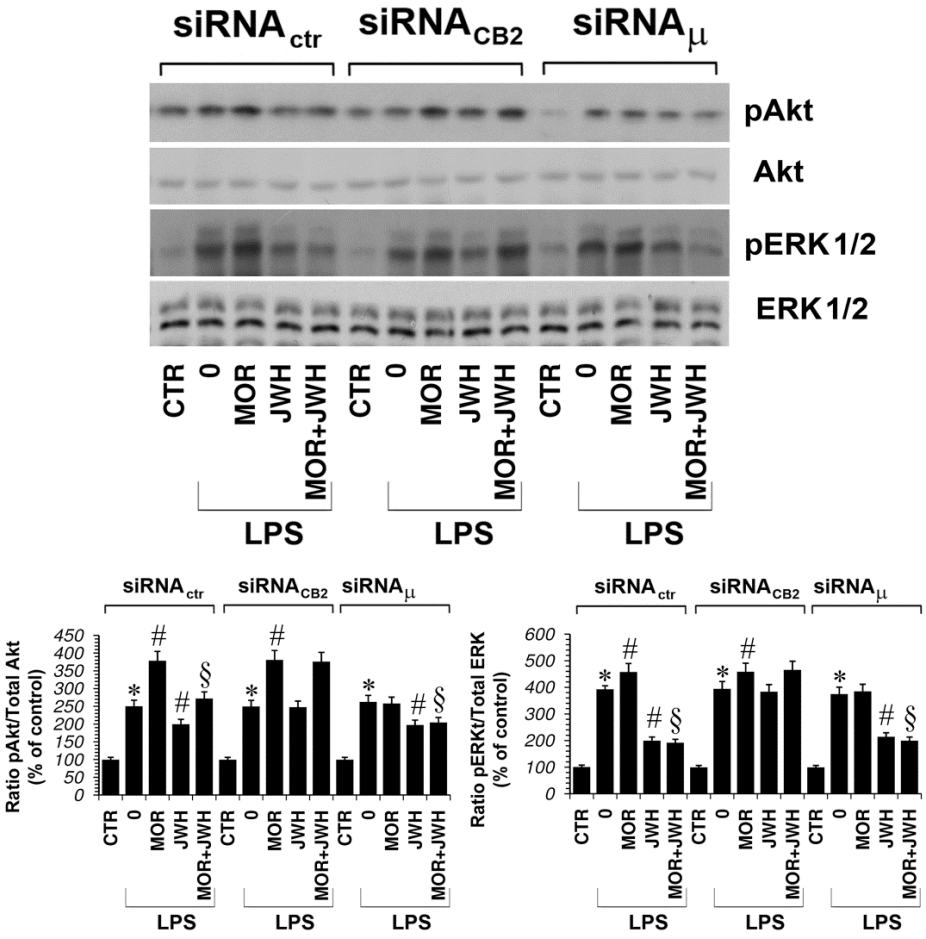
siRNA ctr
siRNA CB2
siRNA μ
pAkt
Akt
pERK1/2
ERK1/2
CTR
0
MOR
JWH
MOR+JWH
LPS
Ratio pAkt/Total Akt (% of control)
Ratio pERK/Total ERK (% of control)

**Figure 20**

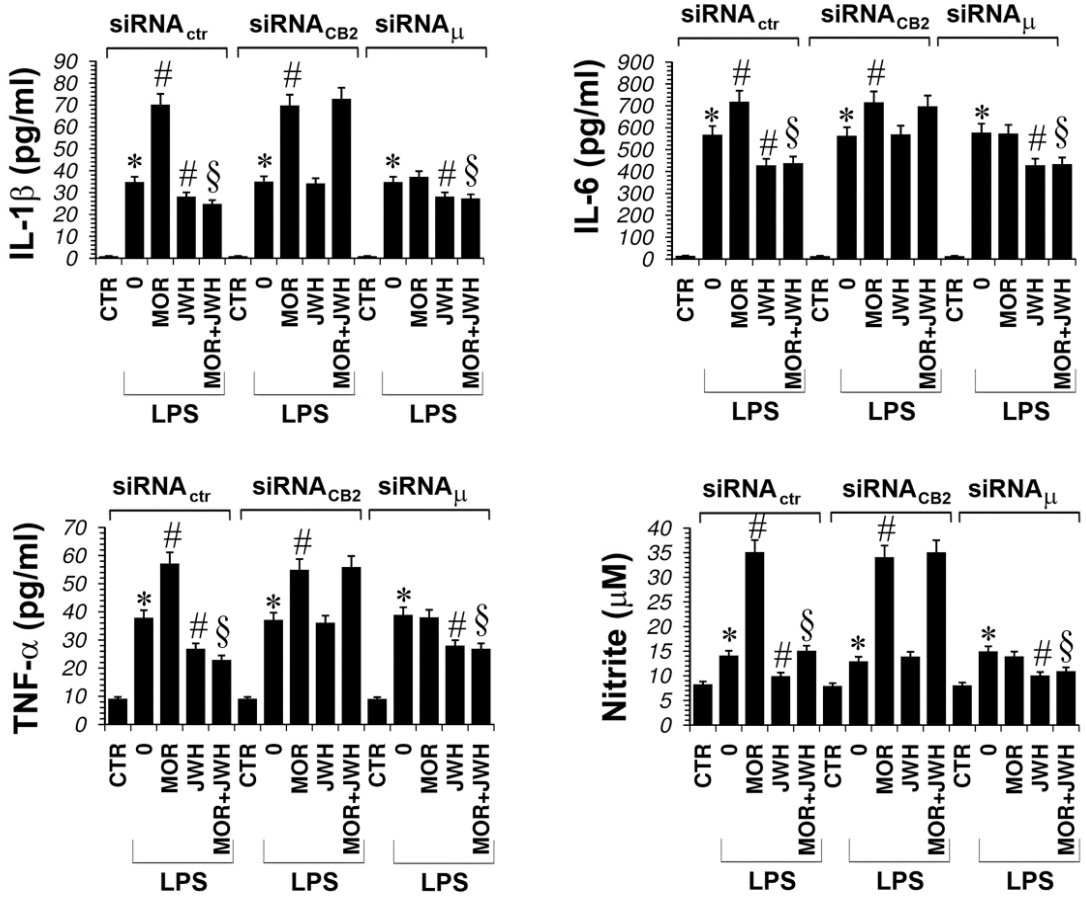
siRNA ctr
siRNA CB2
siRNA μ
IL-1β (pg/ml)
IL-6 (pg/ml)
TNF-α (pg/ml)
Nitrite (μM)
CTR
0
MOR
JWH
MOR+JWH
LPS

# References


Alexander SP, Mathie A, Peters JA (2011). Guide to receptors and channels (GRAC), 5th edition. Br J Pharmacol 164 (Suppl. 1): S1–324.

Alexander SPH, Benson HE, Faccenda E, Pawson AJ, Sharman JL, Catterall WA, Spedding M, Peters JA, Harmar AJ, CGTP collaborators (2013). The Concise Guide to PHARMACOLOGY 2013/2014: Overview. Br J Pharmacol 170: 1449-1458.

Anavi-Goffer S, Baillie G, Irving AJ, Gertsch J, Greig IR, Pertwee RG, Ross RA (2012). Modulation of L-a-lysophosphatidylinositol/GPR55 mitogen-activated protein kinase (MAPK) signaling by cannabinoids. J Biol Chem 287: 91–104.

Atwood BK, Mackie K (2010). $CB_2$: a cannabinoid receptor with an identity crisis. Br J Pharmacol 160: 467–479.

Begg M, Pacher P, Bátkai S, Osei-Hyiaman D, Offertáler L, Mo FM, Liu J, Kunos G (2005). Evidence for novel cannabinoid receptors. Pharmacol Ther 106: 133–145.

Benito C, Tolón RM, Pazos MR, Núñez E, Castillo AI, Romero J (2008). Cannabinoid $CB_2$ receptors in human brain inflammation. Br J Pharmacol 153: 277–285.

Bondarenko AI (2014). Endothelial atypical cannabinoid receptor: do we have enough evidence? Br J Pharmacol 171: 5573-5588.

Cabral GA, Harmon KN, Carlisle SJ (2001). Cannabinoid-mediated inhibition of inducible nitric oxide production by rat microglial cells: evidence for $CB_1$ receptor participation. Adv Exp Med Biol 493: 207–214.

Cabral GA, Raborn ES, Griffin L, Dennis J, Marciano-Cabral F (2008). $CB_2$ receptors in the brain: role in central immune function. Br J Pharmacol 153: 240–251.

Caivano M, Cohen P (2000). Role of mitogen-activated protein kinase cascades in mediating lipopolysaccharide-stimulated induction of cyclooxygenase-2 and IL-1 beta in RAW264 macrophages. J Immunol 164: 3018–3025.

Carlisle SJ, Marciano-Cabral F, Staab A, Ludwick C, Cabral GA (2002). Differential expression of the $CB_2$ cannabinoid receptor by rodent macrophages and macrophage-like cells in relation to cell activation. Int Immunopharmacol 2: 69–82.

Chao CC, Gekker G, Sheng WS, Hu S, Tsang M, Peterson PK (1994). Priming effect of morphine on the production of tumor necrosis factor-α by microglia: implications in respiratory burst activity and human immunodeficiency virus-1 expression. J Pharmacol Exp Ther 269: 198–203.

Chen Y, Sommer C (2009). The role of mitogen-activated protein kinase (MAPK) in morphine tolerance and dependence. Mol Neurobiol 40: 101–107.

Cichewicz DL (2004). Synergistic interactions between cannabinoid and opioid analgesics. Life Sci 74: 1317–1324.

Correa F, Mestre L, Docagne F, Guaza C (2005). Activation of cannabinoid $CB_2$ receptor negatively regulates IL-12p40 production in murine macrophages: role of IL-10 and ERK1/2 kinase signaling. Br J Pharmacol 145: 441–448.

Correa F, Docagne F, Clemente D, Mestre L, Becker C, Guaza C (2008). Anandamide inhibits IL-12p40 production by acting on the promoter repressor element GA-12: possible involvement of the COX-2 metabolite prostamide E(2). Biochem J 409: 761–770.

Correa F, Docagne F, Mestre L, Clemente D, Hernangómez M, Loría F, Guaza C (2009). A role for $CB_2$ receptors in anandamide signalling pathways involved in the regulation of IL-12 and IL-23 in microglial cells. Biochem Pharmacol 77: 86–100.

Correa F, Hernangómez M, Mestre L, Loría F, Spagnolo A, Docagne F, Di Marzo V, Guaza C (2010). Anandamide enhances IL-10 production in activated microglia by targeting $CB_2$ receptors: roles of ERK1/2, JNK, and NF-kappaB. Glia 58: 135–147.

Cui Y, Chen Y, Zhi JL, Guo RX, Feng JQ, Chen PX (2006). Activation of p38 mitogen-activated protein kinase in spinal microglia mediates morphine antinociceptive tolerance. Brain Res 1069: 235–243.

Cunha TM, Roman-Campos D, Lotufo CM, Duarte HL, Souza GR, Verri WA, Funez MI, Dias QM, Schivo IR, Domingues AC, Sachs D, Chiavegatto S, Teixeira MM, Hothersall JS, Cruz JS, Cunha FQ, Ferreira SH (2010). Morphine peripheral analgesia depends on activation of the PI3Kgamma/AKT/nNOS/NO/KATP signaling pathway. Proc Natl Acad Sci USA 107: 4442–4447.

Dhopeshwarkar A, Mackie K (2014). $CB_2$ cannabinoid receptors as a therapeutic target - what does the future hold? Mol Pharmacol 86(4):430-437.

Ehrhart J, Obregon D, Mori T, Hou H, Sun N, Bai Y, Klein T, Fernandez F, Tan J, Shytle RD (2005). Stimulation of cannabinoid receptor 2 ($CB_2$) suppresses microglial activation. J Neuroinflammation 2: 29.

Eljaschewitsch E, Witting A, Mawrin C, Lee T, Schmidt PM, Wolf S, Hoertnagl H, Raine CS, Schneider-Stock R, Nitsch R, Ullrich O (2006). The endocannabinoid anandamide protects neurons during CNS inflammation by induction of MKP-1 in microglial cells. Neuron 49: 67–79.

Fachinetti F, Del Giudice G, Furegato S, Passarotto M, Leon M (2003). Cannabinoids ablate release of TNFα in rat microglial cells stimulated with lypopolysaccharide. Glia 41: 161–168.

Fernández-Ruiz J (2009). The endocannabinoid system as a target for the treatment of motor dysfunction. Br J Pharmacol 156: 1029–1040.

Fernández-Ruiz J, Moreno-Martet M, Rodríguez-Cueto C, Palomo-Garo C, Gómez-Cañas M, Valdeolivas S, Guaza C, Romero J, Guzmán M, Mechoulam R, Ramos JA (2011). Prospects for cannabinoid therapies in basal ganglia disorders. Br J Pharmacol 163: 1365–1378.

da Fonseca Pacheco D, Klein A, de Castro Perez A, da Fonseca Pacheco CM, de Francischi JN, Duarte ID (2008). The mu-opioid receptor agonist morphine, but not agonists at delta- or kappa-opioid receptors, induces peripheral antinociception mediated by cannabinoid receptors. Br J Pharmacol 154: 1143–1149.

Galeotti N, Stefano GB, Guarna M, Bianchi E, Ghelardini C (2006). Signalling pathway of morphine induced acute thermal hyperalgesia in mice. Pain 123: 294–305.

Gertsch J, Leonti M, Raduner S, Racz I, Chen JZ, Xie XQ, Altmann KH, Karsak M, Zimmer A (2008). Beta-caryophyllene is a dietary cannabinoid. Proc Natl Acad Sci USA 105: 9099–9104.

Gobbi G, Mirandola P, Tazzari PL, Ricci F, Caimi L, Cacchioli A, Papa S, Conte R, Vitale M (2003). Flow cytometry detection of serotonin content and release in resting and activated platelets. Br J Haematol 121: 892–896.

González-Scarano F, Baltuch G (1999). Microglia as mediators of inflammatory and degenerative diseases. Annu Rev Neurosci 22: 219–240.

Grace PM, Hutchinsons MR, Maier SF, Watkins LR (2014). Pathological pain and the neuroimmune interface. Nat Rev Immunol 14: 217-231.

Green LC, Wagner DA, Glogowski J, Skipper PL, Wishnok JS, Tannenbaum SR (1982). Analysis of nitrate, nitrite, and [15N]nitrate in biological fluids. Anal Biochem 126: 131–138.

Henstridge CM, Balenga NA, Schröder R, Kargl JK, Platzer W, Martini L, Arthur S, Penman J, Whistler JL, Kostenis E, Waldhoer M, Irving AJ (2010). GPR55 ligands promote receptor coupling to multiple signalling pathways. Br J Pharmacol 160: 604–614.

Hsieh GC, Pai M, Chandran P, Hooker BA, Zhu CZ, Salyers AK, Wensink EJ, Zhan C, Carroll WA, Dart MJ, Yao BB, Honore P, Meyer MD (2011). Central and peripheral sites of action for $CB_2$ receptor mediated analgesic activity in chronic inflammatory and neuropathic pain models in rats. Br J Pharmacol 162: 428–440.

Johnston IN, Milligan ED, Wieseler-Frank J, Frank MG, Zapata V, Campisi J, Langer S, Martin D, Green P, Fleshner M, Leinwand L, Maier SF, Watkins LR (2004). A role for proinflammatory cytokines and fractalkine in analgesia, tolerance, and subsequent pain facilitation induced by chronic intrathecal morphine. J Neurosci 24: 7353–7365.

Jung WK, Lee DY, Park C, Choi YH, Choi I, Park SG, Seo SK, Lee SW, Yea SS, Ahn SC, Lee CM, Park WS, Ko JH, Choi IW (2010). Cilostazol is anti-inflammatory in BV2 microglial cells by inactivating nuclear factor-kappaB and inhibiting mitogen-activated protein kinases. Br J Pharmacol 159: 1274–1285.

Klegeris A, Bissonnette CJ, McGeer PL (2003). Reduction of human monocytic cell neurotoxicity and cytokine secretion by ligands of the cannabinoid-type $CB_2$ receptor. Br J Pharmacol 139: 775 786.

Klein TW, Newton CA (2007). Therapeutic potential of cannabinoid-based drugs. Adv Exp Med Biol 601: 395–413.

Klein TW, Lane B, Newton CA, Friedman H (2000). The cannabinoid system and cytokine network. Proc Soc Exp Biol Med 225: 1–8.

Lauckner JE, Jensen JB, Chen HY, Lu HC, Hille B, Mackie K (2008). GPR55 is a cannabinoid receptor that increases intracellular calcium and inhibits M current. Proc Natl Acad Sci USA 105: 2699–2704.

Lazarczyk M, Matyja E, Lipkowski AW (2010). A comparative study of morphine stimulation and biphalin inhibition of human glioblastoma T98G cell proliferation in vitro. Peptides 31: 1606–1612.

Lehnardt S, Lachance C, Patrizi S, Lefebvre S, Follett PL, Jensen FE, Rosenberg PA, Volpe JJ, Vartanian T (2002). The toll-like receptor TLR4 is necessary for lipopolysaccharide-induced oligodendrocyte injury in the CNS. J Neurosci 22: 2478–2486.

McGrath J, Drummond G, McLachlan E, Kilkenny C, Wainwright C (2010). Guidelines for reporting experiments involving animals: the ARRIVE guidelines. Br J Pharmacol 160: 1573–1576.

Malan TP, Ibrahim MM, Deng H, Liu Q, Mata HP, Vanderah T, Porreca F, Makriyannis A (2001). $CB_2$ cannabinoid receptor-mediated peripheral antinociception. Pain 93: 239–245.

Manzaneres J, Corchero J, Romero JJ, Fernandez-Ruiz JA, Ramos JÁ FJA (1999). Pharmacological and biochemical interactions between opioids and cannabinoids. Trends Pharmacol Sci 20: 287-294.

Marrs WR, Blankman JL, Horne EA, Thomazeau A, Lin YH, Coy J, Bodor AL, Muccioli GG, Hu SS, Woodruff G, Fung S, Lafourcade M, Alexander JP, Long JZ, Li W, Xu C, Möller T, Mackie K, Manzoni OJ, Cravatt BF, Stella N (2010). The serine hydrolase ABHD6 controls the accumulation and efficacy of 2-AG at cannabinoid receptors. Nat Neurosci 13: 951–957.

Massi P, Solinas M, Cinquina V, Parolaro D (2013). Cannabidiol as potential anticancer drug. Br J Clin Pharmacol 75(2): 303-312.

Mayer DJ, Mao J, Holt J, Price DD (1999). Cellular mechanisms of neuropathic pain, morphine tolerance, and their interactions. Proc Natl Acad Sci USA 96: 7731–7736.

Merighi S, Benini A, Mirandola P, Gessi S, Varani K, Leung E, Maclennan S, Borea PA (2005). $A_3$ adenosine receptor activation inhibits cell proliferation via phosphatidylinositol 3-kinase/Akt-dependent inhibition of the extracellular signal-regulated kinase 1/2 phosphorylation in A375 human melanoma cells. J Biol Chem 280: 19516–19526.

Merighi S, Benini A, Mirandola P, Gessi S, Varani K, Simioni C, Leung E, Maclennan S, Baraldi PG, Borea PA (2007). Caffeine inhibits adenosine-induced accumulation of hypoxia-inducible factor-1alpha, vascular endothelial growth factor, and interleukin-8 expression in hypoxic human colon cancer cells. Mol Pharmacol 72: 395–406.

Merighi S, Simioni C, Gessi S, Varani K, Mirandola P, Tabrizi MA et al. (2009). $A_{2B}$ and $A_3$ adenosine receptors modulate vascular endothelial growth factor and interleukin-8 expression in human melanoma cells treated with etoposide and doxorubicin. Neoplasia 11: 1064–1073.

Merighi S, Simioni C, Gessi S, Varani K, Borea PA (2010). Binding thermodynamics at the human cannabinoid $CB_1$ and $CB_2$ receptors. Biochem Pharmacol 79: 471–477.

Merighi S, Gessi S, Varani K, Simioni C, Fazzi D, Mirandola P, Borea PA (2012a). Cannabinoid $CB_2$ receptor modulates microglial cells stimulated with lypopolysaccharide: role of ERK-1/2 kinase signalling in nitric oxide release. Br J Pharmacol 165: 1773–1788.

Merighi S, Gessi S, Varani K, Fazzi D, Borea PA (2012b). Hydrogen sulfide modulates the release of nitric oxide and VEGF in human keratinocytes. Pharmacol Res 66:428-436.

Molina-Holgado F, Lledo A, Guaza C (1997). Anandamide suppresses nitric oxide and TNF-alpha responses to Theiler's virus or endotoxin in astrocytes. Neuroreport 8: 1929–1933.

Molina-Holgado F, Molina-Holgado E, Guaza C, Rothwell NJ (2002). Role of $CB_1$ and $CB_2$ receptors in the inhibitory effects of cannabinoids on lipopolysaccharide-induced nitric oxide release in astrocyte cultures. J Neurosci Res 67: 829–836.

Molina-Holgado F, Pinteaux E, Moore JD, Molina-Holgado E, Guaza C, Gibson RM (2003). Endogenous interleukin-1 receptor antagonist mediates anti-inflammatory and neuroprotective actions of cannabinoids in neurons and glia. J Neurosci 23: 6470–6474.

Morel LJ, Giros B, Daugé V (2009). Adolescent exposure to chronic delta-9-tetrahydrocannabinol blocks opiate dependence in maternally deprived rats. Neuropsychopharmacology 34: 2469–2476.

Olsen P, Rasmussen M, Zhu W, Tonnesen E, Stefano GB (2005). Human gliomas contain morphine. Med Sci Monit 11: MS18–MS21.

Ortega-Gutiérrez S, Molina-Holgado E, Guaza C (2005). Effect of anandamide uptake inhibition in the production of nitric oxide and in the release of cytokines in astrocyte cultures. Glia 52: 163–168.

Parolaro D, Rubino T, Viganò D, Massi P, Guidali C, Realini N (2010). Cellular mechanisms underlying the interaction between cannabinoid and opioid system. Curr Drug Targets 11: 393–405.

Pertwee RG, Howlett AC, Abood ME, Alexander SP, Di Marzo V, Elphick MR, Greasley PJ, Hansen HS, Kunos G, Mackie K, Mechoulam R, Ross RA. et al. (2010). International Union of Basic and Clinical Pharmacology. LXXIX. Cannabinoid receptors and their ligands: beyond $CB_1$ and $CB_2$. Pharmacol Rev 62: 588–631.

Powell KJ, Hosokawa A, Bell A, Sutak M, Milne B, Quirion R, Jhamandas K (1999). Comparative effects of cyclo-oxygenase and nitric oxide synthase inhibition on the development and reversal of spinal opioid tolerance. Br J Pharmacol 127: 631–644.

Puffenbarger RA, Boothe AC, Cabral GA (2000). Cannabinoids inhibit LPS-inducible cytokine mRNA expression in rat microglial cells. Glia 29: 58–69.

Raghavendra V, Rutkowski MD, DeLeo JA (2002). The role of spinal neuroimmune activation in morphine tolerance/hyperalgesia in neuropathic and sham-operated rats. J Neurosci 22: 9980–9989.

Raghavendra V, Tanga FY, DeLeo JA (2004). Attenuation of morphine tolerance, withdrawal induced hyperalgesia, and associated spinal inflammatory immune responses by propentofylline in rats. Neuropsychopharmacology 29: 327–334.

Richardson JD (2000). Cannabinoids modulate pain by multiple mechanisms of action. J Pain 1: 2–14.

Romero-Sandoval EA, Horvath RJ, DeLeo JA (2008). Neuroimmune interactions and pain: focus on glial-modulating targets. Curr Opin Investig Drugs 9: 726–734.

Romero-Sandoval EA, Horvath R, Landry RP, DeLeo JA (2009). Cannabinoid receptor type 2 activation induces a microglial anti-inflammatory phenotype and reduces migration via MKP induction and ERK dephosphorylation. Mol Pain 5: 25.

Satoh M, Minami M (1995). Molecular pharmacology of the opioid receptors. Pharmacol Ther 68: 343–364.

Scherle PA, Jones EA, Favata MF, Daulerio AJ, Covington MB, Nurnberg SA, Magolda RL, Trzaskos JM (1998). Inhibition of MAP kinase kinase prevents cytokine and prostaglandin E2 production in lipopolysaccharide-stimulated monocytes. J Immunol 161: 5681–5686.

Sheng WS, Hu S, Min X, Cabral GA, Lokensgard JR, Peterson PK (2005). Synthetic cannabinoid WIN55,212-2 inhibits generation of inflammatory mediators by IL-1beta-stimulated human astrocytes. Glia 49: 211–219.

Shohami E, Gallily R, Mechoulam R, Bass R, Ben-Hur T (1997). Cytokine production in the brain following closed head injury: dexanabinol (HU-211) is a novel TNF-alpha inhibitor and an effective neuroprotectant. J Neuroimmunol 72: 169–177.

Song P, Zhao ZQ (2001). The involvement of glial cells in the development of morphine tolerance. Neurosci Res 39: 281–286.

Stella N (2010). Cannabinoid and cannabinoid-like receptors in microglia, astrocytes, and astrocytomas. Glia 58: 1017–1030.

Wang Z, Ma W, Chabot JG, Quirion R (2009). Cell-type specific activation of p38 and ERK mediates calcitonin gene-related peptide involvement in tolerance to morphine-induced analgesia. FASEB J 23: 2576–2586.

Watkins LR, Milligan ED, Maier SF (2001). Spinal cord glia: new players in pain. Pain 93: 201–205.

Watkins LR, Milligan ED, Maier SF (2003). Glial proinflammatory cytokines mediate exaggerated pain states: implications for clinical pain. Adv Exp Med Biol 521: 1–21.

Watkins LR, Hutchinson MR, Johnston IN, Maier SF (2005). Glia: novel counter-regulators of opioid analgesia. Trends Neurosci 28: 661–669.

Watkins LR, Hutchinson MR, Ledeboer A, Wieseler-Frank J, Milligan ED, Maier SF (2007). Norman Cousins Lecture. Glia as the 'bad guys': implications for improving clinical pain control and the clinical utility of opioids. Brain Behav Immun 21: 131–146.

Watkins LR, Hutchinson MR, Rice KC, Maier SF (2009). The 'toll' of opioid-induced glial activation: improving the clinical efficacy of opioids by targeting glia. Trends Pharmacol Sci 30: 581–591.

Watters JJ, Sommer JA, Pfeiffer ZA, Prabhu U, Guerra AN, Bertics PJ (2002). A differential role for the mitogen-activated protein kinases in lipopolysaccharide signaling: the MEK/ERK pathway is not essential for nitric oxide and interleukin 1beta production. J Biol Chem 277: 9077–9087.

Wilson AR, Maher L, Morgan MM (2008). Repeated cannabinoid injections into the rat periaqueductal gray enhance subsequent morphine antinociception. Neuropharmacology 55: 1219–1225.

Yrjanheikki J, Keinanen R, Pellikka M, Hokfelt T, Koistinaho J (1998). Tetracyclines inhibit microglial activation and are neuroprotective in global brain ischemia. Proc Natl Acad Sci USA 95: 15769–15774.

Yrjanheikki J, Tikka T, Keinanen R, Goldsteins G, Chan PH, Koistinaho J (1999). A tetracycline derivative, minocycline, reduces inflammation and protects against focal cerebral ischemia with a wide therapeutic window. Proc Natl Acad Sci USA 96: 13496–13500.

# Morphine mediates a proinflammatory phenotype *via* μ-opioid-receptor-PKCε-Akt-ERK1/2 signalling pathway in activated microglial cells

# Introduction

Opioids are potent analgesics and are irreplaceable for the treatment of severe pain and in anesthesia. They mediate their effects via three receptors termed μ-, δ- and κ-opioid receptors. Among these, μ-opioid receptors play an outstanding role, because they mediate effects of morphine and most clinically used opioids (Frolich et al., 2011; Kieffer et al.,2009). However, marked reduction in the analgesic properties of opiates resulting from repeated use significantly hinders the prolonged clinical use of these drugs. Although the exact mechanisms of opiate tolerance remain unknown, it has been suggested that the activation of microglia in response to morphine and the consequent production of pro-inflammatory cytokines plays a key pathogenic role. For this reason, many current studies aim to find substances inhibiting the biosynthesis of pro-inflammatory cytokines.

Recently, we have demonstrated that morphine and the μ-opioid receptor agonist DAMGO induce the activation of Akt and ERKs in microglial cells. In addition, μ-opioid receptors increase NO and pro-inflammatory cytokine secretion, e.g. IL-1β, TNF-α and IL-6, through Akt and ERK signalling (Merighi et al., 2012b). However, the mechanisms that occur in the GPCR signalling by which μ-opioid receptors signal to ERKs have not been studied in detail.

Microglia, brain inflammatory cells, are activated in injured brain where they release inflammatory mediators such as nitric oxide (NO), tumor necrosis factor-alpha (TNF-α), and prostaglandins (Minghetti et al., 1995; Lee et al., 1993; Chao et al., 1992; Grace et al., 2014). The inflammatory mediators could protect tissues from bacterial infection but also could potentiate the damage of neurons (Minghetti et al., 1998). Activated microglial cells in the spinal cord may release proinflammatory cytokines and other substances thought to facilitate pain transmission (Watkins et al., 2003; 2001). Therefore, pharmacological attenuation of glial activation represents a novel approach for controlling pain (Ock et al., 2010; Watkins et al., 2005). Although the intracellular signalling molecules involved in microglial activation have not been fully understood, protein kinase C (PKC) has been considered as an important mediator of microglial activation. In particular, it has been reported that PKC inhibitors reduced NO release from lipopolysaccharide (LPS)-treated microglia (Nakai et al., 1998; Yoon et al., 1994).

# Protein kinase Cε

Among different effectors, PKC has attracted a great deal of attention because of its prominent role in synaptic plasticity and memory. PKC is an integral component of most GPCR signaling pathways to ERK/MAPK (Belcheva et al., 2005). Accordingly, PKC was found to be an early signalling component in the opioid pathway to ERK (Zheng et al., 2008; Bohn et al., 2000; Fukuda et al., 1996). Nevertheless, little is known about the actual isoforms involved in this pathway.

PKC is a multi-gene family with at least 10 members that differ in their tissue expression, subcellular localization, activator and cofactor requirements, and substrate specificity. PKC serine/threonine kinases require diacylclycerol (DAG) and phosphatidyl serine (PS) for their activation, while according to their dependency on $Ca^{2+}$ are classified into conventional, $Ca^{2+}$-dependent cPKCs α, β, and γ, and into novel, $Ca^{2+}$-independent nPKCs δ, ε, η, θ; the newest and atypical PKCs, aPKC ζ and λ/ι require only PS (Freeley et al., 2011; Steinberg et al., 2008). PKC isoforms are regulated by their phosphorylation and translocation; once phosphorylated, PKC isoforms are rendered catalytically competent and are activated upon their translocation to cell membrane. Therefore, activation of PKC isoforms is assessed by their phosphorylation and membrane translocation (Sudan et al., 2012). Most PKC isoforms are widely expressed in the brain with higher concentrations in the cerebral structures and areas known to participate in memory processes. PKCε in particular, a prominent PKC in differentiating and differentiated neurons (Mangoura et al., 2006; Prekeris et al., 1996), is considered critical in learning and memory, and in synaptic remodeling (Hama et al., 2004). There is evidence that PKCε isoform is activated by opiates, raising the possibility that PKCε modulates behavioral responses to opiates. The interactions between the transition from acute to chronic pain and the development of opioid tolerance and dependence are mediated by PKCε (Joseph et al., 2010). Recently, it has been demonstrated that morphine uses the PKCε pathway to induce ERK phosphorylation and receptor desensitization (Zheng et al., 2011). Furthermore, PKC inhibitors can reduce morphine anti-nociceptive tolerance (Smith et al., 2007). Mice that lack PKCε isozyme ($PKC\varepsilon^{-/-}$) show enhanced responses to morphine (Newton et al., 2007) and increased analgesia and thermal behavioral tolerance to specific cannabinoid agonists (Wallace et al., 2009). Several aspects of the immune system in these animals were normal although macrophages were defective in the production of LPS-stimulated TNF-α, IL-1β, $PGE_2$, and NO. There were also deficits in LPS-stimulated MAPK and NFkB activation (Castrillo et al., 2001).

Therefore, the present study was designed to identify in detail the receptor-proximal signalling events that link μ-opioid receptors to activation of Akt and ERKs in microglial cells and to define the molecular mechanism contributing to the ability of morphine to increase inflammatory mediators such as NO, TNF-α, IL-1β and IL-6 in activated microglial cells. In particular, the role of PKCε isoform in μ-opioid-induced inflammatory response in microglia has been here investigated.

# Materials and Methods

## Animals

One-day-old Balb/c mice were obtained from Charles River (Calco, Italy). Animal care procedures conformed to the guidelines issued by the European Council (86/609/EEC) were approved by the local Animal Care and Ethics Committee.

## Reagents and antibodies

Tissue culture media and growth supplements were obtained from Lonza (Euroclone, Milan, Italy). U0126 (MEK-1 and MEK-2 inhibitor, soluble in DMSO) was provided by Promega (Milan, Italy). Phosphorylated p44/42 MAPK (ERK1/2) (Thr $^{202}$/Tyr $2^{204}$) (cat. #4370) and total anti-ERK1/2 pAb, anti-COX-2 (cat. #4842), anti-iNOS (cat. #2977), phosphorylated (Ser 473) (cat. #9271) and total Akt were from Cell Signaling Technology (Euroclone, Milan, Italy). SH5 (inhibitor of Akt) was from Enzo Life Sciences (Vinci-Biochem, Vinci, Florence, Italy). Anti-PKCε (cat. #06-991) used in Western blot assay was from Millipore (Milan, Italy). Anti-PKCε (cat. #NBP1-30126) used in immunofluorescence assay was from Novus Biological (DBA, Milan, Italy). Phosphorylated (Ser 729) (sc-12355) PKCε antibody, small interfering RNA (siRNA) PKCε (sc-36250) and MOR-1 siRNA (sc-35958) were from Santa Cruz Biotechnology (DBA, Milan, Italy). RNAiFect™ Transfection Kit was from Qiagen (Milan, Italy). Unless otherwise stated, all other chemicals were purchased from Sigma (Milan, Italy). Drug and molecular target nomenclature conforms to Alexander et al., 2013.

## Primary microglial cell cultures

Primary glial cultures were prepared as described in a previous study (Merighi et al., 2012a). Briefly, after anesthesia (Zoletil 100, 30 mg·kg$^{-1}$, Virbac Laboratories, France) and decapitation, forebrains from newborn Balb/c mice were excised, meninges removed, and tissue dissociated mechanically. Cells were re-suspended in Dulbecco's modified Eagle medium (DMEM/F12) supplemented with 10% heat-inactivated fetal bovine serum (FBS) and 1% penicillin/streptomycin,

then plated on poly-D-lysine-coated (5 $\mu g \cdot mL^{-1}$) 75 $cm^2$ flasks (Falcon; Euroclone, Milan, Italy). After 15 days, the flasks were shaken vigorously to remove loosely adherent microglia. The supernatant was plated on multi-well culture plates for 2 h, and the medium was changed to remove nonadherent cells. Cells were grown in a humidified environment containing 5% $CO_2$ at a constant temperature of 37°C. The purity of microglial cultures was assessed by examining cell morphology under phase-contrast microscopy, and was confirmed by flow cytometry with Mac-1 anti-CD11b antibody (BD Pharmingen, Milan, Italy).

## Cell cultures

Cells were maintained in DMEM/F12 medium containing 10% FBS, penicillin (100 $U \cdot mL^{-1}$), streptomycin (100 $\mu g \cdot mL^{-1}$) at 37°C in 5% $CO_2$/95% air. Cells were split 2 or 3 times weekly at a ratio between 1:5 and 1:10.

## Flow cytometry of primary microglial cells

Aliquots of 0.5 x $10^6$ cells were incubated for 40 min at 4°C with either specific Phycoerythrin (PE)-labeled antibodies, or isotype-matched irrelevant IgG-PE (Beckman Coulter) as negative control. Cells were washed with PBS and characterized for CD11b and GFAP expression by flow cytometry with PE-labeled anti-CD11b MoAb (BD Pharmingen, Milan, Italy) and the fluorescein isothiocyanate (FITC)-labeled anti-GFAP MoAb (BD Pharmingen, Milan, Italy). In particular, GFAP immunophenotyping was performed in permeabilized cells, using IntraPrep™ fixing/permeabilization reagent (Beckman Coulter) (Gobbi et al., 2003). Analysis was performed on an Epics XL flow cytometer (Beckman Coulter, Fullerton, CA) using Expo ADC software (Beckman Coulter).

## Primary microglial cell exposure to opioids and LPS treatment

LPS, a cell wall component of Gram-negative bacteria, is a potent activator of glia. Hence, microglial cells were treated with 1 $\mu g \cdot mL^{-1}$ LPS (from Escherichia coli, serotype 055:B5) (soluble in cell culture medium) before commencing incubation with opioid ligands. Unless otherwise

stated, the concentration of morphine, naloxone, DAMGO, DPDE, U69593 and CTAP was 100 nM, which is the ligand concentration able to occupy 99% of the receptors at equilibrium. Microglia were then maintained in DMEM/F12 containing opioids or their vehicle, and harvested after treatment at the indicated times.

## PKCε activity

PKCε activity has been modulated by εV1-2 (CEAVSLKPT) peptide conjugated by a cysteine disulfide bound to TAT47–57 (CYGRKKRRQRRR) (Brandman et al., 2007), generously donated by Prof. P. Mirandola, University of Parma, Italy. Briefly, εV1-2 is a specific PKCε inhibitor designed from C2 region of PKCε protein that acts as a competitor of binding between PKCε and its anchoring protein εRACK. Microglial cells were treated with 1 μM of εV1-2.

## Nitrite assay for primary microglial cells

NO synthase activity was assessed indirectly by measuring nitrite ($NO_2^-$) accumulation in the cell culture media using a colorimetric kit (Calbiochem, Milan, Italy). At the end of the treatment period, the nitrite concentration in the conditioned media was determined according to a modified Griess method (Merighi et al., 2012a). Briefly, the NADH-dependent enzyme nitrate reductase was used to convert the nitrate to nitrite prior to quantification of the absorbance, measured at 540 nm by a spectrophotometric microplate reader (Fluoroskan Ascent, Labsystems, Sweden). Values were obtained by comparison with reference concentrations of sodium nitrite.

## Enzyme-linked immunosorbent assay (ELISA)

The levels of IL-1β, TNF-α and IL-6 protein secreted by the cells in the medium were determined by ELISA kits (R&D Systems). In brief, subconfluent cells were changed into fresh medium in the presence of solvent or various concentrations of drugs. The medium was collected, and IL-1β, TNF-α and IL-6 protein concentrations were measured by ELISA according to the manufacturer's instructions. The results were normalized to the number of cells per plate. The data were presented as mean ± S.E. from four independent experiments performed in triplicate.

## Western blotting for primary microglial cells

Western blot assay was performed as previously described (Merighi et al., 2009; 2006). Aliquots of total protein sample (50 μg) were analyzed using antibodies specific for phosphorylated or total p44/p42 MAPK (1:1000 dilution), phosphorylated (1:200) or total (1:1000) PKCε, phosphorylated or total Akt (1:1000 dilution), for μ-opioid receptors. Specific reactions were revealed with Enhanced Chemiluminescence Western blotting detection reagent (Amersham Corp., Arlington Heights, IL). The membranes were then stripped and re-probed with tubulin (1:250) to ensure equal protein loading.

## Densitometry analysis

The intensity of each immunoblot assay band was quantified using a VersaDoc Imaging System (Bio-Rad, Milan, Italy). Mean densitometric data from independent experiments was normalized to the results obtained with control cell cultures. The ratio of phospho-protein to total protein was reported in a densitometric analysis.

## Treatment of primary microglial cells with siRNA

Microglial cells were plated in six-well plates and grown to 50–70% confluence before transfection. Transfection of $siRNA_{PKC\varepsilon}$ or $siRNA_{\mu}$ was performed at a concentration of 100 nM using RNAiFect™ Transfection Kit (Qiagen, Milan, Italy). Cells were cultured in complete media and total proteins were isolated at 24, 48 and 72 h for Western blot analysis of PKCε and μ-opioid receptor protein. A randomly chosen non-specific siRNA was used under identical conditions as control (Merighi et al., 2007; 2005).

## Immunofluorescence

Microglial cells were seeded on glass coverslips in 6-well plates overnight at 37°C in a humidified atmosphere containing 5% $CO_2$. Microglial cells were treated with 1 $\mu g \cdot mL^{-1}$ LPS alone or in combination with morphine 100 nM. After 10 min the medium was removed, cells were washed

twice with PBS, mixed in 4% paraformaldehyde for 10 min, permeabilized in a PBS solution containing 0.2% Triton X-100, 1% BSA and incubated for 1 h with PBS-plus 10% goat serum. Cells were then stained (for 90 min at room temperature) with a 1:200 dilution of an anti-PKCε antibody (Novus Biological) in PBS-plus 1% goat serum. The coverslips were rinsed three times and then the cells were labeled with a FITC-conjugated secondary antibody in PBS for 1 h. Coverslips were stained with 4',6'-diamino-2-phenyl-indole (DAPI), mounted in DABCO glycerol-PBS, and observed on a Nikon fluorescent microscope.

## Statistical analysis

All data are reported as mean ± S.E. of independent experiments and are indicated in the figure legends. Each experiment was performed by using the microglial cells derived from one single mouse, and was performed in triplicate. The experiments were repeated at least four times as indicated from n-values that represent the number of mice used. Data sets were examined by analysis of variance (ANOVA) for comparisons between multiple groups and Dunnett's test for comparing a control group to all other groups (when necessary). A P value of less than 0.05 was considered statistically significant.

# Results

## Morphine alters the LPS-induced expression and activation of PKCε

Expression of the myeloid cell surface antigen CD11b was analyzed in primary microglial cells by flow cytometry. Cells were treated with specific MoAbs or isotype-matched irrelevant MoAbs. Microglia were negative for the astrocyte-specific protein GFAP but showed significant positive staining for CD11b, as compared to the isotype control, thereby indicating high expression levels of the microglial cell marker CD11b (data not shown).

We have studied by immunofluorescence the involvement of PKCε in microglial cells treated with morphine. PKCε protein expression in quiescent microglia was localized to nuclear compartment (Figure 21) while a faint signal was observed in the cytoplasm. Treatment with morphine (100 nM) did not change PKCε expression or localization. On the contrary, LPS 1 $\mu g \cdot mL^{-1}$ alone or LPS + morphine 100 nM increased PKCε expression and a clear cell membrane translocation of this enzyme was also observed. These results were confirmed through the analysis of phosphorylation levels and membrane translocation of PKCε in microglial cells by Western blotting (Figure 22). In particular, microglial cells were treated with either LPS 1 $\mu g \cdot mL^{-1}$ alone or LPS + morphine 100 nM for 0, 5, 10, 15, 30, or 60 min. The cytosolic and membrane fractions of cells were subsequently prepared for Western blot analysis of PKCε. In separate experiments, after treatment, whole-cell lysates were prepared and analyzed by Western blot analysis for phospho-PKCε. The presence of PKCε was determined in unstimulated microglial cells. We found that LPS induces phosphorylation of PKCε in a time-dependent manner, as demonstrated using specific phospho-PKCε antibody, which detects PKCε isoform only when phosphorylated at indicated specific site (Ser-729) (Figure 22A). In the presence of morphine 100 nM, PKCε phosphorylation induced by LPS was significantly higher than LPS alone, with a maximal activation at 10 min (Figure 22B). Consistent with PKCε phosphorylation results, incubation of cells with LPS 1 $\mu g \cdot mL^{-1}$ alone provoked the cytosol-to-membrane translocation and thus activation of PKCε (Figure 22C). In the presence of morphine 100 nM, PKCε translocation was significantly higher than LPS 1 $\mu g \cdot mL^{-1}$ alone and was maximal at 10 min. A decrease in PKCε translocation induced by LPS + morphine was observed at 15 min followed by a further activation at 30 and 60 min (Figure 22D). Furthermore, to confirm that phosphorylation of PKCε leads to membrane localization, we have shown the presence of phosphorylated membranous PKCε. In particular, we have performed a Western blot analysis using specific phospho-PKCε antibody on membrane fractions. We found that PKCε phosphorylation

induced by LPS + morphine (for 10 min) was significantly higher than LPS alone also in the membranous fraction (Figure 22E,F).

## Effect of opioid receptor ligands on LPS-induced expression and activation of PKCε

Morphine-induced PKCε activation was found to be opioid receptor-mediated. Pretreatment of cells with the broad-range opioid receptor antagonist naloxone for 30 min abolished morphine-induced phosphorylation (Figure 23) of PKCε at 10 min in LPS-activated microglial cells. Furthermore, DAMGO (100 nM), a μ-opioid receptor selective agonist, mimicked morphine effects on microglial PKCε activation (Figure 23). Conversely, DPDPE and U-69593, δ- and κ-receptor selective agonists, respectively, had no effect on LPS-induced PKCε activation (Figure 23). Finally, pretreatment of microglial cells with CTAP 100 nM, a μ-opioid receptor selective antagonist, before treatment with DAMGO 100 nM, abolished μ-opioid receptor agonist's effect on LPS-induced PKCε activation (Figure 23). These results demonstrate that morphine activates PKCε in mouse activated microglial cells via the μ-opioid receptor.

## μ-opioid receptor gene silencing in microglial cells

To confirm the apparent role of μ-opioid receptors we reduced their expression in primary microglial cells by siRNA transfection, in order to cause transient knockdown of the μ-opioid receptor gene. Primary microglial cells were transfected with nonspecific random control ribonucleotides (siRNA scramble, $siRNA_{ctr}$) or with small interfering RNAs that target μ-opioid receptor mRNA ($siRNA_{\mu}$) for degradation. As shown in Figure 24A, μ-opioid receptor protein expression was strongly reduced after 48 and 72 h of treatment with $siRNA_{\mu}$. Therefore, 48 h after $siRNA_{\mu}$ transfection, primary microglial cells were treated with either LPS 1 $\mu g \cdot mL^{-1}$, or LPS + morphine 100 nM, for 10 min, after which cytosolic and membrane fractions of cells were subsequently prepared for Western blot analysis of PKCε. In separate experiments, after treatment, whole-cell lysates were prepared and analyzed by Western blot analysis for phospho-PKCε. We found that the inhibition of μ-opioid receptor expression blocks morphine-increases in phospho-PKCε and PKCε translocation in microglia (Figure 24B). These results clearly show the connection

between μ-opioid receptor stimulation, morphine, and PKCε signaling in activated primary microglial cells.

## PKCε isoform modulates morphine-induced Akt and ERK1/2 phosphorylation in activated microglial cells

Because phosphorylation and membrane translocation of PKCε isoform were regulated by morphine, which also regulates Akt and ERK1/2 phosphorylation (Merighi et al., 2012b), we next examined whether the selective inhibition of PKCε isoform by its inhibitor εV1-2 and siRNA regulated morphine-induced signaling through these two kinases in activated microglial cells.

To study the specificity of εV1-2, we treated BALB/c-derived microglial cells with the PKC inhibitor for 2 h followed by stimulation with LPS and morphine for 10 min and studied PKCε isoform activation by membrane translocation. We observed that εV1-2 inhibited morphine-induced translocation of the PKCε isoform for which it was specific (Figure 25). Indeed, to investigate the possible relationship between PKCε and Akt–ERK1/2 kinases, we examined the activation of Akt and ERK1/2 by LPS plus morphine in the presence of εV1-2. On the basis of our earlier study, induction of Akt and ERK1/2 activation by LPS plus morphine was most significant 15 min after treatment. Therefore, cells were pretreated with εV1-2 for 30 min before LPS plus morphine stimulation for 15 min. We found that Akt and ERK1/2 phosphorylation at 15 min following LPS alone or LPS plus morphine treatment is attenuated by the PKCε inhibitor εV1-2 (Figure 25). These results demonstrate that the inhibition of PKCε isoform activation by its translocation inhibitor peptide εV1-2 reduced LPS- and morphine-induced Akt and ERK1/2 phosphorylation in activated microglial cells (Figure 25), indicating that the activation of PKCε occurs upstream of Akt and ERK1/2 kinases. To confirm the role of PKCε and to investigate the involvement of μ-opioid receptors in the signalling under investigation, we examined the effect of $siRNA_{PKC\varepsilon}$ on μ-opioid receptor-elicited Akt and ERK1/2 phosphorylation. In order to cause transient knockdown of PKCε gene we reduced PKCε expression in primary microglial cells by siRNA transfection. Primary microglial cells were transfected with nonspecific random control ribonucleotides (siRNA scramble, $siRNA_{ctr}$) or with small interfering RNAs that target PKCε mRNA ($siRNA_{PKC\varepsilon}$) for degradation. As shown in Figure 26A, PKCε protein expression was strongly reduced after 24 and 48 h of treatment with $siRNA_{PKC\varepsilon}$. Therefore, 24 h after $siRNA_{PKC\varepsilon}$ transfection, primary microglial cells were treated with either LPS 1 $\mu g \cdot mL^{-1}$ alone, LPS + morphine 100 nM, or LPS + DAMGO 100 nM for 15 min, after which ERK1/2- and Akt-phosphorylated protein levels were measured.

The results revealed that inhibition of PKCε expression is sufficient to block ERK1/2 and Akt phosphorylation levels increased by morphine in LPS-treated microglia (Figure 26B). Furthermore, to analyze iNOS protein expression, primary microglial cells were stimulated with LPS in the absence or presence of morphine or DAMGO and Western blotting was performed after 4 h of treatment. As is evident from Figure 26B, iNOS protein was induced by stimulation with LPS (1 $\mu g \cdot mL^{-1}$). This induction was increased by co-treatment with either 100 nM morphine or DAMGO. We found that the inhibition of PKCε expression by siRNA blocks morphine- and DAMGO increases in iNOS protein expression in LPS-treated microglia (Figure 26B). These results clearly show the connection between PKCε, morphine and DAMGO, ERKs and Akt signaling, iNOS protein, in activated primary microglial cells.

Effect of LPS and morphine on another proinflammatory enzyme, COX-2, was examined by Western blot assay. Stimulation of microglial cells with LPS 1 $\mu g \cdot mL^{-1}$ led to increased expression of protein for COX-2 (Figure 26C). However, morphine 100 nM did not modulate the increased expression of COX-2 protein stimulated by LPS (Figure 26C).

## PKCε isoform modulates morphine-induced cytokine and nitrite in activated microglial cells

We measured cytokine and nitrite levels in microglial cells pretreated with the PKCε inhibitor εV1-2. Then, we went on to investigate how the inhibition of PKCε interferes with the signalling pathways modulated by LPS and morphine by maintaining primary microglial cells in LPS-supplemented (1 $\mu g \cdot mL^{-1}$) DMEM in combination with the opioid receptor agonist morphine (100 nM) for 24 h. As shown in Figure 27A, LPS-induced IL-1β, TNFα, IL-6 and nitrite release was significantly increased in the presence of morphine in primary microglial cells. However, the stimulatory response of morphine on cytokine and nitrite production was reversed in the presence of the PKCε inhibitor, εV1-2 (Fig. 27A). We found εV1-2 alone significantly inhibited LPS and LPS plus morphine-induced increase of IL-1β, IL-6, TNF-α and nitrite release. Likewise, we measured cytokine and nitrite levels in microglial cells in which PKCε was down-regulated by siRNA. We found that in microglial cells with PKCε down-regulated, morphine and DAMGO did not significantly increase IL-1β, TNF-α, IL-6 and nitrite protein levels when compared to LPS, after 24 h of treatment (Fig. 27B).

## Activation of PKCε by morphine in reactive microglia occurs upstream Akt, ERK1/2 and iNOS

Microglial cells were pretreated with U0126 and SH-5, inhibitors of ERK1/2 and Akt, respectively, for 30 min before LPS plus morphine stimulation for 10 min. Subsequently, whole-cell lysates were prepared and analyzed by Western blot analysis for phospho-PKCε. Figure 28A shows that morphine 100 nM significantly increased phospho-PKCε in activated microglial cells even in the presence of U0126 and SH-5. These results confirm that activation of PKCε by morphine in reactive microglia occurs upstream Akt and ERK1/2.

Furthermore, microglial cells were pretreated with U0126 and SH-5, for 30 min before LPS plus morphine stimulation for 4 h. Subsequently, whole-cell lysates were prepared for Western blot analysis of iNOS. The results demonstrate that SH-5 and U0126 significantly blocked the ability of morphine to increase iNOS production in the presence of LPS (Figure 28A), indicating that activation of Akt and ERK1/2 occurs upstream iNOS production induced by LPS and morphine in reactive microglia. Moreover, microglial cells pretreated with SH-5 for 30 min before LPS plus morphine stimulation for 10 min were analyzed for ERK1/2 phosphorylation levels. We found that the inhibition of the Akt pathway significantly blocked morphine-induced ERK1/2 phosphorylation in morphine-treated activated microglia (Figure 28B), indicating that Akt proceeds through ERK1/2 activation to mediate chemokine and nitrite production induced by morphine.

Finally, we have investigated the effect of morphine 100 nM alone on signal transduction pathway in microglial cells. Figure 29A shows that morphine did not modulate PKCε activation, iNOS and COX-2 protein expression while slightly increased Akt and ERK1/2 phosphorylation. In addition, we measured cytokine and nitrite levels in microglial cells treated with morphine 100 nM for 24 h. We found that IL-1β, IL-6, TNF-α and nitrite release was not significantly modulated in the presence of morphine in primary microglial cells (Figure 29B).

# Discussion and Conclusions

The studies presented here indicate that PKCε has a critical function in the regulation of a number of signalling pathways that mediate various aspects of microglia activation in response to morphine treatment. In particular, our findings point to an important role for PKCε in morphine-evoked inflammatory pathways leading to chemokine and NO production. By using pharmacological inhibitors and RNA interference, we have clearly demonstrated that morphine-induced iNOS, IL-1β, TNF-α, IL-6 and NO production in primary activated microglial cells is mediated by a signalling pathway involving the sequential activation of PKCε, Akt and MAPK, as illustrated in Figure 30.

The hallmark for PKC activation is a process called translocation, whereby PKC isoforms, once phosphorylated, translocate from the cytosol to subcellular membrane regions (Freeley et al., 2011; Steinberg et al., 2008; Mirandola et al., 2011). Presence of a small fraction of membrane-bound active PKCε form in the unstimulated control cells suggests some activation of PKCε in resting-state cells. There is evidence that PKCε isoform is activated by opiates. In particular, PKC inhibitors can reduce morphine anti-nociceptive tolerance (Smith et al., 2007). Mice that lack PKCε isozyme ($PKC\varepsilon^{-/-}$) show enhanced responses to morphine (Newton et al., 2007) and increased analgesia and thermal behavioral tolerance to specific cannabinoid agonists (Wallace et al., 2009). Now, for the first time, our findings identified that the novel PKC isoform ε was activated by morphine in mouse stimulated microglia.

Our group recently demonstrated that morphine enhances the release of NO and the IL-1β, IL-6, TNF-α proinflammatory cytokines from activated microglial cells through the μ-opioid receptor and by acting on Akt–ERK1/2 signaling (Merighi et al., 2012a). The present study further extends earlier findings that the presence of opioid receptors on glia and the ability of morphine to prime microglia for enhanced production of proinflammatory cytokines supports a possible direct interaction of morphine with glial cells (Chao et al., 1994). It has been reported that, while agonists of the μ-opioid receptor are the most appropriate therapy for moderate to severe pain, important issues of the development of tolerance and dependence diminish their usefulness in patients requiring chronic treatment. Much work has been done to elucidate the cellular mechanisms of opioid-induced analgesia, tolerance and dependence in the hope of finding an analgesic that is capable of enhancing pain relief without initiating the cellular processes involved in tolerance and dependence. The first report linking glia to morphine tolerance demonstrated that chronic systemic morphine increased glia activation in the spinal cord (Song et al., 2001). Other authors have also

shown that chronic morphine administration activates astroglia and microglia (Raghavendra et al., 2002). Activated microglial cells in the spinal cord may release proinflammatory cytokines and other substances thought to facilitate pain transmission. It has been reported that glial inhibitors influence the development of morphine tolerance. Furthermore, glial cells are also considered to be crucial sources of NO, cytokines and cyclooxygenase products that influence synaptic transmission in the CNS. Inhibition of these factors may delay morphine tolerance (Watkins et al., 2003; 2001; 2007). Therefore, pharmacological attenuation of glial activation represents a novel approach for controlling neuropathic pain and tolerance (Ock et al., 2010). It has been indicated that uncontrolled activation of microglial cells after nerve injury can lead to altered activities of opioid systems or opioid-specific signaling (Ock et al., 2010; Watkins et al., 2007). It is already known that microglia release neuroexcitatory substances in response to morphine, thereby opposing its effects (Watkins et al., 2001; 2007; Ock et al., 2010). This raises an older hypothesis that suppression of glial activation and the resulting blockade of proinflammatory cytokine synthesis can improve morphine efficacy (Song et al., 2001; Watkins et al., 2001). The mechanism underlying the involvement of glial cells in morphine tolerance is unclear. It is possible that morphine can act directly on glial cells triggering alterations in their morphology and functions (Raghavendra et al., 2002; 2004). Additionally, glial cells are also considered to be crucial sources of NO, cytokines and cyclooxygenase products that influence synaptic transmission in the central nervous system (CNS). Inhibition of these factors may delay morphine tolerance (Powell et al., 1999).

Many current studies aim to find substances inhibiting the biosynthesis of proinflammatory cytokines. It has been found that propentofylline, minocycline and ibudilast inhibit cytokines and lower astroglia and microglia activation, thereby suppressing the development of neuropathic pain (Romero-Sandoval et al., 2008). The beneficial effects of minocycline are associated with a reduction of inducible NO synthase and cyclooxygenase-2 expression and a decrease in cytokine and prostaglandin release in microglia (Yrjanheikki et al., 1999; 1993). Further studies have shown that minocycline reduced microglial activation by inhibiting p38 MAPK in microglia, and in this way delayed morphine tolerance. It was also suggested that ibudilast may counteract opioid tolerance by blocking the activation of glial cells in the spinal cord in rodents (Romero-Sandoval et al., 2008). PKCε is critically involved at an early stage of LPS-mediated signalling in activated macrophages (Castrillo et al., 2001). Several studies have also implicated MAP kinase activation as a critical event in LPS-mediated signalling (Hambleton et al., 1996; Geppert et al., 1994; Han et al., 1994; Reimann et al., 1994; Weinstein et al., 1992). It has been demonstrated that the extent of ERK1/2 MAP kinase activation is significantly decreased after LPS-stimulation of PKCε$^{-/-}$ macrophages. Furthermore, our results for the first time suggest that PKCε is critical to the

reactivity state of microglia, promoting the morphine-induced release of NO and cytokines from microglial cells. In particular, we found that in activated microglial cells, morphine increased Akt and ERK kinase phosphorylation through PKCε activation. Activation of Akt pathway is found closely linked to PKCε activation in our cellular system, although an earlier report has indicated that Akt pathway may be independent on PKC isoforms (Sun et al., 2009). Distinct stimuli applied to different cells (microglia vs. macrophages) may account for the differential interaction of the intracellular pathways.

In summary, in the present study, we identified for the first time the involvement of PKCε isoform and Akt pathway upstream of ERK1/2 to mediate morphine-induced proinflammatory phenotype in mouse microglial cells. The establishment of PKCε role in morphine-TLR signalling may provide a means to treat opioid development of tolerance and dependence. However, because the increase of the inflammatory cytokines cannot explain the pain tolerance directly, it will be important to measure the pain mediators, such as substance P, in animal study. Certainly, the in vivo observations that PKC inhibitors can reduce morphine antinociceptive tolerance (Smith et al., 2007) provide evidence that selective inhibition of those PKCs involved might provide useful adjuncts to chronic therapy with opioid drugs. Inhibition of a kinase required for so many important biological functions may be expected to result in substantial side effects. However, several inhibitors of PKC have proven to be well tolerated in clinical trials (Budde et al., 2010; Geraldes et al., 2010; Roffey et al., 2009). We may hope for a similar advance with regard to PKCε selective inhibition.

# Figure Legends

**Figure 21**: Cellular localization of PKCε by imunofluorescence. Microglial cells were treated with morphine 100 nM (MOR), LPS 1 $\mu g \cdot mL^{-1}$ alone (LPS) or LPS + morphine (LPS + MOR) for 10 min. Control panels (CTR) were drug-vehicle-treated cells. PKCε was revealed by immunofluorescence with anti-PKCε antibody and detected by goat fluorescein isothiocyanate anti-rabbit IgG. The fluorescent dye DAPI (blue panel) was used to stain the nuclei. Original magnification 40x.

**Figure 22:** Expression and morphine-induced phosphorylation and membrane translocation of PKCε isoform in LPS-activated primary microglia. Microglial cells were treated with either LPS (1 $\mu g \cdot mL^{-1}$) alone or LPS + morphine (100 nM) for 0–60 min. (A) Phospho- and total PKCε expression in whole-cell lysates. (B) Densitometry of phospho-PKCε expression relative to total PKCε. (C) PKCε expression in membrane (m) and cytosolic (c) fractions of cells. (D) Densitometry of membrane vs. cytosolic PKCε. (E) Phospho- and total PKCε expression in membrane fractions (m) of cells. (F) Densitometry of membrane vs. total PKCε. Plots are mean ± S.E. values of four separate experiments (one of which is shown) performed in triplicate (n = 4). *$P < 0.01$ vs. control conditions (absence of drugs, 0); #$P < 0.01$ vs. LPS conditions; analysis was by ANOVA followed by Dunnett's test.

**Figure 23:** Effect of opioid receptor ligands on LPS-induced phosphorylation of PKCε isoform in primary microglia. Microglial cells were treated with either LPS alone, LPS + morphine 100 nM (MOR), LPS + DAMGO 100 nM, LPS + DPDPE 100 nM, LPS + U69593 100 nM, LPS + Naloxone 100 nM (NALOX), or LPS + CTAP 100 nM for 10 min. The antagonists were added 30 min before morphine. (A) Phospho- and total PKCε expression. (B) Densitometry of phospho-PKCε expression relative to total PKCε. Plots are mean ± S.E. values of four separate experiments (one of which is shown) performed in triplicate (n = 4). *$P < 0.01$ vs. control conditions (absence of drugs, CTR); $^{\#}P < 0.01$ vs. LPS conditions (0); $^{\S}P < 0.01$ vs. LPS + MOR; $^{\dagger}P < 0.01$ vs. LPS + DAMGO; analysis was by ANOVA followed by Dunnett's test.

**Figure 24:** μ-opioid receptor expression silencing. (A) Primary microglial cells were treated with either scramble (-) ($siRNA_{control}$) or with $siRNA_{\mu}$ and cultured for 24, 48 and 72 h. Tubulin shows equal loading of protein. Densitometric quantification of μ-opioid receptor by Western blot is shown. Plots are mean ± S.E. values of four separate experiments performed in triplicate (n = 4); *P < 0.01 compared with the control (scramble transfected cells); analysis was by ANOVA followed by Dunnett's test. (B) Primary microglial cells were treated with either $siRNA_{ctr}$ or $siRNA_{\mu}$ for 48 h and cultured with LPS 1 $\mu g \cdot mL^{-1}$ alone or plus morphine 100 nM (MOR) for 10 min. Densitometry of phospho-PKCε expression relative to total PKCε and densitometry of membrane vs. cytosolic PKCε is shown. Plots are mean ± S.E. values of four separate experiments (one of which is shown) performed in triplicate (n = 4). *P < 0.01 vs. control conditions (absence of drugs, CTR); $^{\#}$P < 0.01 vs. LPS conditions; analysis was by ANOVA followed by Dunnett's test.

**Figure 25:** PKCε is involved in mediating morphine-induced Akt and ERK1/2 activation in primary microglial cells. Microglial cells were pretreated with εV1-2 (1 mM) for 2 h before LPS and morphine stimulation for 10 min. Densitometry of membrane vs. cytosolic PKCε is shown. The ratio of phospho-protein to total protein is used. Plots are mean ± S.E. values of four separate experiments (one of which is shown) performed in triplicate (n = 4) and normalized to the result obtained in untreated cell cultures (CTR) set to 100%. *P < 0.01 vs. control conditions (absence of drugs, CTR); $^{\#}$P < 0.01 vs. LPS conditions; $^{\S}$P < 0.01 vs. LPS + MOR; analysis was by ANOVA followed by Dunnett's test.

**Figure 26:** PKCε expression silencing. (A) Primary microglial cells were treated with either scramble (-) ($siRNA_{control}$), or with $siRNA_{PKC\varepsilon}$ and cultured for 24 and 48 h. Tubulin shows equal loading of protein. Densitometric quantification of PKCε by Western blot is shown. Plots are mean ± S.E. values (n = 3); *P < 0.01 compared with the control (scramble transfected cells); analysis was by ANOVA followed by Dunnett's test. (B) Primary microglial cells were treated with either $siRNA_{ctr}$ or $siRNA_{PKC\varepsilon}$ for 24 h and cultured with LPS 1 $\mu g \cdot mL^{-1}$ alone or plus morphine 100 nM (MOR) or DAMGO 100 nM for 10 min (Akt and ERKs) or 4 h (iNOS). The ratio of phospho-protein to total protein is used. The mean values of 3 independent experiments (one of which is shown) were normalized to the result obtained in cells in the absence of LPS. The unstimulated control was set to 100%. *P < 0.05 with respect to unstimulated control (CTR); $^{\#}$P < 0.05 with respect to cells treated with LPS; analysis was by ANOVA followed by Dunnett's test. (C) COX-2

expression in primary microglial cells treated for 4 h either with LPS 1 μg·mL$^{-1}$ alone or in combination with morphine 100 nM. Densitometric analysis is reported. The mean values of 3 independent experiments (one of which is shown) were normalized to the result obtained in cells in the absence of LPS. *P < 0.05 with respect to unstimulated control (CTR); analysis was by ANOVA followed by Dunnett's test.

**Figure 27:** (A) Effect of εV1-2 on morphine-induced production of proinflammatory cytokine and nitrite in activated primary microglial cells. Microglial cells were treated with either LPS alone, LPS + morphine 100 nM (MOR), alone or in the presence of εV1-2. Microglial cells were pretreated with εV1-2 (1 μM) for 2 h before LPS and morphine stimulation for 24 h. Plots are mean ± S.E. values of four separate experiments performed in triplicate (n = 4). *P < 0.01 vs. control conditions (absence of drugs, CTR); $^{\#}$P < 0.01 vs. LPS conditions (0); $^{\S}$P < 0.01 vs. LPS + MOR; analysis was by ANOVA followed by Dunnett's test. (B) Primary microglial cells were treated with either $siRNA_{ctr}$ or with $siRNA_{PKC\varepsilon}$ for 24 h and cultured with LPS 1 μg·mL$^{-1}$ alone or plus morphine 100 nM (MOR) or DAMGO 100 nM for 24 h. The unstimulated control (CTR) was set to 100%. Plots are mean ± S.E. values (n = 3); *P < 0.05 vs. CTR; $^{\#}$P < 0.05 vs. LPS; analysis was by ANOVA followed by Dunnett's test.

**Figure 28:** Primary microglial cells were treated with either LPS 1 μg·mL$^{-1}$ alone or plus SH-5 1 μM, U0126 1 μM, morphine 100 nM (MOR) alone or in combination for 10 min (p-PKC in panel A and pERK1/2 in panel B) or 4 h (iNOS). Densitometry of phospho-PKCε expression relative to total PKCε is shown. Plots are mean ± S.E. values of four separate experiments (one of which is shown) performed in triplicate (n = 4). *P < 0.01 vs. control conditions (absence of drugs, CTR); $^{\#}$P < 0.01 vs. LPS conditions; $^{\S}$P < 0.01 vs. LPS + MOR; analysis was by ANOVA followed by Dunnett's test.

**Figure 29:** Primary microglial cells were treated with morphine 100 nM (MOR) for (A) 10 min (p-PKCε, pAkt, pERK1/2), 4 h (COX-2, iNOS) or (B) 24 h (IL-1β, IL-6, TNF-α, nitrite). Densitometric analysis of phosphorylated isoform is reported. Plots are mean ± S.E. values of four separate experiments (one of which is shown) performed in triplicate (n = 4). *P < 0.01 vs. control conditions (absence of morphine, CTR); analysis was by t-test.

**Figure 30:** Schematic summary of morphine-initiated signal transduction cascade in murine microglia. Morphine binding to μ-opioid receptor (μR) activates PKCε, Akt and ERK kinases, which lead to subsequent expression of proinflammatory chemokines and NO.

**Figure 21**

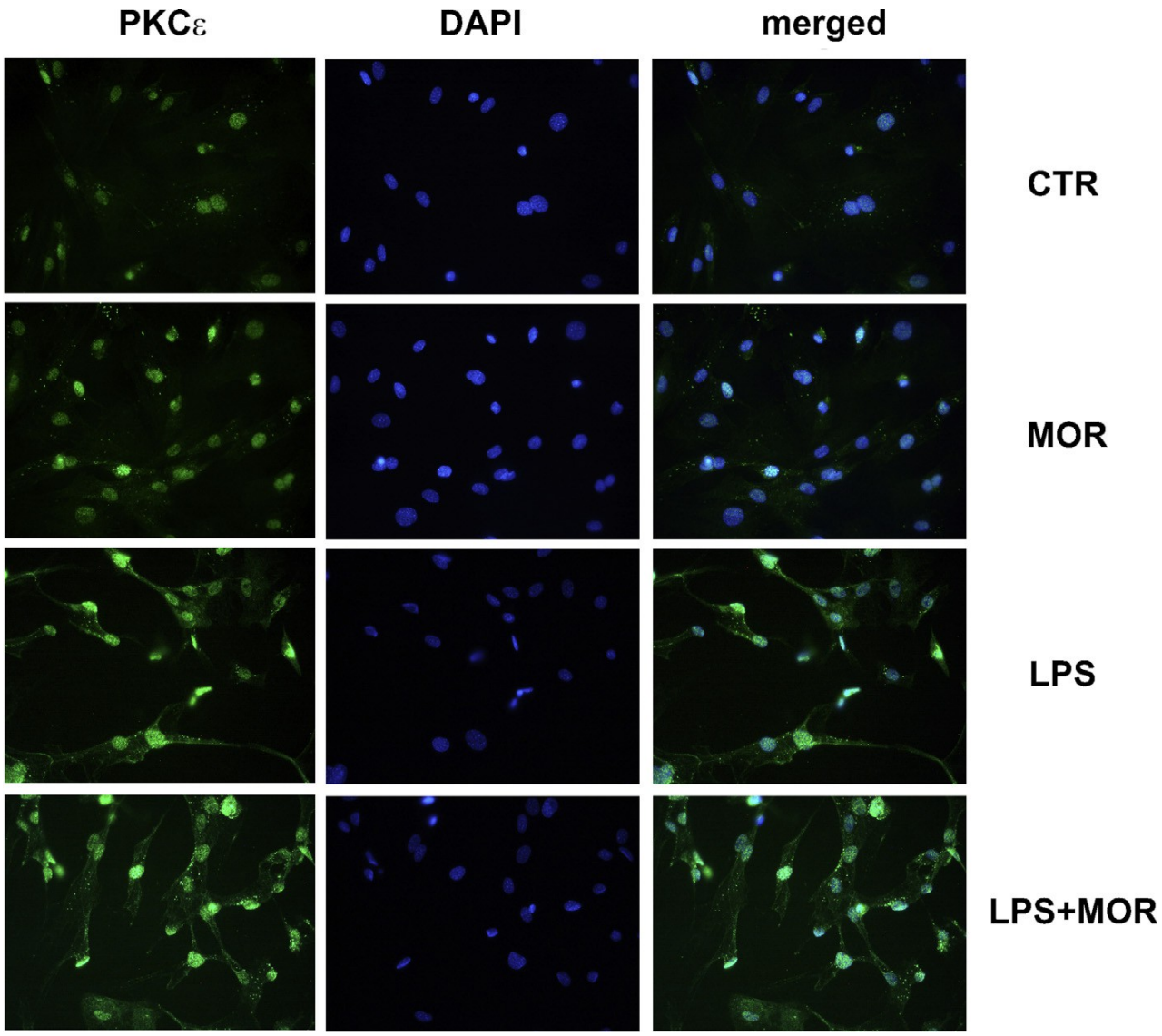

**Figure 22**

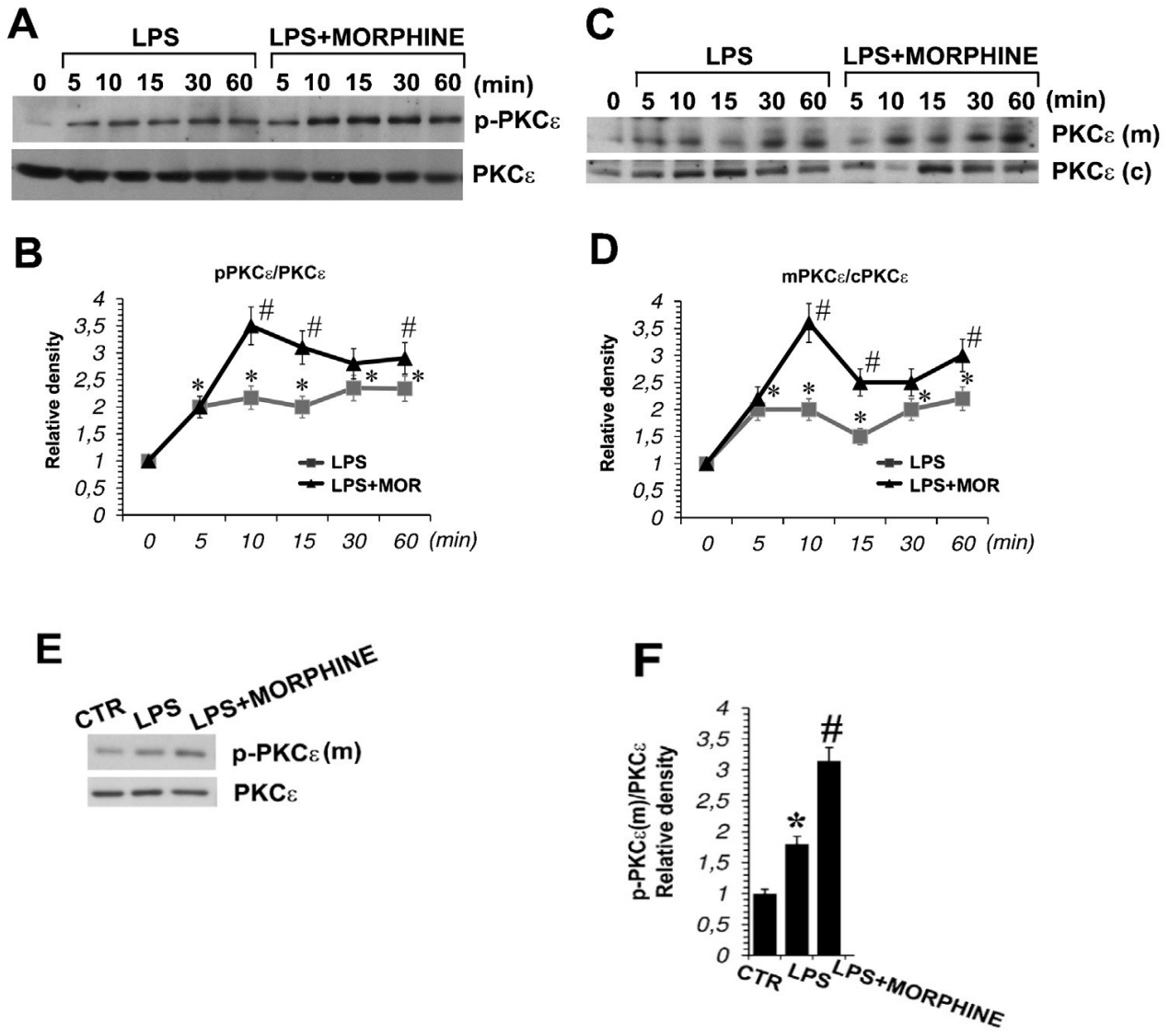


**Figure 23**

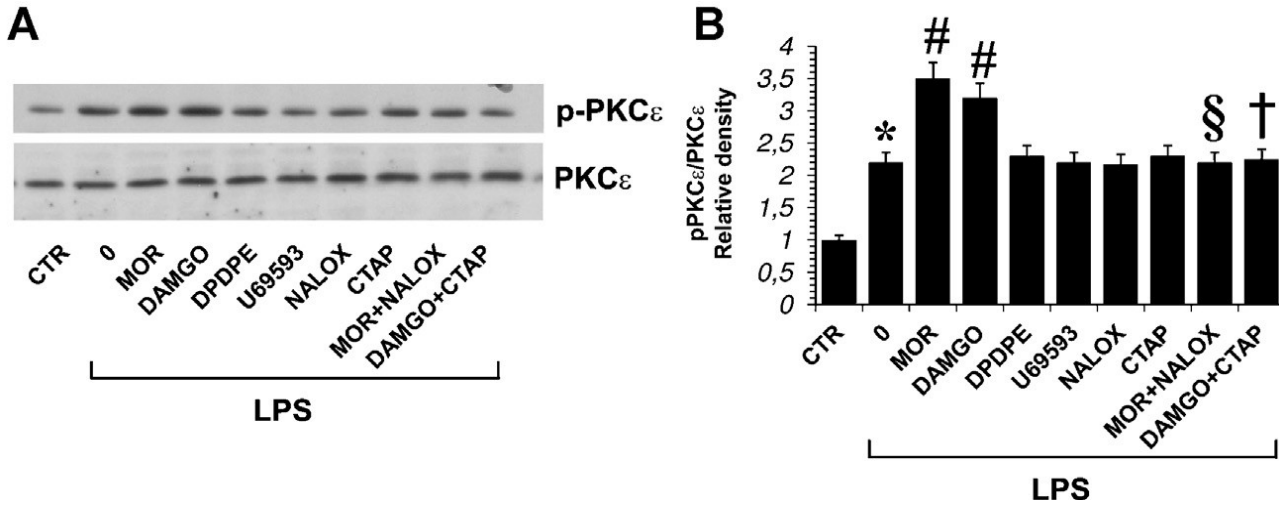

**Figure 24**

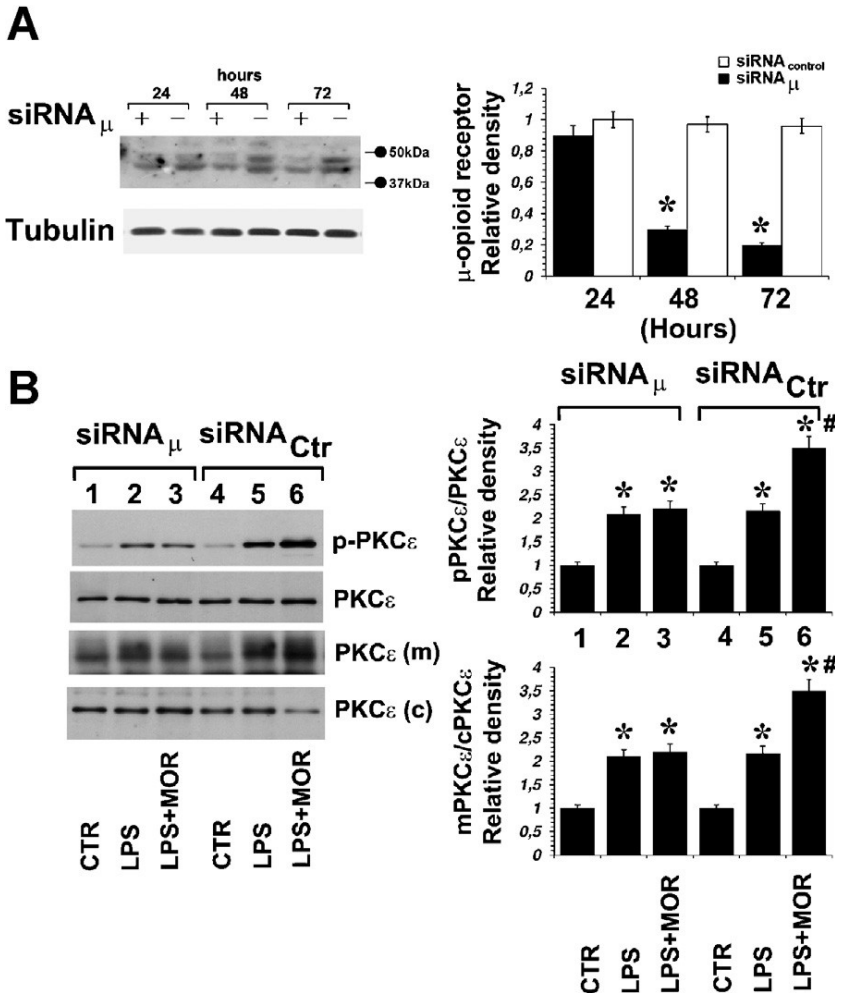


**Figure 25**

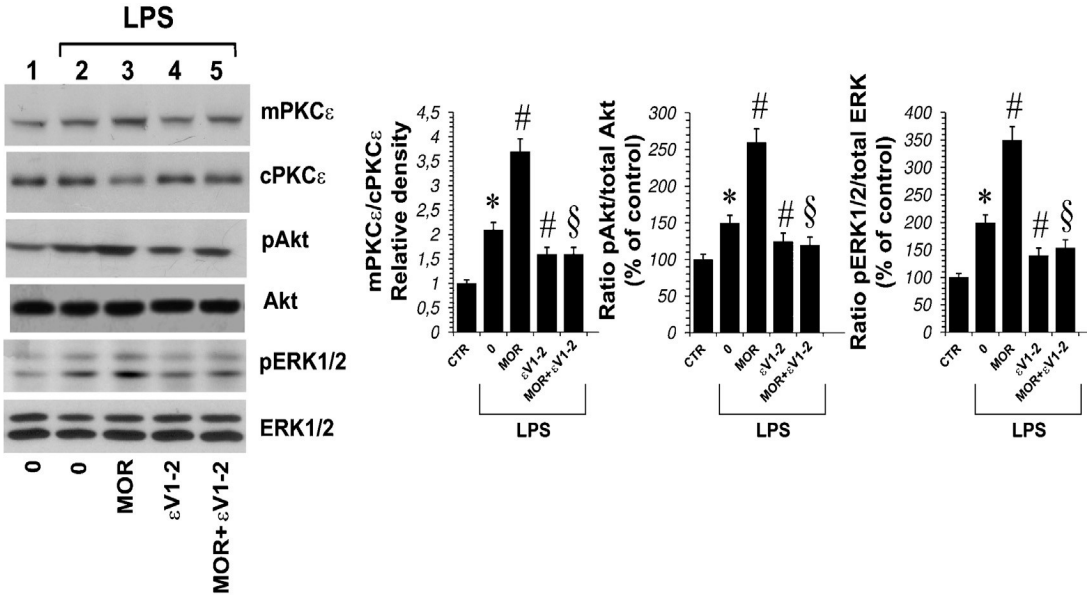

**Figure 26**

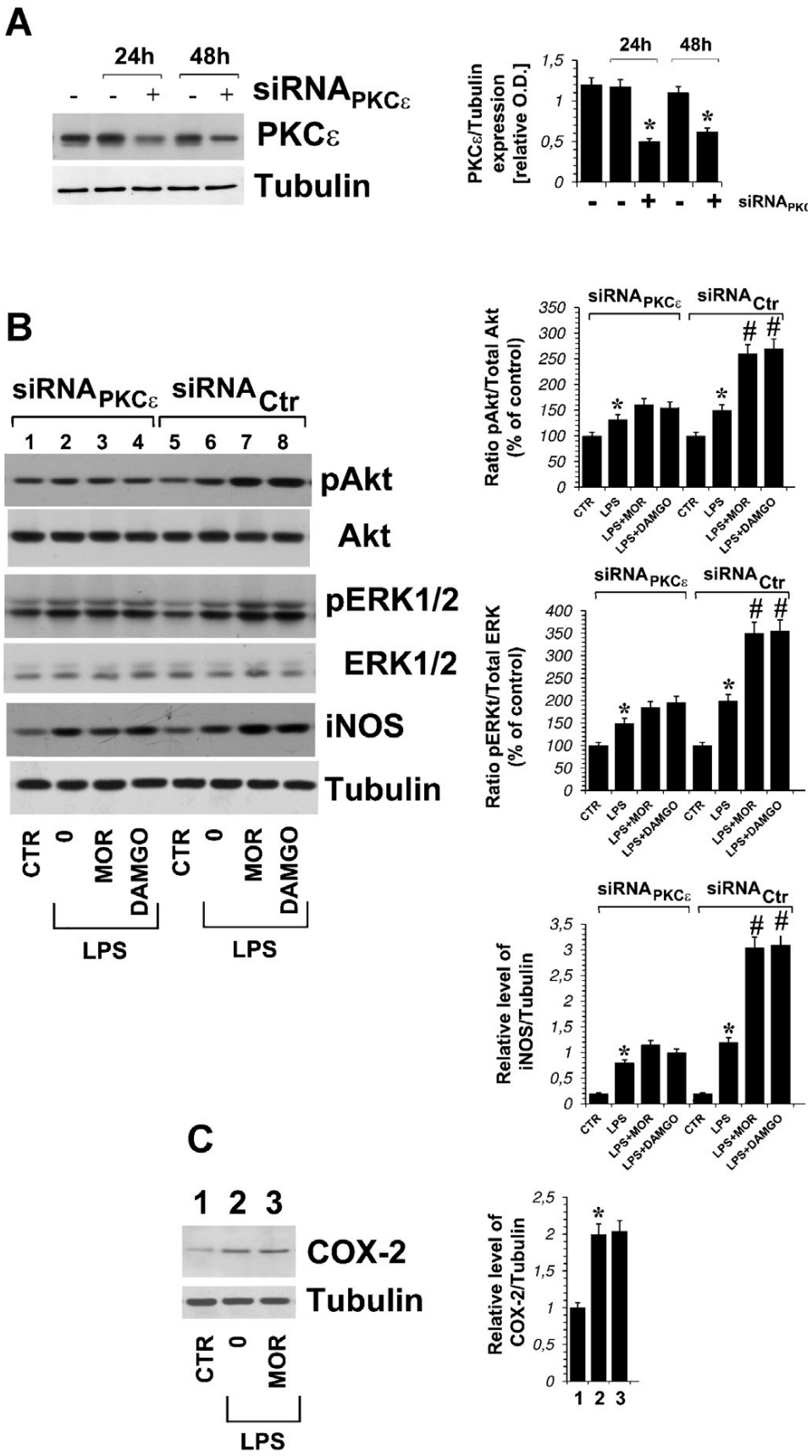
A
24h
48h
siRNA$_{PKC\varepsilon}$
PKCε
Tubulin
PKCε/Tubulin expression [relative O.D.]
B
siRNA$_{PKC\varepsilon}$
siRNA$_{Ctr}$
pAkt
Akt
pERK1/2
ERK1/2
iNOS
Tubulin
CTR
0
MOR
DAMGO
LPS
Ratio pAkt/Total Akt (% of control)
Ratio pERKt/Total ERK (% of control)
Relative level of iNOS/Tubulin
LPS+MOR
LPS+DAMGO
C
COX-2
Relative level of COX-2/Tubulin

**Figure 27**

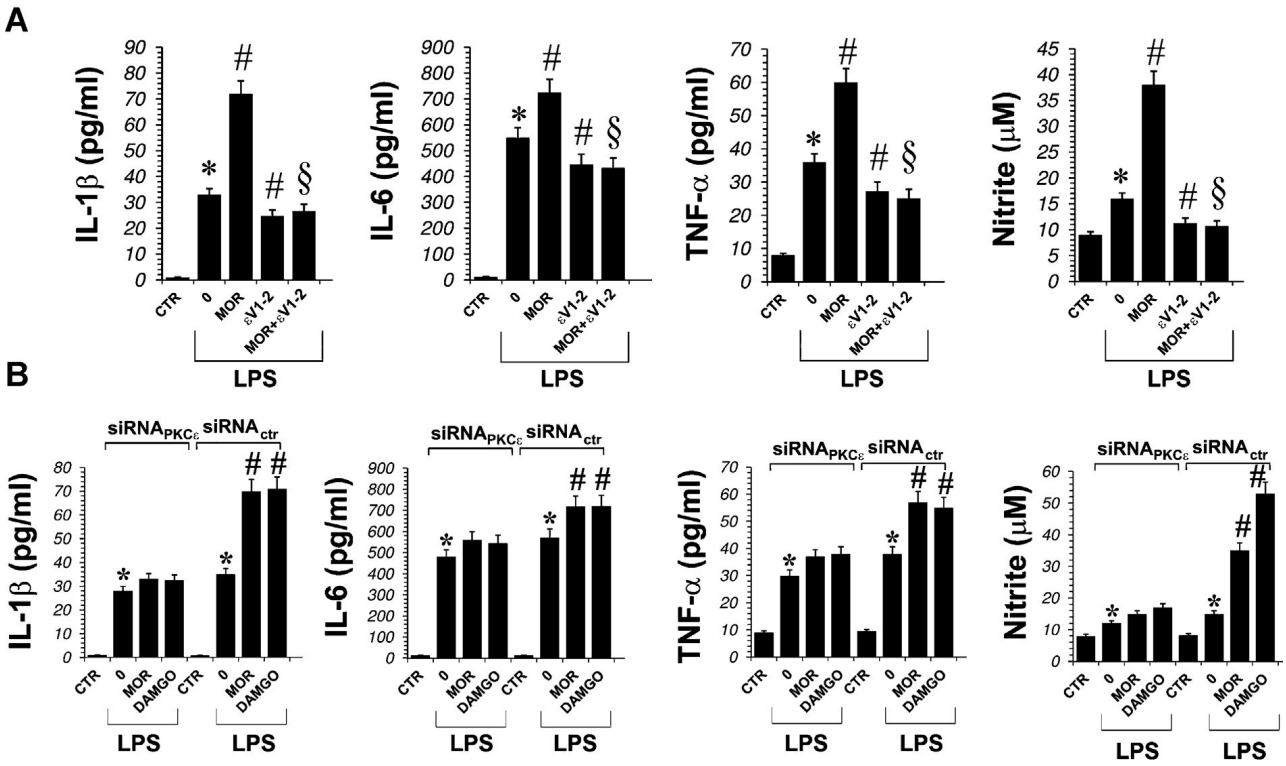
A
IL-1β (pg/ml)
IL-6 (pg/ml)
TNF-α (pg/ml)
Nitrite (μM)
CTR
0
MOR
εV1-2
MOR+εV1-2
LPS
B
siRNA PKCε
siRNA ctr
DAMGO

**Figure 28**

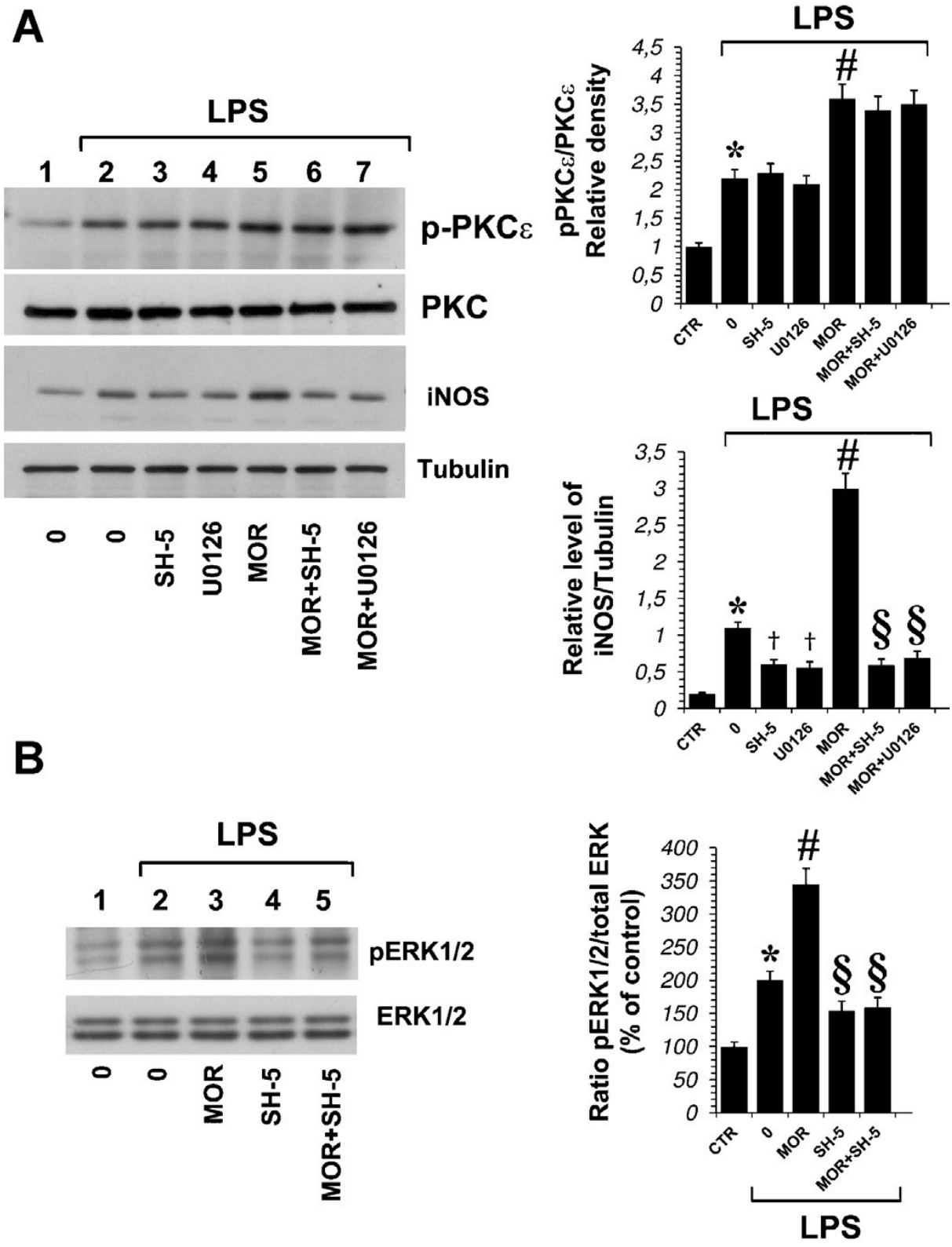
A
LPS
1 2 3 4 5 6 7
p-PKCε
PKC
iNOS
Tubulin
0 0 SH-5 U0126 MOR MOR+SH-5 MOR+U0126
pPKCε/PKCε Relative density
CTR 0 SH-5 U0126 MOR MOR+SH-5 MOR+U0126
Relative level of iNOS/Tubulin
B
LPS
1 2 3 4 5
pERK1/2
ERK1/2
0 0 MOR SH-5 MOR+SH-5
Ratio pERK1/2/total ERK (% of control)
CTR 0 MOR SH-5 MOR+SH-5
LPS

**Figure 29**

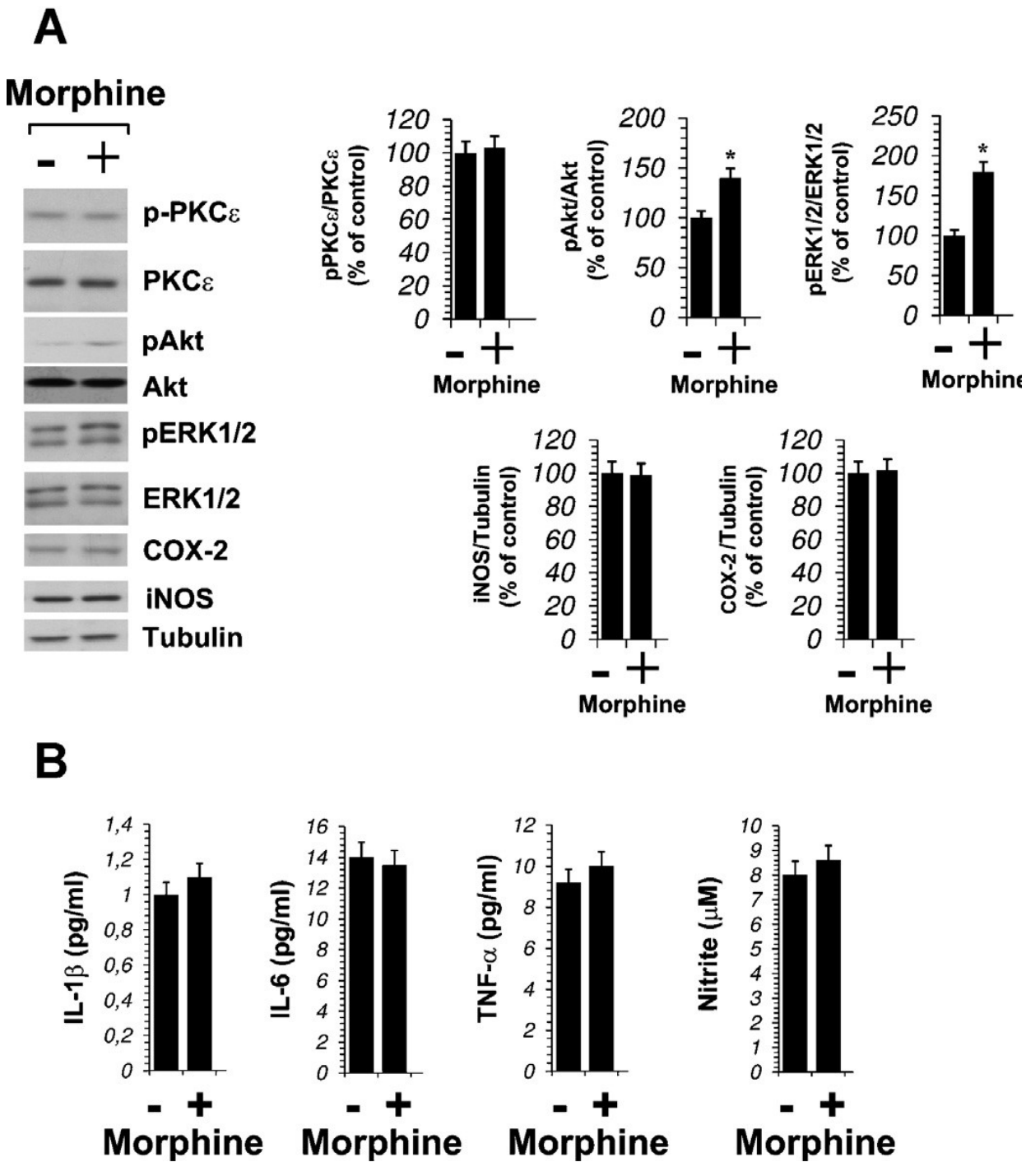
A
Morphine
- +
p-PKCε
PKCε
pAkt
Akt
pERK1/2
ERK1/2
COX-2
iNOS
Tubulin
pPKCε/PKCε (% of control)
120
100
80
60
40
20
0
- +
Morphine
pAkt/Akt (% of control)
200
150
100
50
0
*
pERK1/2/ERK1/2 (% of control)
250
200
150
100
50
0
iNOS/Tubulin (% of control)
COX-2/Tubulin (% of control)
B
IL-1β (pg/ml)
1,4
1,2
1
0,8
0,6
0,4
0,2
0
IL-6 (pg/ml)
16
14
12
10
8
6
4
2
0
TNF-α (pg/ml)
12
10
8
6
4
2
0
Nitrite (μM)
10
9
8
7
6
5
4
3
2
1
0

**Figure 30**

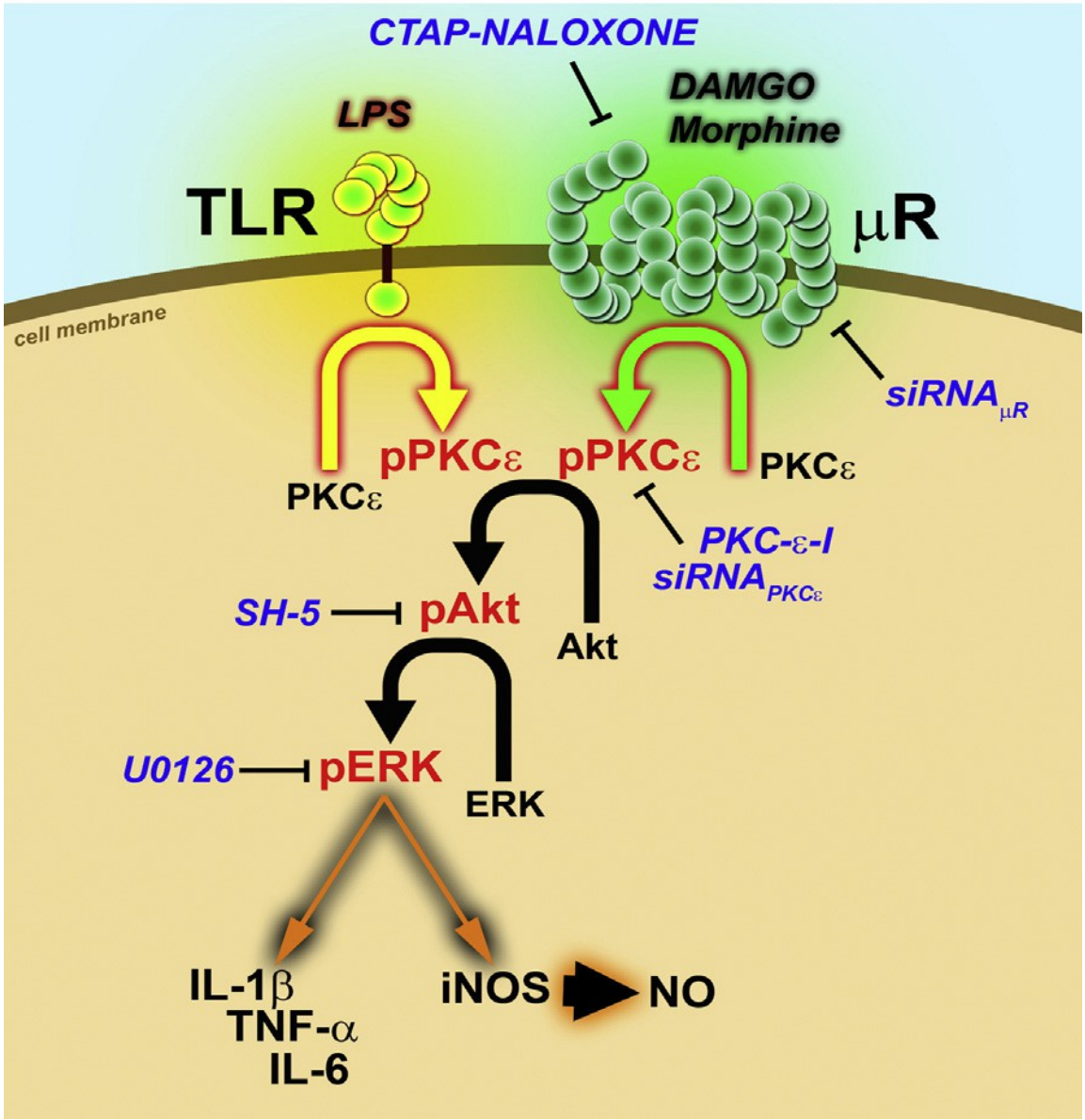
CTAP-NALOXONE
DAMGO
Morphine
LPS
TLR
μR
cell membrane
siRNA μR
pPKCε
pPKCε
PKCε
PKCε
PKC-ε-I
siRNA PKCε
SH-5
pAkt
Akt
U0126
pERK
ERK
IL-1β
TNF-α
IL-6
iNOS
NO

# References

Alexander SPH, Benson HE, Faccenda E, Pawson AJ, Sharman JL, Catterall WA, Spedding M, Peters JA, Harmar AJ, CGTP collaborators (2013). The Concise Guide to PHARMACOLOGY 2013/2014: Overview . Br J Pharmacol 170: 1449-1458.

Belcheva MM, Clark AL, Haas PD, Serna JS, Hahn JW, Kiss A, Coscia CJ (2005). Mu and kappa opioid receptors activate ERK/MAPK via different protein kinase C isoforms and secondary messengers in astrocytes. J Biol Chem 280: 27662–27669.

Bohn LM, Belcheva MM, Coscia CJ (2000). Mitogenic signaling via endogenous kappa-opioid receptors in C6 glioma cells: evidence for the involvement of protein kinase C and the mitogen-activated protein kinase signaling cascade. J Neurochem 74: 564–573.

Brandman R, Disatnik MH, Churchill E, Mochly-Rosen D (2007). Peptides derived from the C2 domain of protein kinase C epsilon (epsilon PKC) modulate epsilon PKC activity and identify potential protein–protein interaction surfaces. J Biol Chem 282: 4113–4123.

Budde K, Sommerer C, Becker T, Asderakis A, Pietruck F, Grinyo JM, Rigotti P, Dantal J, Ng J, Barten MJ, Weber M (2010). Sotrastaurin, a novel small molecule inhibiting protein kinase C: first clinical results in renal-transplant recipients. Am J Transplant 10: 571–581.

Castrillo A, Pennington DJ, Otto F, Parker PJ, Owen MJ, Boscà L (2001). Protein kinase C epsilon is required for macrophage activation and defense against bacterial infection. J Exp Med 194: 1231–1342.

Chao CC, Hu S, Molitor TW, Shaskan EG, Peterson PK (1992). Activated microglia mediate neuronal cell injury via a nitric oxide mechanism. J Immunol 149: 2736–2741.

Chao CC, Gekker G, Sheng WS, Hu S, Tsang M, Peterson PK (1994). Priming effect of morphine on the production of tumor necrosis factor-α by microglia: implications in respiratory burst activity and human immunodeficiency virus-1 expression. J Pharmacol Exp Ther 269: 198–203.

Freeley M, Kelleher D, Long A (2011). Regulation of protein kinase C function by phosphorylation on conserved and non-conserved sites. Cell Signal 23: 753–762.

Frölich N, Dees C, Paetz C, Ren X, Lohse MJ, Nikolaev VO, Zenk MH (2011). Distinct pharmacological properties of morphine metabolites at G(i)-protein and β-arrestin signalling pathways activated by the human μ-opioid receptor. Biochem Pharmacol 81: 1248–1254.

Fukuda K, Kato S, Morikawa H, Shoda T, Mori K (1996). Functional coupling of the delta-, mu- and kappa-opioid receptors to mitogen-activated protein kinase and arachidonate release in Chinese hamster ovary cells. J Neurochem 67: 1309–1316.

Geppert TD, Whitehurst CE, Thompson P, Beutler B (1994). Lipopolysaccharide signals activation of tumor necrosis factor biosynthesis through the ras/raf-1/MEK/MAPK pathway. Mol Med 1: 93–103.

Geraldes P, King GL (2010). Activation of protein kinase C isoforms and its impact on diabetic complications. Circ Res 106: 1319–1331.

Gobbi G, Mirandola P, Tazzari PL, Ricci F, Caimi L, Cacchioli A, Papa S, Conte R, Vitale M (2003). Flow cytometry detection of serotonin content and release in resting and activated platelets. Br J Haematol 121: 892–896.

Grace PM, Hutchinsons MR, Maier SF, Watkins LR (2014). Pathological pain and the neuroimmune interface. Nat Rev Immunol 14: 217-231.

Hama H, Hara C, Yamaguchi K, Miyawaki A (2004). PKC signaling mediates global enhancement of excitatory synaptogenesis in neurons triggered by local contact with astrocytes. Neuron 41: 405–415.

Hambleton J, Weinstein SL, Lem L, DeFranco AL (1996). Activation of c-Jun N-terminal kinase in bacterial lipopolysaccharide-stimulated macrophages. Proc Natl Acad Sci USA 93: 2774–2778.

Han J, Lee JD, Bibbs L, Ulevitch RJ (1994). A MAP kinase targeted by endotoxin and hyperosmolarity in mammalian cells. Science 265: 808–811.

Kieffer BL, Evans CJ (2009). Opioid receptors: from binding sites to visible molecules in vivo. Neuropharmacology 56: 205–212.

Joseph EK, Reichling DB, Levine JD (2010). Shared mechanisms for opioid tolerance and a transition to chronic pain. J Neurosci 30: 4660–4666.

Lee SC, Liu W, Dickson DW, Brosnan CF, Berman JW (1993). Cytokine production by human fetal microglia and astrocytes. Differential induction by lipopolysaccharide and IL-1 beta. J Immunol 150: 2659–2567.

Mangoura D, Sun Y, Li C, Singh D, Gutmann DH, Flores A, Ahmed M, Vallianatos G (2006). Phosphorylation of neurofibromin by PKC is a possible molecular switch in EGF receptor signaling in neural cells. Oncogene 25: 735–745.

Merighi S, Benini A, Mirandola P, Gessi S, Varani K, Leung E, Maclennan S, Borea PA (2005). $A_3$ adenosine receptor activation inhibits cell proliferation via phosphatidylinositol 3-kinase/ Akt-dependent inhibition of the extracellular signal-regulated kinase 1/2 phosphorylation in A375 human melanoma cells. J Biol Chem;280:19516–19526.

Merighi S, Benini A, Mirandola P, Gessi S, Varani K, Leung E, Maclennan S, Borea PA (2006). Adenosine modulates vascular endothelial growth factor expression via hypoxia-inducible factor-1 in human glioblastoma cells. Biochem Pharmacol 72: 19–31.

Merighi S, Benini A, Mirandola P, Gessi S, Varani K, Simioni C, Leung E, Maclennan S, Baraldi PG, Borea PA (2007). Caffeine inhibits adenosine-induced accumulation of hypoxia-inducible factor-1alpha, vascular endothelial growth factor, and interleukin-8 expression in hypoxic human colon cancer cells. Mol Pharmacol 72: 395–406.

Merighi S, Simioni C, Gessi S, Varani K, Mirandola P, Tabrizi MA, Baraldi PG, Borea PA (2009). $A_{2B}$ and $A_3$ adenosine receptors modulate vascular endothelial growth factor and interleukin-8 expression in human melanoma cells treated with etoposide and doxorubicin. Neoplasia 11: 1064–1073.

Merighi S, Gessi S, Varani K, Simioni C, Fazzi D, Mirandola P, Borea PA (2012a). Cannabinoid $CB_2$ receptors modulate ERK-1/2 kinase signalling and NO release in microglial cells stimulated with bacterial lipopolysaccharide. Br J Pharmacol 165: 1773–1788.

Merighi S, Gessi S, Varani K, Fazzi D, Mirandola P, Borea PA (2012b). Cannabinoid $CB_2$ receptor attenuates morphine-induced inflammatory responses in activated microglial cells. Br J Pharmacol 166: 2371–2385.

Minghetti L, Levi G (1995). Induction of prostanoid biosynthesis by bacterial lipopolysaccharide and isoproterenol in rat microglial cultures. J Neurochem 65: 2690–2698.

Minghetti L, Levi G (1998). Microglia as effector cells in brain damage and repair: focus on prostanoids and nitric oxide. Prog Neurobiol 54: 99–125.

Mirandola P, Gobbi G, Masselli E, Micheloni C, Di Marcantonio D, Queirolo V, Chiodera P, Meschi T, Vitale M (2011). Protein kinase Cε regulates proliferation and cell sensitivity to TGF-1β of CD4+ T lymphocytes: implications for Hashimoto thyroiditis. J Immunol 187: 4721–4732.

Nakai M, Hojo K, Taniguchi T, Terashima A, Kawamata T, Hashimoto T, Maeda K, Tanaka C (1998). PKC and tyrosine kinase involvement in amyloid beta (25-35)-induced chemotaxis of microglia. NeuroReport 9:3467–3470.

Newton PM, Kim JA, McGeehan AJ, Paredes JP, Chu K, Wallace MJ, Roberts AJ, Hodge CW, Messing RO (2007). Increased response to morphine in mice lacking protein kinase C epsilon. Genes Brain Behav 6: 329–338.

Ock J, Kim S, Yi KY, Kim NJ, Han HS, Cho JY, Suk K (2010). A novel anti-neuroinflammatory pyridylimidazole compound KR-31360. Biochem Pharmacol 79: 596–609.

Powell KJ, Hosokawa A, Bell A, Sutak M, Milne B, Quirion R, Jhamandas K. (1999). Comparative effects of cyclo-oxygenase and nitric oxide synthase inhibition on the development and reversal of spinal opioid tolerance. Br J Pharmacol 127: 631–644.

Prekeris R, Mayhew MW, Cooper JB, Terrian DM (1996). Identification and localization of an actin-binding motif that is unique to the epsilon isoform of protein kinase C and participates in the regulation of synaptic function. J Cell Biol 132: 77–90.

Raghavendra V, Rutkowski MD, DeLeo JA (2002). The role of spinal neuroimmune activation in morphine tolerance/hyperalgesia in neuropathic and shamoperated rats. J Neurosci 22: 9980–9989.

Raghavendra V, Tanga FY, DeLeo JA (2004). Attenuation of morphine tolerance, withdrawal-induced hyperalgesia, and associated spinal inflammatory immune responses by propentofylline in rats. Neuropsychopharmacology 29: 327–334.

Reimann T, Bu¨ scher D, Hipskind RA, Krautwald S, Lohmann-Matthes ML, Baccarini M (1994). Lipopolysaccharide induces activation of the Raf-1/MAP kinase pathway. A putative role for Raf-1 in the induction of the IL-1 beta and the TNF-alpha genes. J Immunol 153: 5740–5749.

Roffey J, Rosse C, Linch M, Hibbert A, McDonald NQ, Parker PJ (2009). Protein kinase C intervention: the state of play. Curr Opin Cell Biol 21: 268–279.

Romero-Sandoval EA, Horvath RJ, DeLeo JA (2008). Neuroimmune interactions and pain: focus on glial-modulating targets. Curr Opin Investig Drugs 9: 726–734.

Smith FL, Gabra BH, Smith PA, Redwood MC, Dewey WL (2007). Determination of the role of conventional, novel and atypical PKC isoforms in the expression of morphine tolerance in mice. Pain 127: 129–139.

Song P, Zhao ZQ (2001). The involvement of glial cells in the development of morphine tolerance. Neurosci Res 39: 281–286.

Sudan R, Srivastava N, Pandey SP, Majumdar S, Saha B (2012). Reciprocal regulation of protein kinase C isoforms results in differential cellular responsiveness. J Immunol 188(5):2328-2337.

Sun J, Ramnath RD, Tamizhselvi R, Bhatia M (2009). Role of protein kinase C and phosphoinositide 3-kinase-Akt in substance P-induced proinflammatory pathways in mouse macrophages. FASEB J 23: 997–1010.

Steinberg SF (2008). Structural basis of protein kinase C isoform function. Physiol Rev 88: 1341–1378.

Wallace MJ, Newton PM, McMahon T, Connolly J, Huibers A, Whistler J, Messing RO (2009). PKC epsilon regulates behavioral sensitivity, binding and tolerance to the $CB_1$ receptor agonist WIN55,212-2. Neuropsychopharmacol 34: 1733–1742.

Watkins LR, Milligan ED, Maier SF (2001). Spinal cord glia: new players in pain. Pain 93: 201–205.

Watkins LR, Milligan ED, Maier SF (2003). Glial proinflammatory cytokines mediate exaggerated pain states: implications for clinical pain. Adv Exp Med Biol 521: 1–21.

Watkins LR, Hutchinson MR, Johnston IN, Maier SF (2005). Glia: novel counter-regulators of opioid analgesia. Trends Neurosci 28: 661–669.

Watkins LR, Hutchinson MR, Ledeboer A, Wieseler-Frank J, Milligan ED, Maier SF (2007). Norman Cousins Lecture. Glia as the bad guys: implications for improving clinical pain control and the clinical utility of opioids. Brain Behav Immun 21: 131–146.

Weinstein SL, Sanghera JS, Lemke K, DeFranco AL, Pelech SL (1992). Bacterial lipopolysaccharide induces tyrosine phosphorylation and activation of mitogenactivated protein kinases in macrophages. J Biol Chem 267: 14955–14962.

Yoon HJ, Jun CD, Kim JM, Rim GN, Kim HM, Chung HT (1994). Phorbol ester synergistically increases interferon-gamma-induced nitric oxide synthesis in murine microglial cells. Neuroimmunomodulation 1: 377–382.

Yrjanheikki J, Keinanen R, Pellikka M, Hokfelt T, Koistinaho J (1998). Tetracyclines inhibit microglial activation and are neuroprotective in global brain ischemia. Proc Natl Acad Sci USA 95: 15769–15774.

Yrjanheikki J, Tikka T, Keinanen R, Goldsteins G, Chan PH, Koistinaho J (1999). A tetracycline derivative, minocycline, reduces inflammation and protects against focal cerebral ischemia with a wide therapeutic window. Proc Natl Acad Sci USA 96: 13496–13500.

Zheng H, Loh HH, Law PY (2008). Beta-arrestin-dependent mu-opioid receptor-activated extracellular signal-regulated kinases (ERKs) translocate to nucleus in contrast to G protein-dependent ERK activation. Mol Pharmacol 73: 178–190.

Zheng H, Chu J, Zhang Y, Loh HH, Law PY (2011). Modulating micro-opioid receptor phosphorylation switches agonist-dependent signaling as reflected in PKC epsilon activation and dendritic spine stability. J Biol Chem 286: 12724–12733.

# Curriculum vitae

**2007** Degree in Chemistry and Pharmaceutical Technology at the University of Ferrara.

**2008-2014** Research Fellowship at the Department of Medical Sciences, Section of Pharmacology, University of Ferrara.

**2012-2014** PhD Student in "Pharmacology and Molecular Oncology", Department of Medical Sciences, Section of Pharmacology, University of Ferrara.

# List of Publications

Gessi S, Merighi S, **Fazzi D**, Stefanelli A, Varani K, Borea PA (2011). Adenosine receptor targeting in health and disease. Expert Opin Investig Drugs 20(12): 1591-609.

Merighi S, Gessi S, Varani K, Simioni C, **Fazzi D**, Mirandola P, Borea PA (2012). Cannabinoid $CB_2$ receptor modulates microglia cells stimulated with lypopolysaccharide: role of ERK-1/2 kinase signaling in nitric oxide release. B J Pharmacol 165(6): 1773-88.

Merighi S, Gessi S, Varani K, **Fazzi D**, Mirandola P, Borea PA (2012). Cannabinoid $CB_2$ receptor attenuates morphine-induced inflammatory responses in activated microglial cells. Br J Pharmacol 166(8): 2371-85.

Merighi S, Gessi S, Varani K, **Fazzi D**, Borea PA (2012). Hydrogen sulfide modulates the release of nitric oxide and VEGF in human keratinocytes. Pharmacol Res 66(5): 428-36.

Merighi S, Gessi S, Varani K, **Fazzi D**, Stefanelli A, Borea PA (2013). Morphine mediates a proinflammatory phenotype via μ-opioid receptor-PKCε-Akt-ERK1/2 signalling pathway in activated microglial cells. Biochem Pharmacol 86(4): 487-96.

Gessi S, Merighi S, Stefanelli A, **Fazzi D**, Varani K, Borea PA (2013). $A_1$ and $A_3$ adenosine receptors inhibit LPS-induced hypoxia-inducible factor-1 accumulation in murine astrocytes. Pharmacol Res 76: 157-70.

Tabrizi MA, Baraldi PG, Baraldi S, Preti D, Prencipe F, Saponaro G, Romagnoli R, Gessi S, Merighi S, Stefanelli A, **Fazzi D**, Borea PA, Maia RC, Romeiro NC, Fraga CAM, Barreiro EJ (2014). Synthesis and Biological Evaluation of Pyrazolo-[3,4-b]pyridin-4-ones as a New Class of Topoisomerase II Inhibitors. Med Chem, in press.

# Poster

Gessi S, Merighi S, Stefanelli A, **Fazzi D**, Varani K, Borea PA (2011). HIF-1 neuroprotection through erythropoietin increase in hypoxia: a role for $A_1$ adenosine receptors. Bologna, 14-17 settembre 2011 - Società Italiana di Farmacologia.

Merighi S, Gessi S, Varani K, **Fazzi D**, Stefanelli A, Mirandola P, Borea PA (2011). Cannabinoid $CB_2$ receptor modulates microglial cell activation: role of ERK-1/2 kinase signalling. Bologna, 14-17 settembre 2011 - Società Italiana di Farmacologia.

Stefanelli A, Gessi S, Merighi S, Mirandola P**,** Bonfatti A, Fini S, Sensi A, **Fazzi D**, Varani K, Vesce F, Borea PA (2012). Downregulation of $A_1$ and $A_{2B}$ adenosine receptors in human trisomy 21 mesenchymal cells from first-trimester chorionic villi. Rimini, 16-19 Settembre 2012, 16° Seminario Nazionale SIF Dottorandi e Assegnisti di Ricerca.

**Fazzi D**, Merighi S, Gessi S, Varani K, Stefanelli A, Mirandola P, Borea PA (2012). Cannabinoid $CB_2$ receptor attenuates morphine-induced inflammatory responses in activated microglial cells. Rimini, 16-19 Settembre 2012, 16° Seminario Nazionale SIF Dottorandi e Assegnisti di Ricerca.

Gessi S, Merighi S, Stefanelli A, Mirandola P, Bonfatti A, Fini S, Sensi A, **Fazzi D**, Varani K, Vesce F, Borea PA (2012). Downregulation of $A_1$ and $A_{2B}$ adenosine receptors in human trisomy 21 mesenchymal cells from first-trimester chorionic villi. Annual Purine club meeting 2012.

Merighi S, Gessi S, Varani K, **Fazzi D**, Stefanelli A, Borea PA (2013). Morphine mediates a proinflammatory phenotype via μ-opioid receptor-PKCε-Akt-ERK1/2 signaling pathway in activated microglial cells. Torino, 23-26 Ottobre 2013, 36° Congresso Nazionale della Società Italiana di Farmacologia.

Gessi S, Merighi S, Stefanelli A, **Fazzi D,** Varani K, Borea PA (2013). $A_1$ and $A_3$ adenosine receptors inhibit LPS-induced Hypoxia-inducible factor-1 accumulation in hypoxic murine astrocytes. Torino, 23-26 Ottobre 2013, 36° Congresso Nazionale della Società Italiana di Farmacologia.

# Meetings

**2008** Attestato di partecipazione al convegno: “Bambini ed anziani: la Farmacovigilanza nelle età a maggior rischio” (FE).

**2009** Attestato di partecipazione al workshop: “Il placebo nelle sperimentazioni cliniche: Aspetti farmacologici ed etici”

**2012** Attestato di partecipazione al workshop: Convegno Monotematico “Cannabinoidi: presente e futuro” (FE).

**2012** Attestato di partecipazione : “XVI Seminario Nazionale SIF Dottorandi ed assegnisti di Ricerca” Rimini.

**2014** Attestato di partecipazione al corso sul trattamento degli animali utilizzati a fini sperimentali: aspetti etico-legali, sicurezza, best practice svoltosi presso l’Università degli Studi di Ferrara.

# Acknowledgements

The research described in this thesis was carried out in the Laboratory of Cellular and Molecular Pharmacology, Institute of Pharmacology, Department of Medical Sciences, University of Ferrara.

I wish to express my gratitude to Dr.ssa Stefania Merighi and to Prof. Pier Andrea Borea.

Special thanks are due to my colleagues Martina, Serena and Luca for giving me support and friendship.

I would like to thank Alessandro, my son Nicola and my daughter Chiara for their support.